**SHIP STRUCTURE SUBJECTED TO EXTREME ICE LOADING: FULL SCALE**

**LABORATORY EXPERIMENTS USED TO VALIDATE NUMERICAL**

**ANALYSIS**

by

© Mike Manuel, B. Eng.

A Thesis submitted to the School of Graduate Studies

in partial fulfillment of the requirements for the degree of

Master of Engineering

Memorial University of Newfoundland

**August 2014**

# ABSTRACT

As the amount of activity in the Arctic increases, the response of ship structures to ice loading is becoming ever more important. Plastic limit states design is utilized for the design of ship structures for ice conditions. This thesis includes the discussion of full-scale laboratory experiments involving ice-structure interaction. Stiffened panels representative of full-scale polar ship structure are loaded with laboratory-grown ice blocks quasi-statically to extreme load levels. These experiments are unique in scale for a laboratory environment.

Finite element analysis of the laboratory experiments is performed, and high fidelity is achieved. The close match between real-life results and finite element simulation validates the methods used in this thesis.

Using the laboratory experiments as validation, the plastic response of polar class ship structure along the midbody ice belt of a longitudinally framed, PC7, 12,000 tonne ship is evaluated using finite element analysis. Different stiffener cross-section types are evaluated, including T-section, L-section, bulb flat, and flat bar-section. Full discussion of the results is included.

# ACKNOWLEDGEMENTS

# Table of Contents

vi

# List of Tables

# List of Figures

# List of Appendices

# 1. Introduction

## 1.1. Background: Arctic exploration and operation in ice

Ships have been transiting ice-infested and polar waters for more than 400 years. Finding a route through the Arctic to Asia from Europe has long been a goal. In 1850, the ships of Sir John Franklin were lost in the Canadian Arctic, and the Canadian Government continues today to search for these lost ships. It was not until 1878 and 1906 that the first successful voyages from the Atlantic Ocean to the Pacific were made through the North East, and North West passages, respectively. Throughout the 1900's, ice breaker designs were developed and built by northern countries such as Canada, Russia, Finland, USA, and others.

In 2007, the Northwest Passage, in the Canadian Arctic, opened during the summer to ships without the need of an icebreaker escort. In 2013, the first commercial cargo ship made a transit of the Northwest Passage. Recently the Northern Sea Route in the Russian Arctic has seen a higher degree of success, opening shipping traffic to foreign vessels seeking shorter transit times on international voyages. In the offshore industry, natural resource production in the Arctic has been occurring for some time. The first offshore oil in the Arctic was produced in Prudhoe Bay in the late 1970s and pumped to shore via a pipeline. In 2014, for the first time in the Russian Arctic, offshore oil was produced, offloaded, and shipped via shuttle tanker to Europe. Offshore exploration is actively taking place throughout the Arctic, with plans for production in various regions. With this trend of increased activity in Arctic waters, there is great interest and investment in

improving the associated technology to operate and explore these remote and harsh regions safely and efficiently. The design of polar ships and structures is one particular area where technology is progressing forward and research and development efforts are advancing the state of the art.

## 1.2. Development of Icebreakers and Ice Class Rules

The first ship designed for icebreaking operations was *City Ice Boat No. 1*, a wooden paddle boat built for the city of Philadelphia in 1837. The Russian *Pilot*, built in 1864, was an iron hulled icebreaker with a rounded hull used to push up onto the ice and break it in bending. This ship is the predecessor to the modern icebreaker. Leading into the early 20th century, ice breaking ships were built by various northern countries.

### 1.2.1. Finnish-Swedish Ice Class Rules

The Finnish government was the first to introduce regulations for ships in ice, in 1890. The first Finnish rules for the strength of ship hulls operating in the Baltic sea during winter months were released in 1920, using the "percentage rule" system, meaning that the scantlings for ships operating in ice had to be some percentage increase over those of ships operating in open water. It was not until 1971, with the release of the Finnish-Swedish Ice Class Rules (FSICR), that the results of ice damage surveys (Johanssen, 1967) were used to estimate ice load magnitudes on ships. Design ice pressures were established for each ice class. Together with engineering equations, structural requirements, and new requirements for machinery systems were introduced. An

interesting and comprehensive technical review of the long-term development of the FSICR can be found in Riska & Kamarainen (2013).

### 1.2.2. Classification Societies

The regulation of ship structure design for ice class ships in general has been evolving for more than 100 years. Historically, different classification societies developed empirically-based rules based on experience gained from their classed fleets. The majority of this experience was isolated to geographical regions where the individual classification societies were most active. More recently, however, classification societies have very much become international organizations; and with the formation of the International Association of Classification Societies (IACS) in 1968, classification rules continue to converge and harmonize towards unified requirements.

### 1.2.3. Polar Class Structural Rules

A multi-year joint research effort by IACS member societies and other coastal state authorities began in 1992 and led to the development of the IACS Unified Requirements Concerning Polar Class (UR I1, I2, and I3). The new harmonized rule set came into effect in 2008. The structural rules (UR I2) work in a hierarchical manner. First, the expected operating condition dictates what *Polar Class* an owner should select for a ship. There are 7 Polar Classes, ranging from PC1 to PC7. PC1 classed ships are intended to operate year-round in all polar waters, and PC7 ships should be limited to summer operation in thin first-year ice which may include old ice inclusions.  Based on the expected conditions, the design ice loads can be derived from a design scenario, which is a

3

glancing collision with an ice edge. Using energy methods, based on ice indentation and collision mechanics, the ice pressure under the design scenario can be calculated. Various *Class Factors* include assumptions about ice strength properties, interaction parameters, ship hull form, and hull areas which establish the strength levels for each polar class. Using these class factors, ice pressure values and line loads can be developed, which are used to generate the width and height of the horizontally-oriented ice design load patch. Once the ice load parameters are established, they are coupled with strength formulations for framing and plating which set the minimum scantlings.

The current polar structural rules are based on a combination of analytical analysis, finite element (FE) analysis, and experience with existing rules and ships. The derivation of plastic framing requirements for polar ships has been well-explained (Daley, 2002). As well, several practical methods of the application of plastic framing requirements for polar ships have been presented (Daley, 2002).

### 1.3. Ship Structure Design

At a basic level, the shell of a ship is a stiffened plate structure, with an outer steel plate that is reinforced and strengthened by transverse and/or longitudinal members. This reinforced plating is designed to have the highest strength to weight ratio possible while meeting strength criteria, as required by classification societies.

#### 1.3.1. Plastic Limit-state Design

Classification societies have recently been moving towards a plastic limit state design approach for ice class structural rules. This is based on the fact that complex structures

4

have enormous reserve strength in plastic deformation beyond initial yield. Instead of designing structures to limit stresses below a certain level under design loads, the structure is designed to undergo a prescribed structural response under design loads. Paik (2006) has some discussion of the limit states design of ships and offshore structures. Figure 1-1 shows a typical stress-strain curve for tensile testing of structural steel. Figure 1-1 is actually taken from tensile tests described later in this thesis. It can be seen that the ultimate strength of the material is not substantially higher than the yield strength, and while there is a lot of energy absorbed in the plastic deformation, there is limited reserve capacity in terms of stress beyond the point of yield.
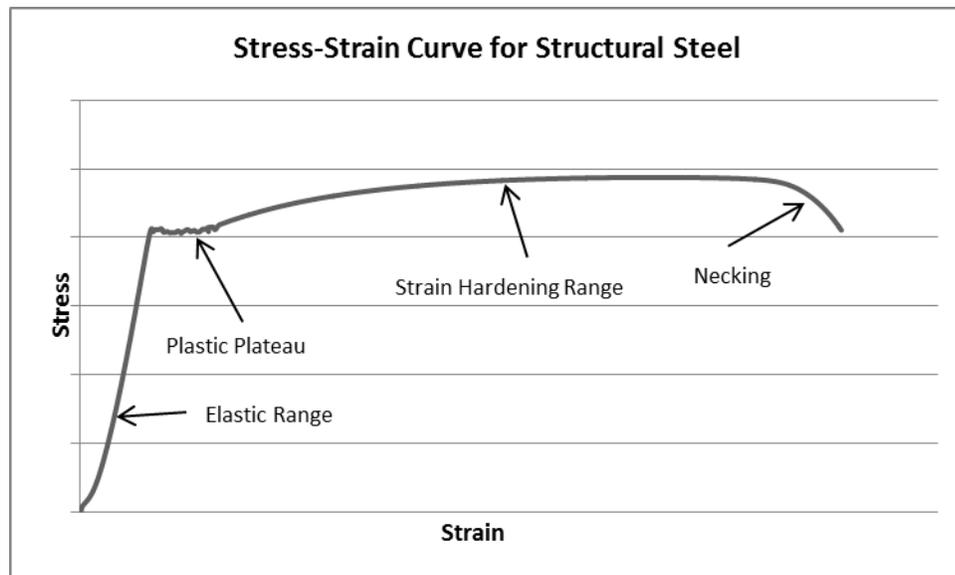


**Figure 1-1: Typical stress-strain curve for structural steel**

In contrast, Figure 1-2 shows a load-deflection curve for a stiffened panel structure. It can be seen that there is great reserve strength beyond the point of yield. In fact, the majority of the loading capacity of a stiffened panel is in the plastic range. Plastic-limit state

5

design acknowledges that designing against yield criteria (meaning keeping the stresses under a prescribed yield stress under design conditions) produces an extremely conservative structure.
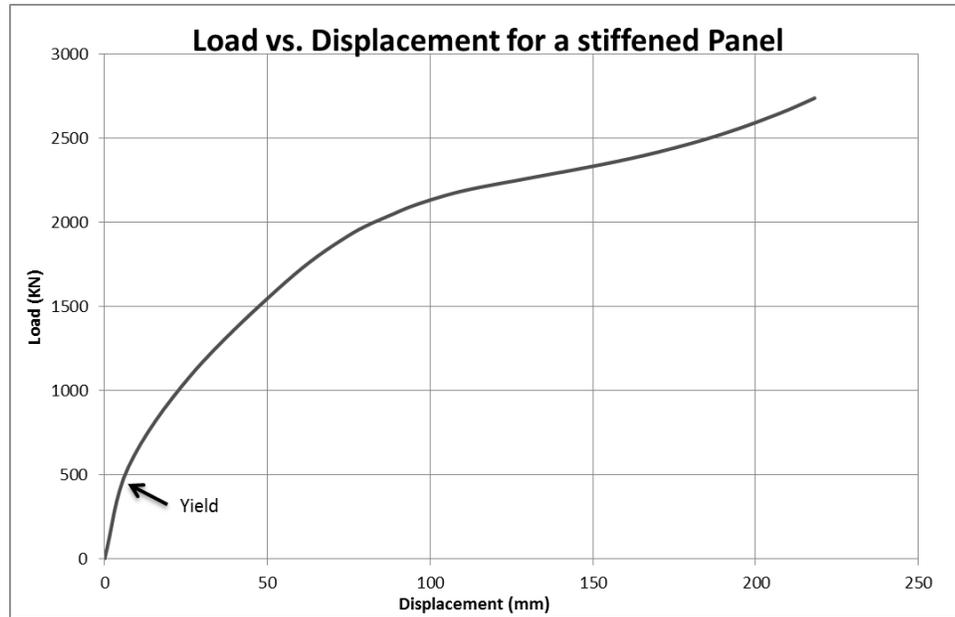


**Figure 1-2: Load-displacement for a stiffened panel**

The International Association of Classification Societies (IACS) has developed universal rules for polar class ships that utilize plastic limit state design. The structural reserve strength is being taken into consideration in the class rules, so some plastic deformation is expected and considered acceptable (Daley, 2002). This approach allows for significantly lighter structures, which in turn, are less expensive to manufacture. Daley et al. (2007) provides a discussion of current structural design rule practices.

6

### 1.3.2. IACS Unified Structural Rules in Practice

A hull structure for a ship exists globally as a stiffened shell, and locally as a stiffened panel. The shell plating is stiffened by transverse and longitudinal local frames, load-carrying stringers and web frames. Based on the design ice loads, as explained above, the design engineer must meet the IACS Structural Requirements, which include:

- Shell plate requirement; specifying the minimum thickness

- Main Frame Requirement; shear area, plastic section modulus and stability criteria

- Web Frame Requirements, which must be dimensioned such that the combined effects of shear and bending do not exceed the limit state defined by the Classification Society. This results in the web frames being required to meet a minimum shear area and a minimum net effective plastic section modulus. Web frames must also meet the structural stability requirement, specifically the maximum slenderness ratio requirements for Tee, L, and bulb shaped sections

- Stringer member requirements, which follow the same requirements as the web frames

### 1.4. Ice Mechanics

While this thesis focuses mostly on the analysis of ship structural response to ice loading, the mechanics of the ice need be understood. Much work has been done in ice mechanics. A common test to provide insight into the strength of ice is the uniaxial compression test. Crushing a cylinder of ice to the point of failure has shown that ice is a very complicated, anisotropic material. Its strength depends on many factors including temperature, salinity,

grain size, grain orientation, as well as strain rate. Other tests have been done to determine the strength of ice, such as direct and ring tensile tests, four-point beam bending tests, and cantilever bending tests. At Memorial University, research in conical ice tests has been ongoing for several years. These tests include ice cone compression tests, ice cone-structural loading tests, and ice cone friction tests. This research has provided significant data for the investigation of the pressure-area relationship during an ice loading event. Full-scale ice ramming tests have been done on various ice breakers to study the local pressure distribution during ice loading.

## 1.5. Ice-Structure Interaction

During an ice loading event on a structure, the ice being forced against the structure will have areas of high pressure and areas of low pressure, with these areas changing constantly as the ice experiences cracking and spalling events in the high pressure areas, effectively changing the contact area and creating new localized areas of high pressure. Figure 1-3 illustrates the key components of ice-structure contact.
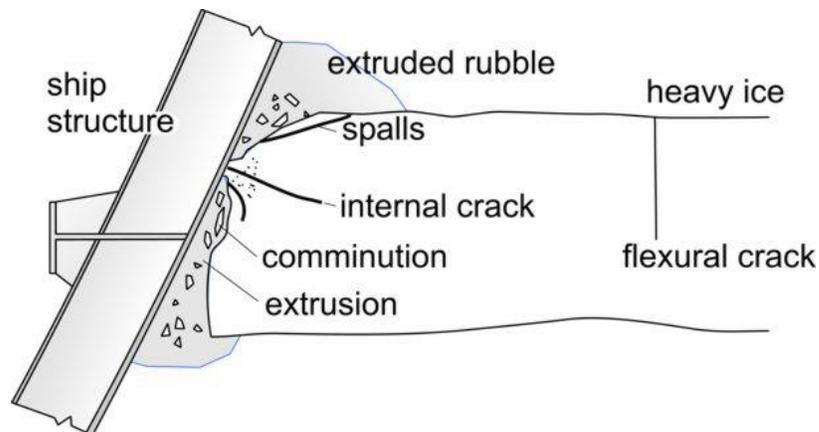
**Figure 1-3: key components of ice-structure contact. Taken from ENGI 8074/9096 notes, CG Daley.**

The nominal pressure (ie. total force divided by total area) during ice loading is easy

enough to determine, however, the true pressure at any given point in the loading area is

likely either much higher, or much lower than the nominal pressure.

Spatial pressure during an ice loading event describes the distribution of pressure over the

ice contact area at a given instant in time, and can be very hard to determine. The spatial

pressure-area relationship during an ice loading event can be estimated by an array of

pressure panels. However, there is a limit to the resolution of any pressure panel array,

and the as-measured pressure is a best estimate of the true pressure distribution. An

accurate estimate of the spatial pressure-area relationship is important in determining

localized loads on a structure. Figure 1-4 illustrates the difference in nominal, true, and

as-measured pressures during an ice loading event.
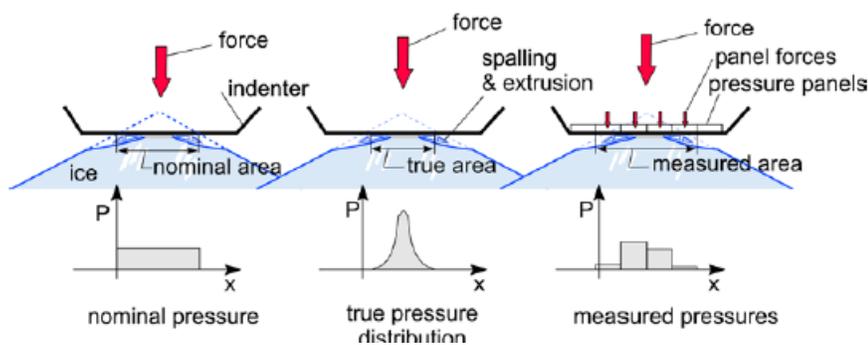


**Figure 1-4: Nominal, true, as-measured ice pressures. Taken from ENGI 8074/9096 notes, CG Daley.**

9

The process pressure-area relationship describes how the average pressure changes during an ice loading event. The process pressure area is used to determine the total force during ice loading, which is important for the global design of structures for an ice environment. Daley (2004) thoroughly discusses the link between spatial and process pressure area relationships based on full scale measurements.

## 1.6. Background of Research

Physical, analytical, and numerical research in the area of the plastic response of ship structures has been ongoing at Memorial University for quite some time now. The physical experiments have evolved from investigating the plastic response of single ship frames loaded with steel indenters (Daley et al, 2003), small stiffened panels (grillages) loaded with steel indenters (Butler, 2002), large grillages loaded with steel indenters (Abraham, 2008), and finally, in the work described in Chapter 3 of this thesis, large grillages loaded with ice cones.

## 1.7. Research Objectives and Scope of Work

The purpose of this work is to add to the understanding and knowledge of the plastic response of stiffened panel structures to ice loading. Through full-scale tests and numerical modelling, this thesis discusses the plastic capacity of ship structure during ice loading events.

The objectives of the research undertaken in this study are:

- Objective 1: Perform full-scale laboratory experiments of ship structure being quasi-statically loaded with ice blocks at extreme load levels.

10

- Objective 2: Develop high-fidelity numerical models of the full-scale laboratory experiments, validating the numerical modelling techniques.

- Objective 3: Develop numerical models to predict the response of IACS Polar Class ship structure to ice loading under design, and overload conditions.

- Objective 4: Compare the relative strengths of IACS rule-compliant ship structure with four different stiffener types.

These objectives will be realized by performing laboratory experiments and by developing numerical models that will demonstrate the accuracy of the methods through comparison with physical results. Finally, based on the validated numerical model, the work will be extrapolated to analysis of a realistic ship framing exercise. This work will demonstrate that full scale experiments on ice impacts can be accurately modeled using finite element methods, and that this FE analysis methodology can be subsequently employed to analyze alternative structural arrangements as a useful tool for optimizing icebreaking ship structural design.

The full scale, large grillage experiments described in this thesis are the first of their kind. In a laboratory setting, full scale ship structure is loaded quasi-statically with laboratory-grown ice blocks to extreme overloads, to several times the design load. The level of control and observation made during these tests greatly exceeds that which is practically possible in full scale real-world tests on vessels, while the scale of the tests provide a realistic indication of the true ice-structure interaction forces.

There are currently no analytical solutions to accurately predict the response of structure to ice loading. However, numerical analysis methods are continuously improving in

11

ability to predict structural response, and full scale laboratory experiments are used in this thesis to validate numerical analysis.

Numerical analysis is then used to estimate the capacity of stiffened panel response to ice loading, while comparing the capacity of different stiffener types. Tee, L, flat bar, and bulb flat stiffener cross sections are considered in a design scenario where each of the stiffener types is used in a similar configuration.

## 2. Large Grillage Ice Loading Laboratory Experiments

### 2.1. Experiment Overview

The large grillage experiments are a set of experiments that took place between November 2012 and April 2013. The goal of these experiments was to observe quantitatively and qualitatively the reaction of steel grillage structure during ice loading. During these experiments, ice cones were loaded quasi-statically into a steel grillage structure representative of full-scale ship structure. The experiment took place in a controlled environment in a laboratory setting. A total of four separate ice cones were loaded into a total of two steel grillage structures. Grillage A was centrally loaded with a single ice cone, in three loading steps. Grillage B was loaded with three separate ice cones in three separate locations.

The setup for these experiments includes a rigid (or nearly rigid) test frame that holds the grillage, a hydraulic ram, a cone of ice inside an ice holder, and a data acquisition system. The rigid test frame is constructed from large steel I-beams and thick steel plates. It is designed to hold the grillage via bolted connections. The frame is designed to experience

12

minimal elastic deflections during loading. Due to the forces involved being on the scale

of $10^6$ N, zero deflection of the holding frame is impractical to achieve, so the relatively

small deflection of the test frame is measured during experimentation. A 3D model of the

rigid test frame is shown in Figure 2-1.
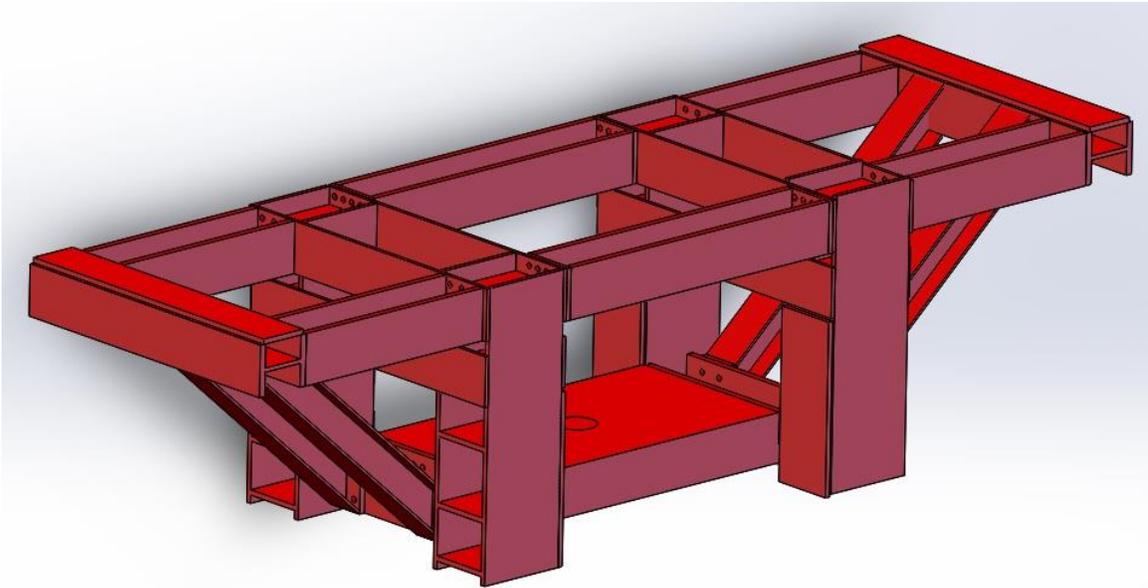


**Figure 2-1: Rigid test frame**

The ice cone samples can be described as a cylinder with a diameter of 1 m and a height

of 300 mm with a 30 degree conical tip on top of the cylinder. The mechanical properties

of the artificially grown ice cylinders have previously been investigated via controlled ice

crushing experiments using a high-resolution ice pressure panel at an earlier stage of the

STePS$^2$ project (Reddy et al, 2012). These previous ice crushing experiments determined

an effective ice growth method and a suitable cone tip angle. An ice cone ready to be

crushed is shown in Figure 2-2.

13

**Figure 2-2: Prepared ice cone**

The hydraulic ram used for loading the ice cone into the grillage is capable of a maximum force of approximately 2.75 MN, with a maximum stroke length of 450 mm. The grillage is representative of a full-scale ship structure. It includes a shell plate, two transverse frame members and three longitudinal stiffeners with the webs and flanges of the stiffeners having T cross-sections.

## 2.2. Grillage Design

The two grillages were designed to closely resemble polar class ship structure while experiencing a suitable amount of deformation from the applied load. The grillages were fabricated by Memorial University Technical Services. The driving factors of the design are as follows:

- The grillage must fit onto existing rigid test frame, matching the existing bolt hole pattern;

14

- The grillage must experience a reasonable amount of elastic and plastic deformation while being loaded to the maximum capacity of the in-house hydraulic system, which has the capability of delivering approximately 2750 kN force;

- The grillage must resemble IACS polar class structure; and,

- The grillage must be loaded to several times the design point for Baltic ice rules, and IACS Polar Class rules.

The grillage, as designed, closely resembles a frame span for a longitudinally framed IACS PC7 structure at the midbody ice belt of a 10,000 tonne vessel. A reasonable design load for this particular grillage is about 500 kN, and it is to be loaded to more than 5 times that amount.

The grillages consist of shell plating, two transverse web frames, three longitudinal T-stiffeners, two longitudinal side stiffeners, and a mounting configuration at the longitudinal ends of the structure. An unmounted grillage is shown in Figure 2-3. The final dimensions of the large grillage are depicted in Figure 2-4.

**Figure 2-3: Undeformed grillage**

**6756**

**6036**

360 · 2000 · 18 · 2000 · 18 · 2000

2420

30

1440

30

A

B

B

A

C

C

Large Grillage
Top View



75 x 10

100 x 30

200 x 8

10

4 @ 350 = 1400

Section A-A    Grillage X-section



18

2420

120 x 18

Cutout Detail 'A'

325

325 x 18

cutout
90 x 30

480   376   350   350   354   30   480

Tie Detail (LG-3)

Section C-C   Stringer
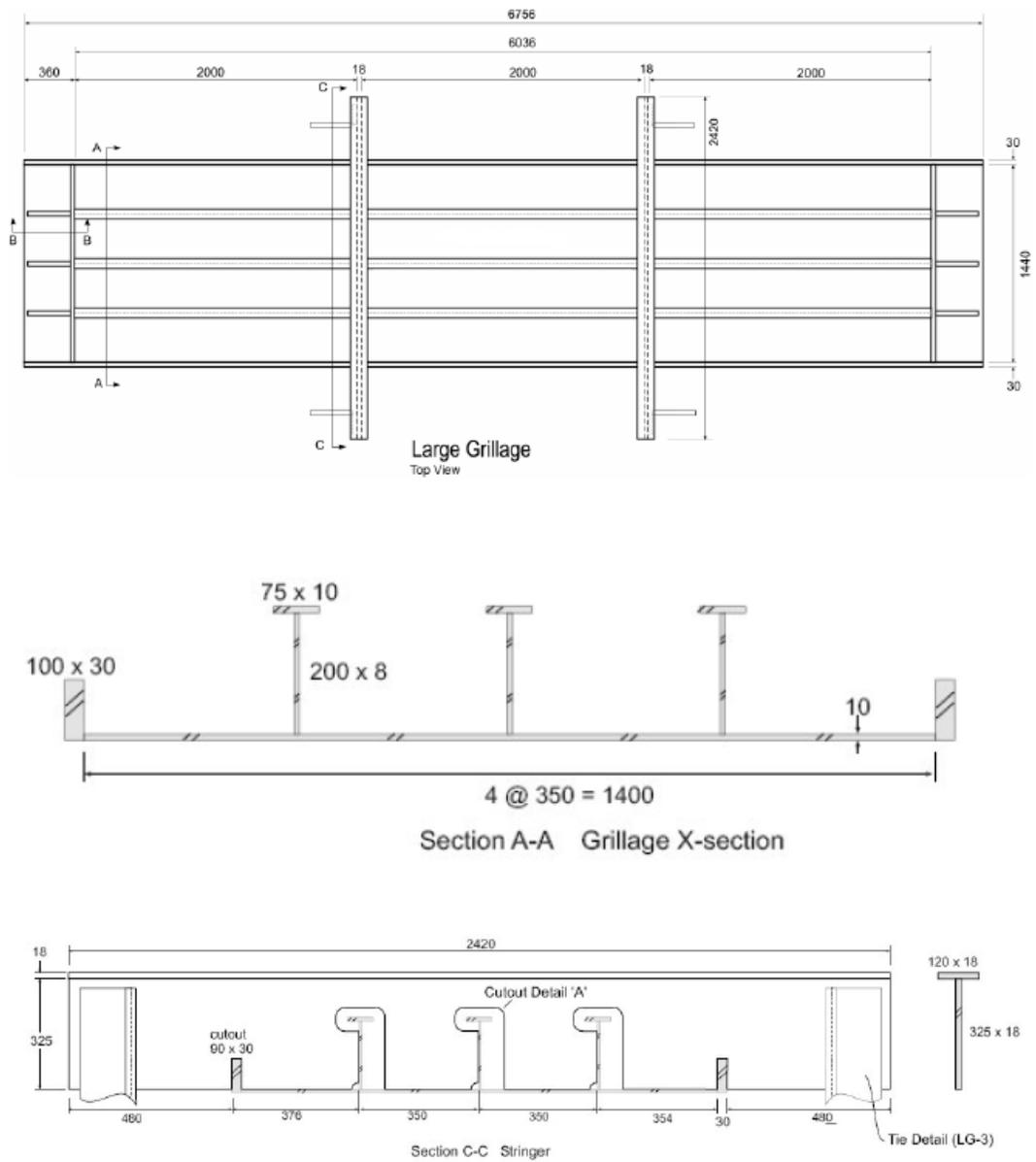
**Figure 2-4: Large grillage dimensions**

17

### 2.3. Ice Cone Design & Construction

The ice cones used for the experiments are based on the results from earlier STePS[2] experiments where ice cones of different properties were loaded into a high-resolution pressure panel (Reddy et al, 2012).

### 2.4. Ice sample Growth

The ice cones are prepared through a series of steps. First, ice cubes made from purified water are crushed in a commercial ice crusher, producing ice chips between 1/8" and 3/8" in diameter. Enough chips to produce an ice cone are made and stored at -10°C temporarily. These ice chips are then mixed with 0°C water at an ice chip volume to water volume ratio of 2:1. This mixing process is done inside the ice cone holder with a removable extension attachment to provide the height required for the cone tip. The cone tip is roughly formed by a top piece that is constructed out of insulating foam. This piece decreases freezing and shaping time of the ice sample, as less ice chips are required to form the shape of the ice cone compared to if a cylinder shape was initially used. The mixing process takes place at an ambient temperature of -10°C. During the mixing process, water and ice chips are evenly poured over the mixture while the mixture is stirred to ensure even mixing and to prevent surface layers from freezing before the mixing process is completed. Once the ice-water mixing is complete, the sample is kept at -10°C for a minimum of 96 hours for freezing.

## 2.5. Ice cone shaping

The 30 degree angle cone tip is formed through machining of the rough ice cone on a custom shaping machine. The shaping machine is a device that spins the ice sample at a constant rate, while a blade is lowered and shaves off ice until a 30 degree cone tip is formed on the ice sample. The ice sample is turned by an electric motor and the blade is lowered using a manual crank and worm gear.

When the ice sample is shaped, it is placed back in the holder and stored at -10°C until it is tested during a grillage experiment.

## 2.6. Experimental Setup

The instrumentation for data acquisition included several components. The first is the string potentiometers. Six in total, these string potentiometers are used to measure the deflection of the rigid test frame during experimentation, as well as measure the stroke of the hydraulic ram. There are two string potentiometers attached to each end of the rigid test frame. The instrument housing is secured to the concrete laboratory floor, while the end of the wire is secured to the rigid frame using a magnet. The ram stroke is measured in a similar way. The plate that the hydraulic ram is positioned on has its vertical deflection measured from underneath using a string potentiometer. An ice cone, loaded onto the ram, and ready for testing is shown in Figure 2-5.

19

**Figure 2-5: Ice cone mounted on hydraulic ram, ready for experiment**

The load is calculated using a pressure gauge on the hydraulic ram.

To measure the strains in the grillage, a total of 74 strain gauges are mounted to the grillage surface. The strain gauges are arranged to measure strains at critical points on the grillage. In order to get multi-directional strain measurements, both linear and rosette-configuration gauges are used. The strain gauges are mounted to the grillage using epoxy adhesive.

One linear variable differential transducer (LVDT) is used on the grillage to measure the vertical deflection of the middle stiffener. The LVDT is positioned above the grillage on a free-standing instrumentation over-frame. This frame provides a stationary, independent datum from which to measure the stiffener deflection.

20

The data from the string potentiometers, LVDT, and strain gauges is recorded in a data acquisition system in a text format.

A Microscribe® is also used to measure the before-and-after grillage form. The Microscribe® is a three-jointed arm that uses optical encoders in the joints to accurately measure the position of the scribe tip in three dimensional space. When the user chooses, the point in space is recorded in a 3D CAD program. Each recorded point on the grillage is recorded both before and after the experiment to create accurate 3D models of the grillage both undeformed and deformed.

The experiment is also recorded through four high speed cameras at a frame rate of 120 frames per second. As well, a DSLR camera takes time-lapse photos during intervals throughout the experiment.

## 2.7. Experimental Procedure

The experimental procedure involves many small steps. Planning and practice are essential to a successful experiment, especially considering the time sensitive nature of the ice cone to the above-freezing temperatures in the laboratory where the experiments take place.

The ice cone and instrumentation are prepared before the test takes place. The ice cone is prepared and stored in a refrigerated room until the experiment. On the day of the test, all cameras are tested, and instrumentation is calibrated. Once this is done, the ice cone is removed from the cold room, and brought into position using a fork lift in combination with an overhead gantry crane. The cone is placed on the hydraulic ram and secured via

21

bolted connections. Safety chains are attached to the ram. The hydraulics are started and a final instrumentation and safety check is carried out before the experiment begins.

## 2.8. Results

The results in this thesis include deflection data from the LVDT and force data from the hydraulic ram. The Microscribe® was used to validate the starting and final deflection of the grillage. Strain gauge data was recorded during all tests; however that data is not included in this work.

### 2.8.1. Grillage A

Grillage A was loaded at the center with a single ice cone, in three steps. The first step was to pretest the setup by applying a "setting load" to the grillage. This setting load was designed to stress the grillage to the onset of plastic yield. This provided an opportunity to test all of the instrumentation prior to subjecting the grillage to significant plastic deformation. Test 1 used the full stroke capacity of the ram to deform the grillage, but did not reach the maximum force capacity of the ram. After raising the base of the ram, during Test 2 the ram was used to produce its maximum force. Figure 2-6 shows Grillage A under maximum deflection, during Test 2.

**Figure 2-6: Grillage A at maximum deflection**

### 2.8.1.1.    Grillage A, Pretest

The ice cone was pressed into the grillage at a rate of 0.3 mm/s up to a load of 393 kN,

and the load was subsequently reduced back to zero. Raw load-displacement data is

shown in Figure 2-7. The load value is taken from the hydraulic ram, while the

displacement value is obtained with the LVDT. The deformation therefore represents the

vertical deflection of the center of the flange at the midpoint of the middle stiffener.
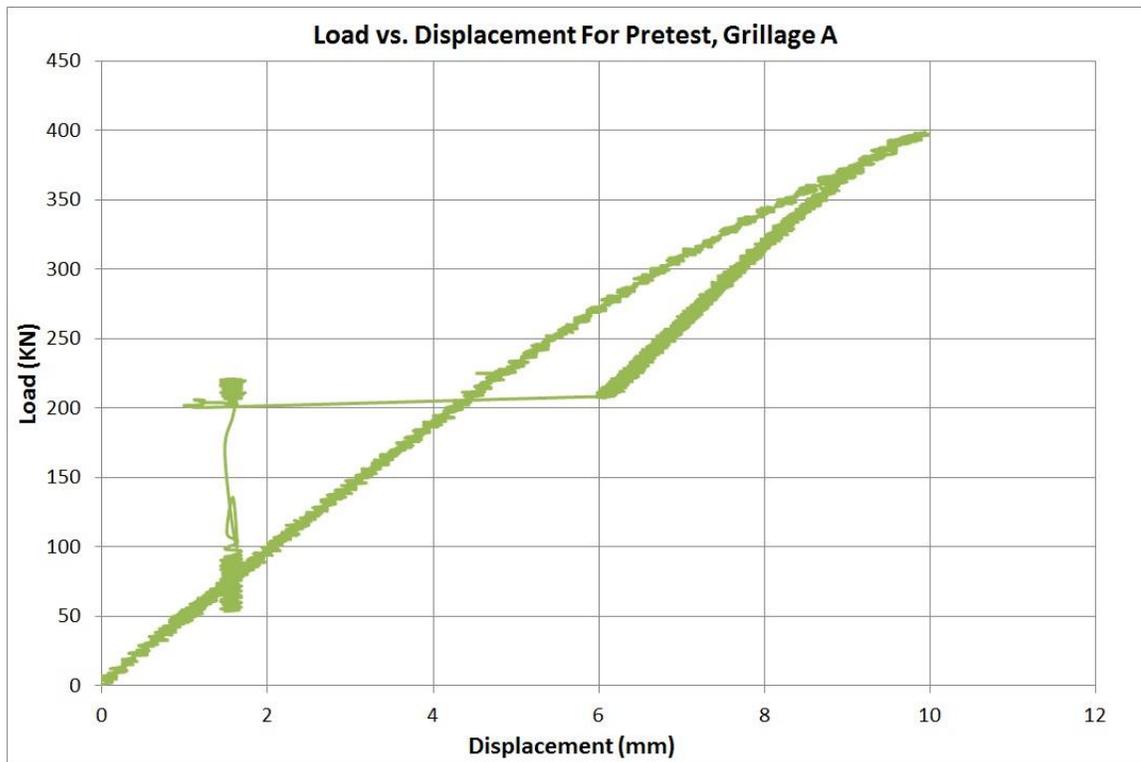
**Figure 2-7: Load vs. displacement for pretest, grillage A**

During the unloading of the grillage, as the displacement reaches 6 mm, the displacement suddenly drops, while the load is held constant. This is due to error in the hydraulic control and pressure measurement. It is common to all of the grillage tests that while unloading, at around 200-210 kN, the load is erroneously recorded while the displacement suddenly drops. Figure 2-7 should actually have a trend in the unloading phase having the same slope as the elastic portion of the loading phase.

It can be seen in Figure 2-7 that the slope of the unloading phase is steeper than the slope of the loading phase. This demonstrates that, in addition to strengthening through strain hardening, the grillage has become stiffer as a result of the plastic deformation.

24

The pretest produced an elastic deformation of 9.9 mm and a plastic deformation of the grillage of 1.6 mm.

### 2.8.1.2. Grillage A, Test 1

The same ice cone used for the pretest was used for test 1. The plan for this test was to push the hydraulic ram to the extent of its stroke, or to the hydraulic force limit. The results from Test 1 are show in Figure 2-8.
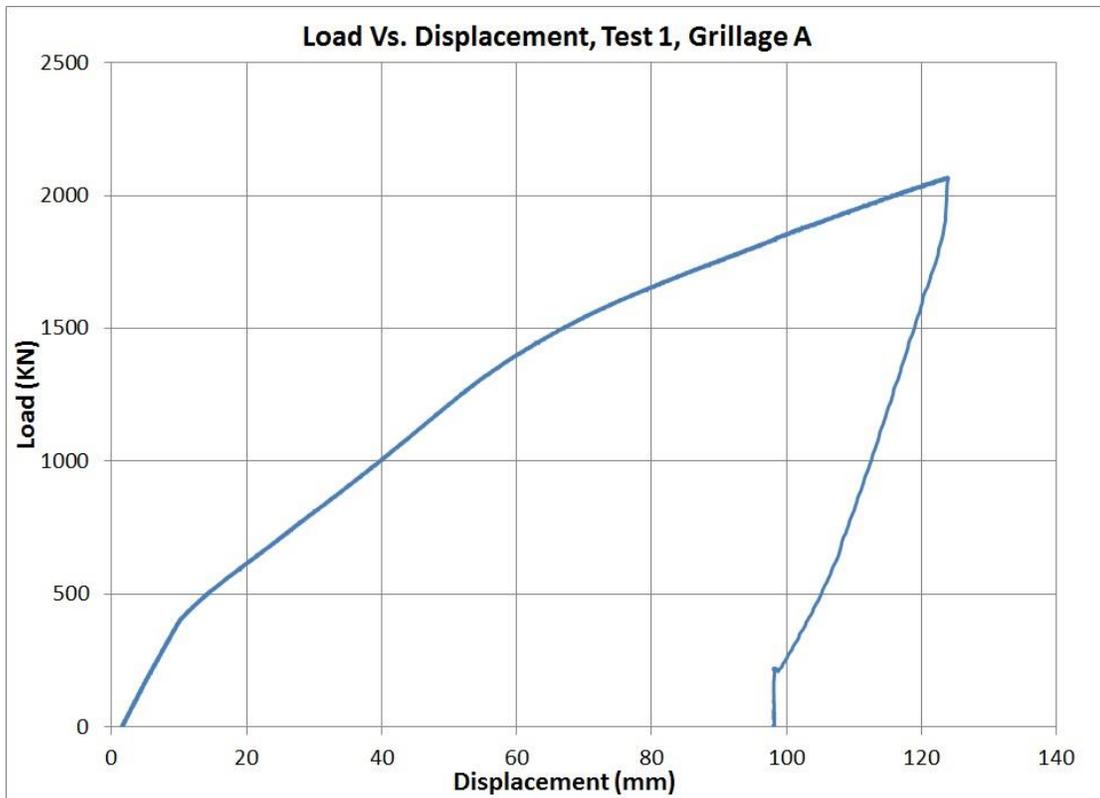


**Figure 2-8: Load vs. displacement, test 1, grillage A**

The test starts with the grillage plastically deformed 1.6 mm due to the pretest. The grillage is then loaded up to 2069 kN, and then the ram is reversed at the same rate as

when the load was being applied. The ram was loaded to the point of maximum stroke. This test was stopped because of the limitation of the hydraulic ram stroke, and not due to any issues with the grillage or other parts of the experimental setup.

Similar to during the pretest, it can be seen in Figure 2-8 that the slope of the unloading phase is steeper than the slope of the loading phase. This demonstrates that, in addition to strengthening through strain hardening, the grillage has become stiffer as a result of the plastic deformation.

Test 1 produced an elastic deformation of 123.8 mm from the original undeformed shape of Grillage A, and a plastic deformation of 98.3 mm. The same error is seen in Figure 2-8 as in Figure 2-7 during the unloading phase.
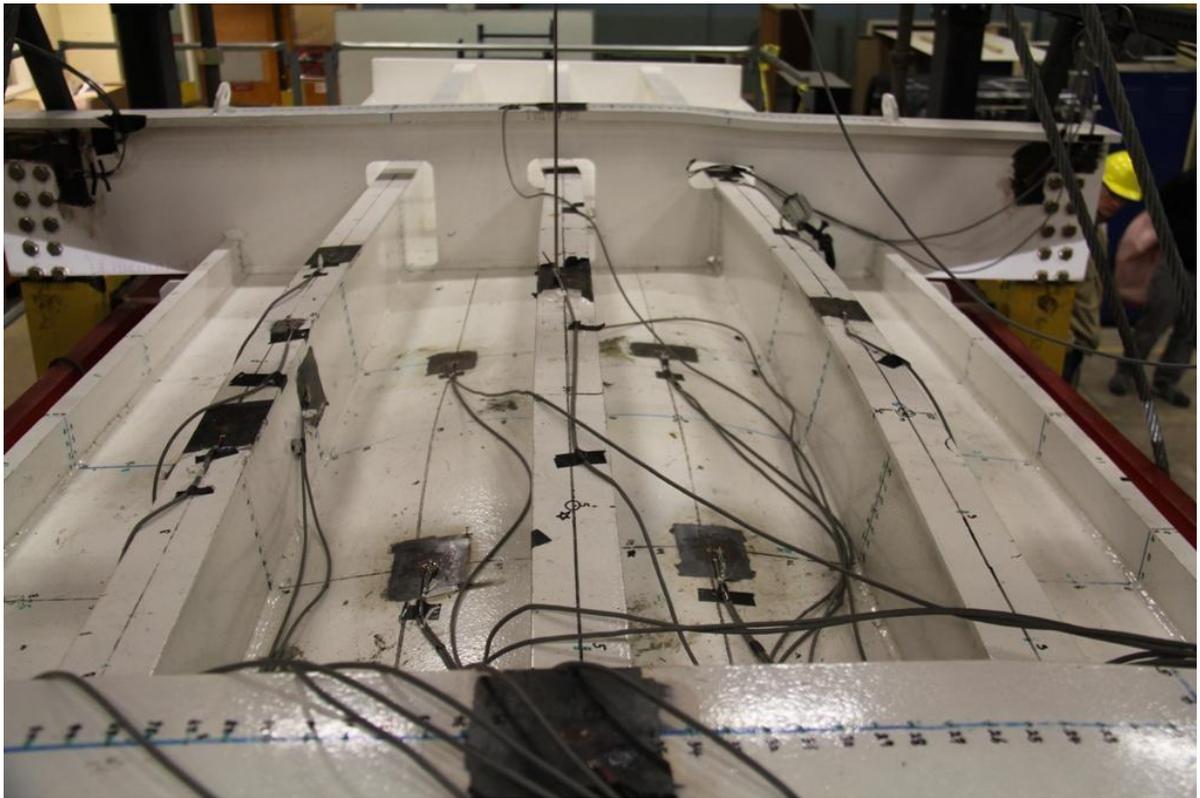


**Figure 2-9: Deformation of grillage A after test 1**

Figure 2-9 depicts grillage A after test 1. Obvious deflection of the shell plating and web frame can be seen. It is also seen that the stiffener flanges are no longer straight.

### 2.8.1.3.    Grillage A, Test 2

With test 1 being ended due to the hydraulic ram reaching the extent of its stroke, for test 2 several steel plates were placed underneath the ram to extend the stroke. The results of Test 2, Grillage A are shown in Figure 2-10. It should be noted that Figure 2-10 is not entirely a direct plot of raw LVDT data. During Test 2, from loads of 2410 kN to 2470 kN, the flange of the center stiffener began to fold, causing the apparent displacement to remain constant while the load continued to increase. At this point, the LVDT probe fell from the stiffener and onto the shell plating of the grillage. The data used to produce this plot was modified to compensate for the sudden drop of the LVDT probe, so the event of the probe falling from the flange onto the shell plating is not represented, while the folding of the flange is represented by the sudden vertical trend in the curve at 2410 kN.

**Figure 2-10: Load vs. displacement, test 2, grillage A**

The test began with the grillage in a permanently deformed state with 98.1 mm of permanent plastic vertical deflection. The ice cone was raised into the grillage at a rate of 0.3mm/s, up to a maximum force of 2728 kN. This is the maximum force that the hydraulic ram is capable of delivering. Test 2 caused a total deformation of 219.2 mm. There was an error in the force-displacement data at this point, so the unloading phase is not shown in the plot.
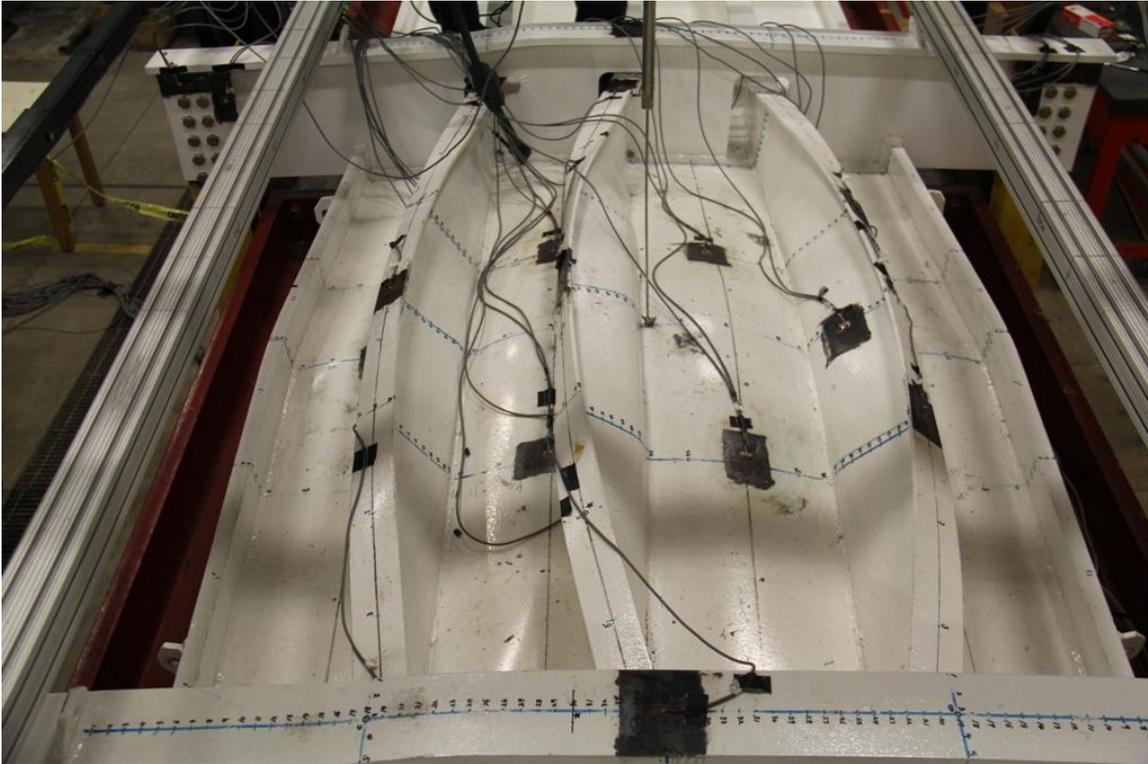
**Figure 2-11: Final shape of grillage A**

Figure 2-11 shows Grillage A after Test 2. The webs of the stiffeners have folded over

significantly, the web frames have deformed significantly, and the shell plating is now in

a dome shape. There was also possible cracking of welds in some locations. The most

severe apparent crack is depicted in Figure 2-12 below.
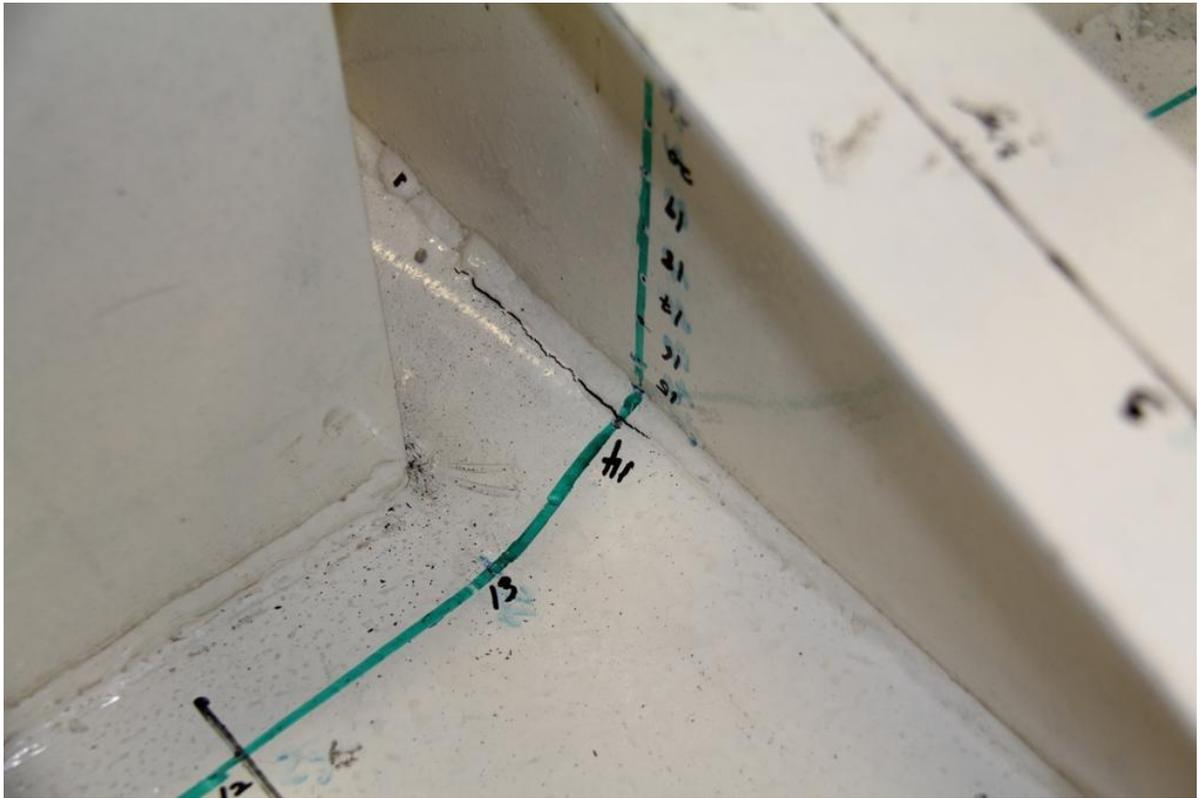
**Figure 2-12: Possible crack in shell-stiffener weld on grillage A**

A plot of the combined loadings of Grillage A is shown in Figure 2-13. It can be seen that the curves for the tests correlate very well. A significant amount of strain hardening is displayed between tests 1 and 2. The slope of the elastic portion of test 2 lines up very well with the unloading portion of the Test 1 curve.

**Figure 2-13: Load vs. displacement, grillage A**

### 2.8.2.   Grillage B

Grillage B is identical to grillage A. However, unlike grillage A which was centrally

loaded with a single ice cone, grillage B was loaded in three separate locations with three

separate ice cones. During test B1 (grillage B, test 1), the grillage was loaded with an ice

cone in the "South" (North and South were used to designate the longitudinal directions

of the grillage, as the grillage was mounted in a north-south orientation in the laboratory)

end of the center span between the web frames. During test B2, it was loaded in the center

of the center span with an ice cone. During test B3, it was loaded in the "North" end of

the center span. This loading pattern was done in part to mimic a more realistic "moving"

31

ice load moving along a stiffener between two web frames. The grillage was loaded to get an equal amount of vertical plastic deformation at the locations of center of loading of the three ice cones used.

### 2.8.2.1. Grillage B, Test 1

This test consisted of loading a new ice cone into the grillage shell plating at a location close to the South end of the main span between the grillage web frames, on the central test stiffener. The load and deformation of the grillage during test B1 is shown in Figure 2-14. The lack of linearity through the first 100 kN loading should be noted.
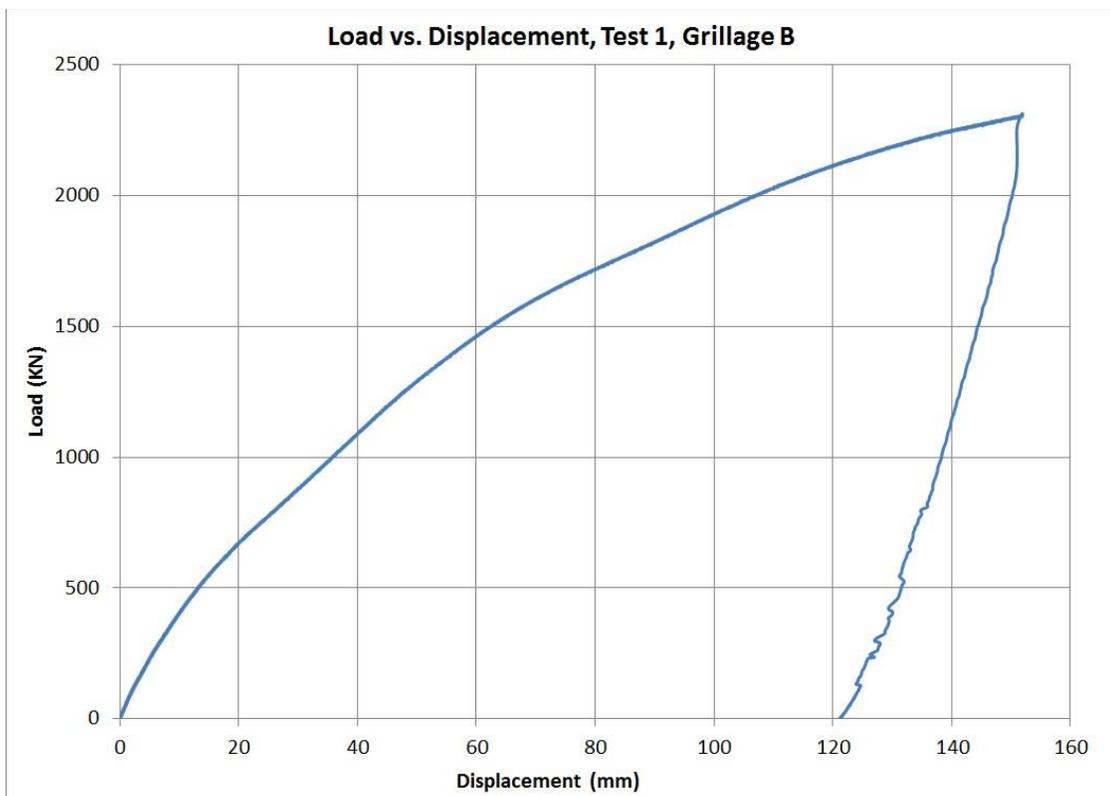


**Figure 2-14: Load vs. displacement, test 1, grillage B**

It can be seen in Figure 2-14 that the grillage experiences a total deformation under load of 151.8 mm and a total plastic deformation of 121.4 mm. This deformation was measured using the LVDT as the vertical displacement of the center test flange at the location of the center of loading (directly above tip of ice cone).  The maximum load applied by the hydraulic ram was 2314 kN. It can be seen in Figure 2-14 that there is some error in the unloading phase of the test as the load is reduced. This is caused by issues in the hydraulic pressure monitor.

### 2.8.2.2.    Grillage B, Test 2

Test B2 consisted of loading a new ice cone into the grillage shell plating at the center of the main span of the grillage, centered on the center test stiffener. The load and deformation of the grillage during test B2 is shown in Figure 2-15.

**Figure 2-15: Load vs. deformation, test 2, grillage B**

It can be seen in Figure 2-15 that the test begins with the grillage already plastically deformed 101.7 mm at the point of measurement. This plastic deformation was caused by Test 1. During Test B2, the grillage experiences a total elastic deformation (compared to the original undeformed shape) of 143.1 mm, and a total plastic deformation of 121.4 mm. This deformation was measured using the LVDT as the vertical displacement of the center test flange at the location of the center of loading (directly above tip of ice cone). The maximum load applied by the hydraulic ram was 2066 kN. Test B2 had a similar error to previous tests during the unloading phase. The final displacement, however, is correct and was confirmed by post-test measurements.

34

### 2.8.2.3. Grillage B, Test 3

Test B3 consisted of loading a new ice cone into the grillage shell plating at the North end of the main span of the grillage, centered on the center test stiffener. The load and deformation of the grillage during test B3 is shown in Figure 2-16.



**Figure 2-16: Load vs. displacement, test 3, grillage B**

It can be seen in Figure 2-16 that the test begins with the grillage already plastically deformed 91.1 mm at the point of measurement. This plastic deformation was caused by Tests B1 and B2. During Test B3, the grillage experienced a total elastic deformation (compared to the original undeformed shape) of 152.8 mm and a total plastic deformation of 125.2 mm. This deformation was measured, using the LVDT, as the vertical

35

displacement of the center test flange directly above the tip of the ice cone. The maximum force produced was 2257 kN. Test B3 had a similar error to previous tests during the unloading phase. The final displacement, however, is correct.

### 2.9. Conclusion

The large grillage test results provide practical, real-world information about ship-ice interaction. Testing full-scale ship structure in a laboratory setting allows for a level of control, observation, and data collection not possible (or impractically expensive) with a ship in an ice environment. To intentionally overload and significantly damage the structure of a ship in operation simply would not be practical.

These tests are useful as a validation of existing ship design rules. They provide insight to the actual ice load a ship can handle without sustaining catastrophic structure failure (ie tearing or puncture of the shell plating). Although the structure was not pushed to the point of failure, and it is not known at what load level that might happen, it is a testament to the load capacity of these structures that they withstood several times the design load without failure.

The slope of the unloading phase is steeper than the slope of the loading phase. This demonstrates that, in addition to strengthening through strain hardening, the grillage becomes stiffer as a result of the plastic deformation.

A major limitation of these experiments is that due to the size, man hours, and cost involved, it was not possible to repeat the tests with more grillages to get more experimental runs. Ideally, the large grillage tests would be repeated several times to display some consistency of the structural response to the ice loading and explore the

effects of strain rate. As well, grillages with different stiffener types could be investigated to compare the performance of the stiffener types under identical conditions. Numerical analysis comparing grillage structures with stiffeners of different cross-sectional shapes is explored in Chapter 4 of this thesis.

A major drawback in using the LVDT as the main measure of real-time vertical deflection during the experiments is that the data may be somewhat inaccurate. This is due to the web of the centre stiffener (which is where the LVDT was measuring the vertical displacement) folding over. Figure 2-11 shows the folded over stiffener, with the LVDT resting on the shell plating.

## 2.10.  Recommendations

Having completed the large grillage testing program, it was observed that there are some areas in which it could have been improved.

The number of strain gauges used may have been excessive. Taking about four weeks per grillage, mounting and wiring the strain gauges was the most time consuming part of the experimental setup. There are millions of data points from the strain gauges during the tests and it is not yet clear if the strain gauge data is going to be used for any analysis of the experiments. It is certainly potentially useful data, but it may not be used.

While not included in this thesis, the Microscribe® was used as a tool to gather confirmation of the displacement data obtained by the LVDT, as well as to provide a detailed outline of the shape of the stiffeners, showing any buckling or twisting that would not be shown via LVDT data. A grid pattern was used to map the form of the entire grillage before and after every test. The number of data points collected may have

37

been significantly more than required. Reducing the number of data points collected would reduce the time required to complete the task and reduce the lag time between experiments.

A load cell on the hydraulic ram would be a necessary improvement for any future tests. Using a pressure gauge on the hydraulics proved to be insufficient for gathering accurate load data during the unloading phase of the experiments.

With respect to the experiments conducted on grillage B, it would be ideal to have a LVDT positioned above each ice cone position during all three tests. This would provide load-response data plots for the position of each cone for the three experiments.

## 3. Validation of Finite Element Analysis Using Large Grillage Results

Validation of the numerical analysis in this work is done by comparing the actual results of the large grillage experiments with the results of ANSYS finite element analysis of the grillage. A model representative of the large grillage was developed and subsequently analyzed in ANSYS. A numerical model of the Grillage experiment is used to validate the FE analysis described later in this thesis.

During the laboratory experiment, the real-time spatial pressure distribution was not (and could not have been) observed. As well, at no point during the experiments was the exact area of ice-structure interaction known. This makes the task of achieving a high-fidelity FE simulation of the experiments quite challenging. Without knowing how the loading area changes with time, or knowing how the pressure distribution changes with load level,

there is no way to exactly model the grillage experiments. Therefore, a reasonable

representation of the patch load size and pressure distribution within the patch size must

be made. Through preliminary FE analysis, while evaluating different circular patch load

diameters and pressure distribution patterns, it was decided that using a single, uniformly

loaded patch size would produce reasonable results. As well, it was the simplest way of

running the analysis, reducing computational time.

Inital FE model results are displayed in Figure 3-1. There was a great deal of variance in

the results based on the selected material properties. Using bilinear isotropic hardening

material properties, through changing the yield strength and the post-yield tangent

modulus, a large degree of variance in the results can achieved. Destructive material

testing was performed on samples of the steel used in the grillage to determine actual

material properties. This is discussed in the next section.
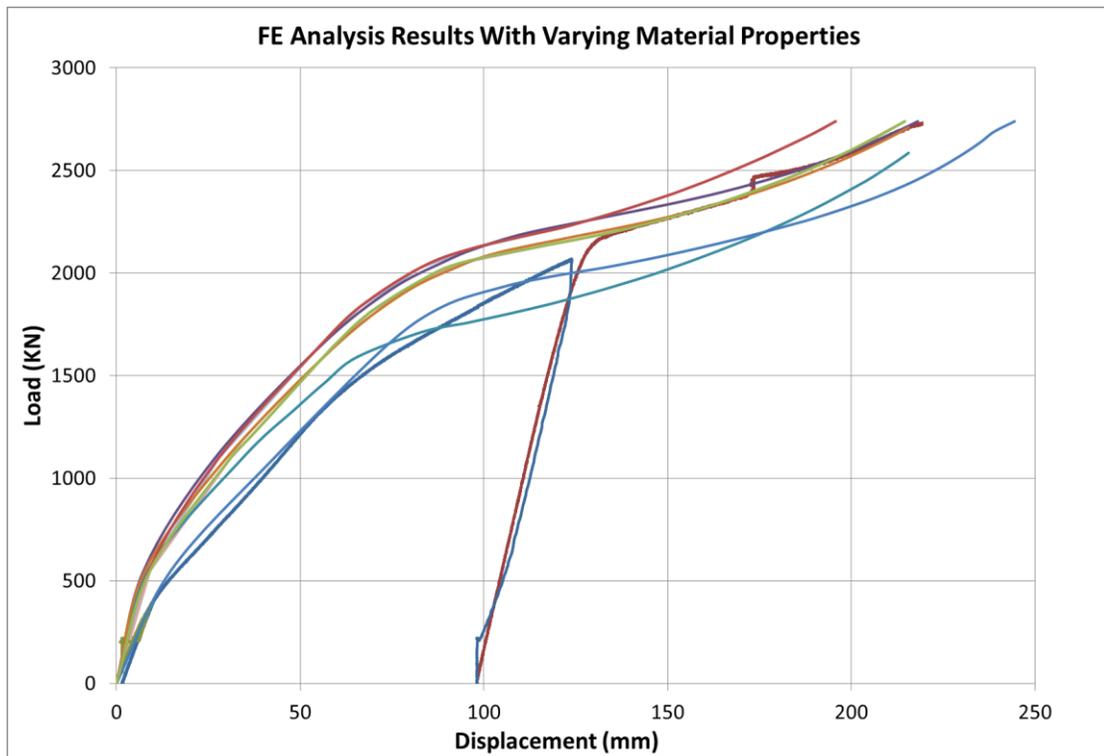
**Figure 3-1: FE analysis results using varying material properties**

## 3.1. Material Property Testing

The steel used to construct the large grillage was 350W shipbuilding steel. This steel has minimum required yield strength of 355 MPa. To ensure accuracy in the finite element analysis, tensile tests were carried out on samples of the steel used in the grillage. Steel was cut out of the shell plating in two undeformed areas of the post-experiment grillage structure. From these two specimens, a total of ten tensile coupon test specimens were cut. The tensile specimens were machined to ABS standards (ABS, 2012) and the tensile tests were carried out using an INSTRON testing machine. The testing setup is shown in Figure 3-2.

**Figure 3-2: Tensile testing setup**

A sample stress-strain plot is shown in Figure 3-3.
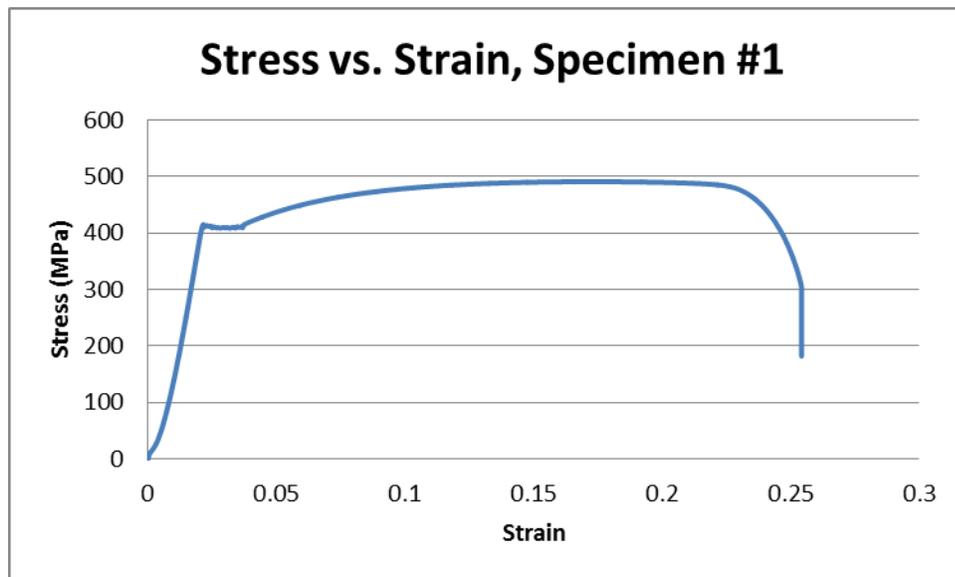


**Figure 3-3: Tensile test results from grillage steel sample**

41

The yield strength results are shown in Table 3-1. The average yield strength of the

specimen is 409.6 MPa. This is much higher than the specified  355MPa. The actual yield

strength will be used during the FE analysis.

**Table 3-1: Grillage steel tensile test results**

| Specimen | Yield Strength (MPa) |
|----------|----------------------|
| 1 | 413.3 |
| 2 | 413.3 |
| 3 | 405.8 |
| 4 | 405 |
| 5 | 408.2 |
| 6 | 406.4 |
| 7 | 411.5 |
| 8 | 405.8 |
| 9 | 412.2 |
| 10 | 414.3 |
| Average | 409.6 |

### 3.2. Model Construction

The large grillage 3D model was created using SOLIDWORKS, and imported into

ANSYS as IGES files. This was done due to the ease of modelling in SOLIDWORKS,

compared to using ANSYS DesignModeller to build the models.

42

### 3.3. Meshing

Solid elements were used for the FE analysis. It has been documented that while both solid and shell elements are suitable for estimating the capacity of a frame, the shape of deformation of stiffened panels is more realistic while using solid elements than using shell elements (Abraham, 2008). The drawback to using solid elements is in the fact that it is much more time consuming to run solid element simulations than to run shell element simulations.

Tetrahedrons were used for the mesh of the large grillage simulation. In ANSYS 14.0, the program automatically controls many of the meshing details by default, while the user has the choice to control any aspects of the mesh. The model is a solid assembly, which was exported as an IGES file using ANSYS SOLID186 element type. SOILD186 is a quadratic element with midbody nodes. Each edge has three nodes, so the SOLID186 element has 20 nodes per element. It can be generated in cubic, tetrahedron, and prism shapes.

It was ensured that all plates in the mesh had at least five nodes through the thickness, which means a minimum of a two-element thickness at all points. Finer meshes were used in critical locations of the grillage. To determine the ideal mesh sizing, a convergence study was carried out. This study is explained in detail in section 3.6.

### 3.4. Boundary Conditions

In the physical experiments, web frames are fixed to the support tabs via bolted connections. The bolted connections were removed from the model because they

43

introduced a significant number of elements (and therefore increase computation time) while not changing the accuracy of the results significantly. The ends of the web frames are fixed in rotation and translation. The faces of the end plates are also fixed. Similar to the connection at the web frames, the bolted connections are not modelled, but the entire faces are fixed. The locations of the fixed supports are shown in Figure 3-4 and Figure 3-5.
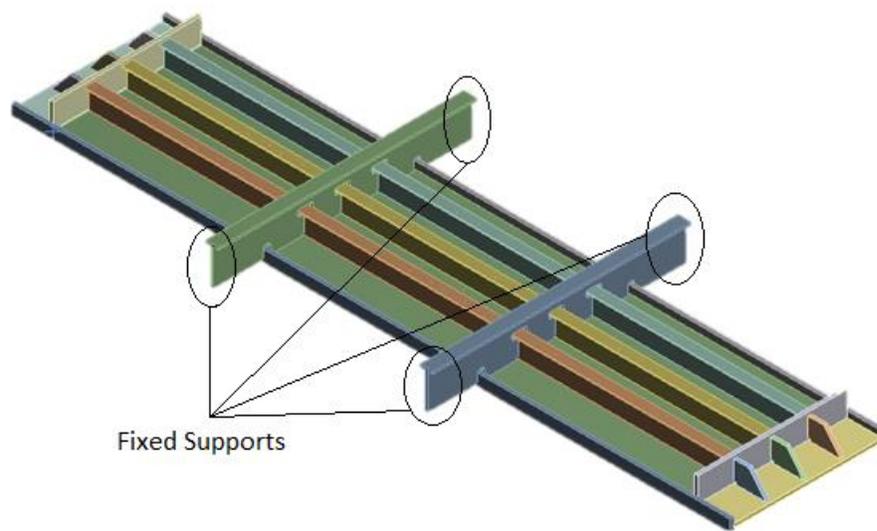


**Figure 3-4: Locations of web frame fixed supports**
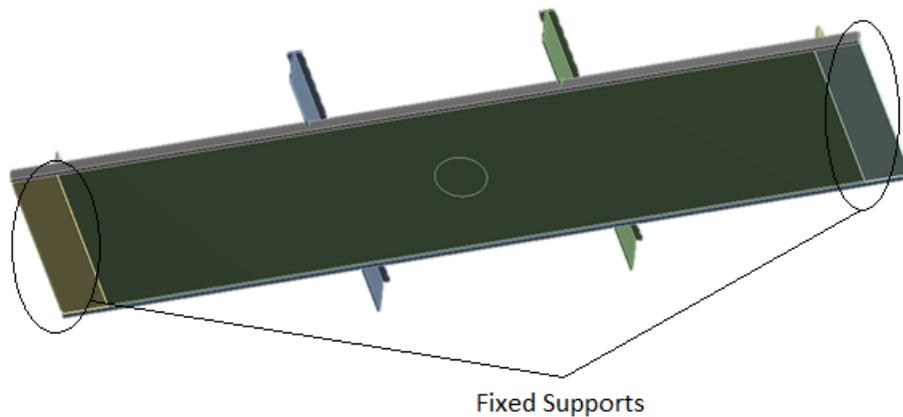


**Figure 3-5: Location of end plate fixed supports**

### 3.5. Ice Loading Representation

The ice is not modelled in the numerical analysis. The ice is represented by a force load, evenly distributed over a 40 cm diameter circular patch area on the shell plate. Several different patch sizes were tried, with both uniform and non-uniform pressure distribution within the load patch. To simplify the mesh, a single patch uniform pressure load area was chosen to be used for the model validation since it produced acceptable results.  The actual ice cone was 100 cm in diameter, but the entire ice cone did not come into contact with the shell plate during the physical experiment. 40 cm was chosen to be an appropriate size patch for the load, and displayed reasonable results.

### 3.6. Convergence Study

A finer mesh typically means more accurate and refined results. However, there is a balance between element sizing and result accuracy at which an acceptable result can be achieved while keeping the computation time to a reasonable level. A convergence study was done to find the point at which increasing the mesh size no longer improved the results, with the results converging on a solution as the mesh continued to be refined. Figure 3-6 shows the grillage model with a coarse mesh. Figure 3-7 shows the load vs. deformation results of the mesh convergence study performed on the grillage FE analysis validation.
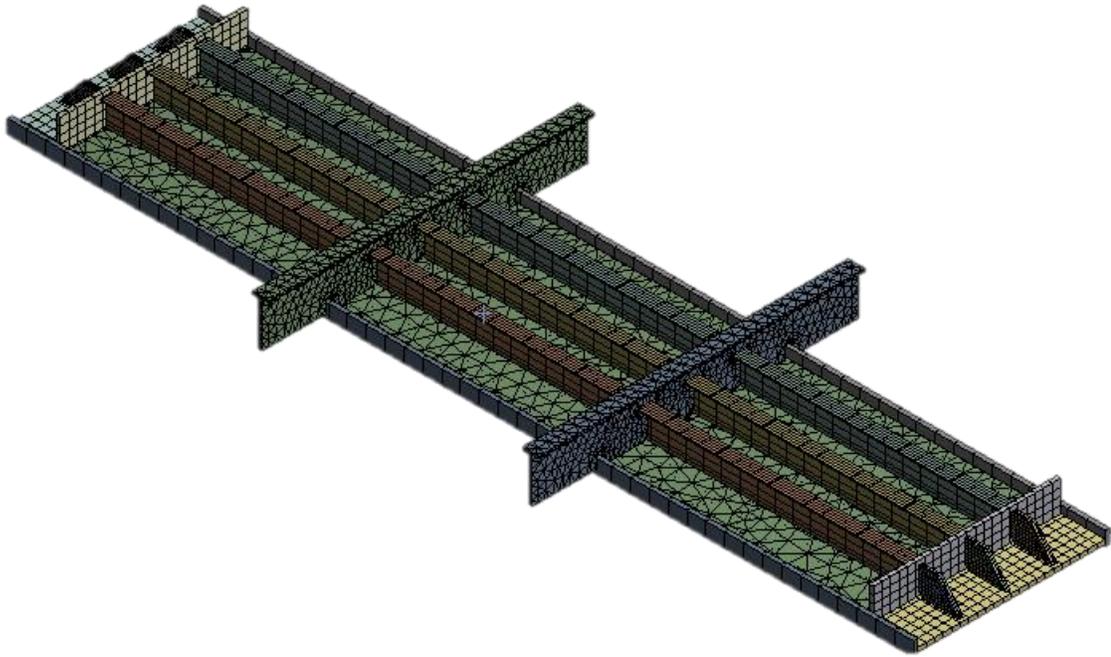
**Figure 3-6: example of grillage model with coarse mesh**

In ANSYS, when using program-controlled mesh sizing, the use can select the mesh

"relevance center". This defines, at a global scale, how fine a mesh will be. Once the

relevance center is selected, the use can select the relevance, which is controllable on a

scale from -100 to +100. Positive numbers increase the mesh fineness, while negative

numbers reduce the mesh fineness. All of the meshes used 1 level of refinement, and as

the mesh fineness was increased, the results converged on a solution. In Figure 3-7, the

results for fine mesh with a relevance level of 40 cannot be seen, because it perfectly

overlaps with the fine mesh with relevance 60 results. Therefore, the FE analysis large

grillage validation simulations use a fine mesh with a relevance of 40.
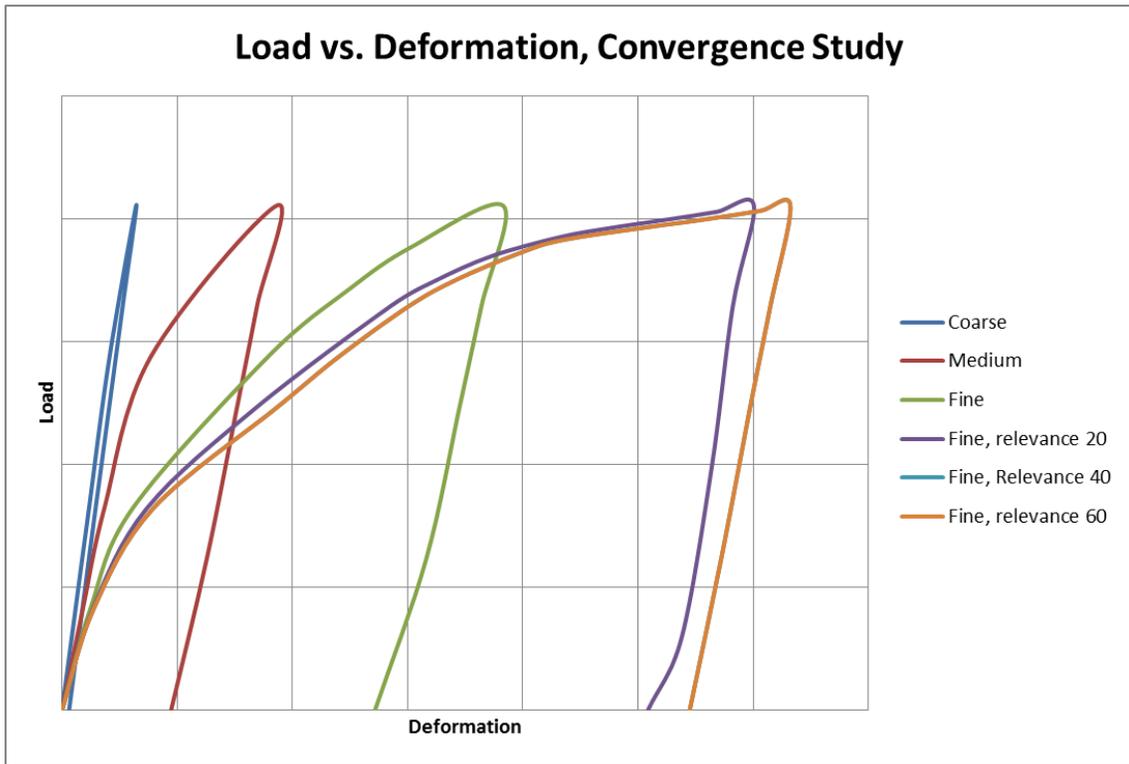
**Figure 3-7: Load vs. deformation of large grillage, ANSYS convergence study**

### 3.7. Results, Comparison to Laboratory Results

The results of grillage A's test 1 result, and the FE analysis results of the same

experiment are shown in Figure 3-8, Figure 3-9, and Figure 3-10. For the FE model, the

line represents the vertical displacement of the grillage at the intersection of the shell

plating and the center stiffener's web. The experimental result is the LVDT data, showing

the vertical displacement at the top of the center stiffener's flange. The material

properties used for the model are shown in Table 3-2.

47

**Table 3-2: Grillage model material properties**

| Grillage Material Properties | |
|---|---|
| Yield Strength [Mpa] | 409 |
| Ultimate Strength [MPa] | 460 |
| Young's Modulus [GPa] | 200 |
| Poisson's Ratio | 0.3 |
| Tangent Modulus | 1500 |

Figure 3-8 displays the elastic range of loading, with each curve reflecting a loading of up to 500 kN, which is the approximate design load for this grillage. It is shown that there is very good agreement between the experimental laboratory data and the FE analysis data. The FE model appears to be very slightly stiffer in the elastic range.
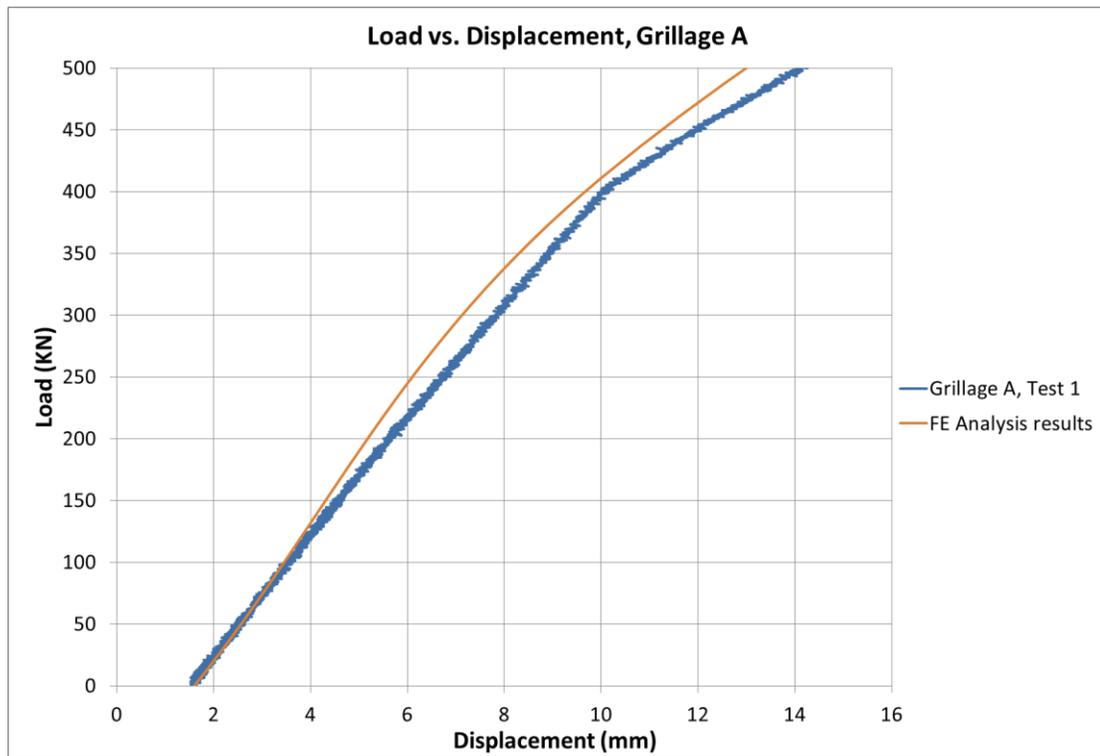
**Figure 3-8: Grillage A, Test 1 laboratory results and FE analysis results up to 500 kN**

Figure 3-9 displays the laboratory results and the FE analysis results for Grillage A, Test 1 up to about 1400 kN of loading, which is almost triple the design load. In this loading range, the FE model is slightly stiffer than the laboratory model. At 60 mm of deflection, the laboratory results show a load of 1400 kN, while the FE analysis results show a load of 1450 kN, representing slightly more than 3% discrepancy in loading capacity at this level of deformation.

49

**Figure 3-9: Grillage A, Test 1 laboratory results and FE analysis results up to 1400 kN**

Figure 3-10 shows the total loading and unloading of Grillage A, Test 1 laboratory results and FE analysis results. The results show greater discrepancy in response as the load increases. At a peak load of 2050 kN, the FE model had 111 mm of total deflection, while the laboratory results displayed 124 mm of total deflection. This represents a 10.5% increase in loading capacity in the FE model over the laboratory results.

When unloaded, the FE model has 92 mm of permanent deformation, while the laboratory results showed 98 mm of permanent deformation. The FE model therefore had 6.1% less permanent plastic deformation during the test.
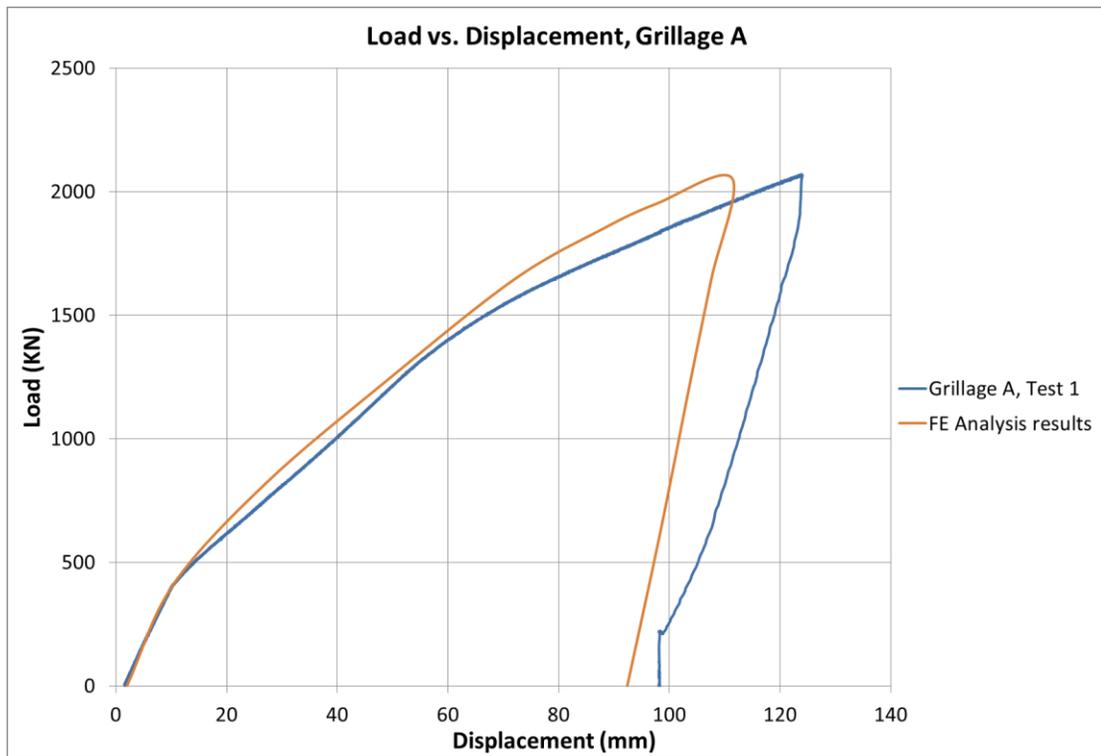
**Figure 3-10: Grillage A, Test 1 laboratory results and FE analysis results**

Figure 3-11 shows the permanent deflection of the finite element model of the grillage.

51
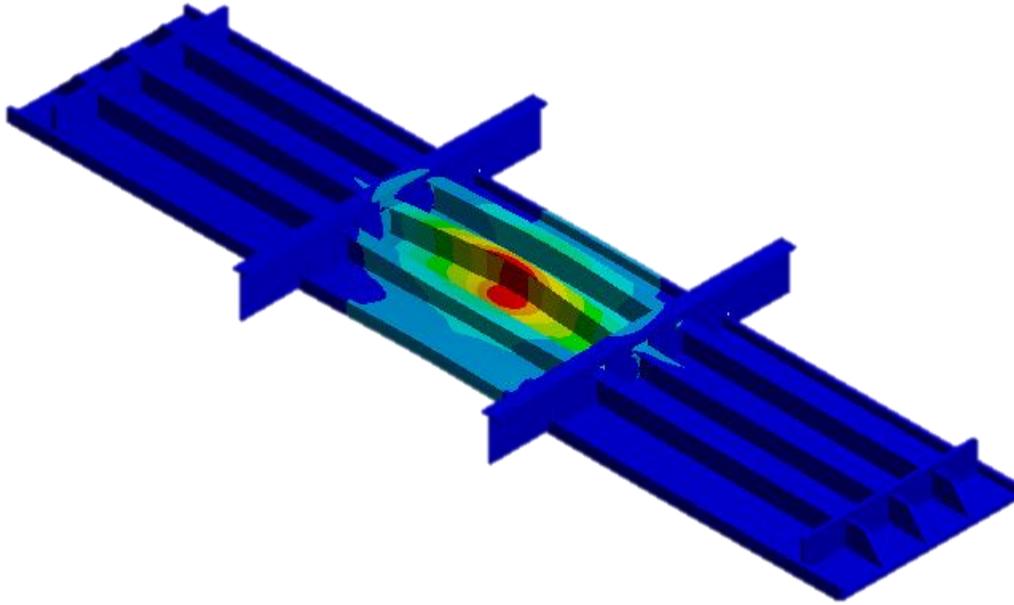
**Figure 3-11: FE model showing permanent deflection of grillage**

### 3.8. Conclusion

The comparison of Grillage A, test 1 experimental results and FE analysis results shows that under design load conditions, the FE analysis closely models the actual response of the grillage to ice loading. As well, under overload conditions up to triple the design load, the FE model is a good representation of the experimental response.

There were several assumptions and simplifications made in the FE model of the grillage experiment, and results were still satisfactory. Using a single load patch size with uniform pressure to represent the ice loading proved to be an acceptable simplification to the model.

# 4. Finite Element Analysis of IACS Polar Class Structure

## 4.1. Introduction

This analysis is done to evaluate the capacity of grillage structure under ice loading conditions when different stiffener cross-sections are used, while meeting design requirements. Four different common stiffener cross-sections are being tested:

- Flat bar

- T-Section

- L-Section

- Bulb section

The grillages meet Polar Class design requirements for the midbody ice belt of a longitudinally framed 12,000 tonne PC7 vessel. All the grillages have a common shell plating thickness, and common web frames. All of the calculated dimensions in the grillage designs have been validated against the ABS polar rules quick check software. Non-linear numerical analysis of each of the grillages was conducted in ANSYS, using the Newton-Raphson Method. This is an iterative method of finding the roots of an equation, which can be used for finding successively better approximations for the balance of external loads and structural response. The load is applied in steps and sub-steps, and the external loads and nodal forces are balanced at each sub-step before moving onto the next sub-step.

53

## 4.2. Grillage Design

### 4.2.1. Design Load

The design ice load patch size and average pressure ($P_{avg}$) are determined by first

calculating the force (F) and line load (Q), as follows (IACS 2013):

$$F = 0.36 \cdot CF_C \cdot DF \qquad\qquad \text{[MN]}$$

where

      $CF_C =$  Crushing Force Class Factor      (IACS (2013))

      $DF =$    ship displacement factor        (IACS (2013))

      $Q = 0.639 \cdot F^{0.61} \cdot CF_D$              [MN/m]

where

      $CF_D =$  Load Patch Dimensions Class Factor      (IACS (2013))

The design load patch size is determined as:

$$W = F / Q \qquad\qquad \text{[m]}$$

$$b = w / 3.6 \qquad\qquad \text{[m]}$$

The average pressure within the design load patch is determined as:

$$P_{avg} = F / (b \cdot w) \qquad\qquad \text{[MPa]}$$

The above calculations for the design case are shown in Table 4-1.

**Table 4-1: Design load calculation values**

| Factor | Value |
|---|---|
| Crushing Force Class Factor | 1.8 |
| Ship Displacement Factor | 4.9054 |
| Displacement Class Factor | 22 |
| Force [MN] | 3.1787 |
| Load Patch Dimension Class Factor | 1.11 |
| Line Load [MN/m] | 1.4361 |
| Load Patch Width [m] | 2.213 |
| Load Patch height [m] | 0.6148 |
| Average Pressure [Mpa] | 2.3359 |

This design load must then be multiplied by the hull area factor for area in question. In the case of the midbody icebelt, the hull area factor is 0.45. This produces a design load at the midbody icebelt of 1.4301 MN.

### 4.2.2. Shell Plating

The shell plating thickness (t) is determined by calculating the plate thickness required to resist ice loads ($t_{net}$), with an added corrosion and abrasion allowance ($t_s$), given by IACS (2013):

$$t = t_{net} + t_s \qquad \text{[mm]}$$

$$t_{net} = 500 \cdot s \cdot ((AF \cdot PPF_p \cdot P_{avg}) / \sigma_y)_{0.5} / (1 + s / (2 \cdot l)) \qquad \text{[mm]}$$

55

where

$s =$ frame spacing [m]

$AF =$ Hull Area Factor from IACS (2013)

$PPF_p =$ Peak Pressure Factor from IACS (2013)

$l =$ distance between frame supports [m]

The above calculations for the design case are shown in Table 4-2.

Table 4-2: Shell plating design calculation values

| Factor | Value |
|---|---|
| Main Frame Spacing [m] | 0.35 |
| Peak Pressure Factor- Plate | 1.78 |
| Hull Area Factor | 0.45 |
| Minimum Required Net Shell Plate Thickness [mm] | 11.68 |
| Minimum Required Gross Shell Plate Thickness [mm] | 12.68 |
| Actual Shell Plate Thickness [mm] | 13 |

### 4.2.3. Web Frames

The polar class rules do not include specific requirements for web frames, but state "the member web frames and load-carrying stringers are to be dimensioned such that the combined effects of shear and bending do not exceed the limit state(s) defined by each member society. Where these members form part of a structural grillage system, appropriate methods of analysis are to be used" (IACS 2013). In addition, the web frames

56

must meet structural stability requirements, specifically a web slenderness ratio for bulb,

tee, and angle sections as:

$$h_w / t_{wn} \leq 805 / (\sigma_y)^{0.5}$$

where

$h_w =$     web height        [mm]

$t_{wn} =$     net web thickness        [mm]

The above minimum slenderness ratio is required for all structural framing members.

ABS Structural Requirements for Polar Class Vessels (2013) is used to design the web

frame dimensions. All of the grillages being analyzed use common T cross-sectioned web

frames.

The requirements include a minimum net effective shear area, a minimum net effective

plastic section modulus, and web stability requirements.

The actual net shear area, Aw, of web frame or load-carrying stringer is given by:

$$A_w = h \cdot t_{wn} \cdot \sin \cdot \phi_w / c_4{}^2$$

$$[cm^2]$$

where

$c_4 = 10$

$h_w =$ height of the web frame or load-carrying stringer        [mm]

$t_{wn} =$ net web thickness of the web frame or stringer ($t_{wn} = t_w - t_c$)        [mm]

$t_w =$ as-built web thickness for the web frame or stringer        [mm]

$t_c =$ corrosion deduction        [mm]

$\phi_w$ = smallest angle between shell plate and web of the web frame or load-carrying

stringer, measured at the midspan of the web frame or load-carrying.

The above calculations for the design case for the web frames are shown in Table 4-3.

**Table 4-3: Web frame dimensions**

| Factor | Value |
|---|---|
| Web Frame spacing [mm] | 2000 |
| Height of Web Frame Stringer [mm] | 350 |
| Net Web Thickness [mm] | 19 |
| As-Built Web Thickness [mm] | 20 |
| web thickness corrosion reduction [mm] | 1 |
| Flange width corrosion reduction [mm] | 1 |
| Net Flange Width [mm] | 118 |
| As-built Flange Width [mm] | 120 |
| Net Flange Thickness [mm] | 18 |
| As-Built Flange Thickness [mm] | 19 |
| Flange thickness corrosion reduction [mm] | 1 |
| shell plate-web angler [degrees] | 90 |
| $c_4$ | 10 |
| Required Net effective Shear Area of Web Frame [cm$^2$] | 62.7 |
| Actual Net effective Shear Area of Web Frame [cm$^2$] | 69.9 |

There are two possible equations for determining the net effective plastic section modulus, depending on whether the cross-sectional area of the web frame or load-carrying stringer is greater or less than the cross-sectional area of the attached flange shell plating. Since the cross-sectional area of the web frames and each longitudinal stiffener is less than the cross-sectional area of the attached flange shell plating, the actual net plastic section modulus can be obtained by the following equation:

$$Z_p = b_{eff} \cdot t_p^2 / (2c_4^2) + h_w^2 \cdot t_w \cdot \sin\phi_w / (2c_4^3) + b_f t_f (h_{fc} \cdot \sin\phi_w - b_w \cdot \cos\phi_w) / c_4^3$$

$$[cm^2]$$

where

$c_4 = 10$

$b_f$ = width of flange of the web frame or load-carrying stringer [mm]

$t_f$ = net thickness of flange of the web frame or load-carrying stringer [mm]

$t_p$ = net thickness of an effective attached flange of shell plate [mm]

$b_{eff}$ = width of the effective attached flange of shell plate [mm]

= distance between adjacent web frame for the calculation of Zp of the web frame

= distance between adjacent load-carrying stringers for the calculation of Zp of the load-carrying stringer

$h_{fc}$ = distance from the mid thickness plane of the web frame or load-carrying stringer to the center of the flange width [mm]

The above calculations for the design case for the web frames are shown in Table 4-4.

**Table 4-4: Web frame design calculation values**

| Factor | Value |
|---|---|
| Required net effective plastic Section Modulus [cm$^3$] | 1992.1 |
| Actual net effective plastic Section Modulus [cm$^3$] | 1987.1 |
| Net thickness of effective attached flange of shell plate [mm] | 12 |
| Width of effective attached flange of shell plate [mm] | 2000 |
| Net x-sectional area of effective attached flange of shell plate [cm$^2$] | 240.0 |
| Net x-sectional area of web frame or load carrying stringer [mm$^2$] | 88.1 |
| height of local frame measured to center of the flange area [mm] | 359.1 |
| Distance from mid thickness plane of local frame web frame to the center of the flange area [mm] | 0 |

The slenderness ratio requirement is met for the web frames, as shown in Table 4-5.

**Table 4-5: Web frame slenderness ratio calculation values**

| Factor | Value |
|---|---|
| height of Web Frame Stringer [mm] | 350 |
| Net Web Thickness [mm] | 18 |
| Slenderness Ratio | 18.4 |
| Maximum Allowable Slenderness Ratio | 42.7 |

### 4.2.4. Longitudinal Stiffeners

The longitudinal stiffeners must meet the minimum requirements for net effective shear area, as well as net effective plastic section modulus, as found in UR I2.

The actual net effective shear area of the frame, Aw, is to comply with the following condition: $A_w \geq A_L$, where:

$$A_L = 1002 \cdot (AF \cdot PPFs \cdot Pavg) \cdot 0.5 \cdot b_1 \cdot a / (0.577 \cdot \sigma_y) \qquad [cm2]$$

where

AF = Hull Area Factor

PPFs = Peak Pressure Factor

Pavg = average pressure within load patch                    [MPa]

$b_1 = ko \cdot b2$                                           [m]

ko = 1 - 0.3 / b'

b' = b / s

b = height of design ice load patch                          [m]

s = spacing of longitudinal frames                           [m]

$b_2 = b \cdot (1 - 0.25 \cdot b')$                           [m]

a = longitudinal design span                                 [m]

$\sigma_y$ = minimum upper yield stress of the material      [N/mm2]

The actual net effective plastic section modulus of the plate/stiffener combination, $Z_p$, is to comply with the following condition: $Z_p \geq Z_{pL}$, where:

61

$$Z_{pL} = 1003 \cdot (AF \cdot PPFs \cdot Pavg) \cdot b1 \cdot a_2 \cdot A_4 / ( 8 \cdot \sigma_y) \qquad [cm3]$$

where:

$$A_4 = 1 / (2 + k_{wl} \cdot [(1 - a_4{}^2)^{0.5}-1)$$

$$a_4 = A_L / A_w$$

$A_L$ = minimum shear area for longitudinal          [cm2]

$A_w$ = net effective shear area of longitudinal          [cm2]

$$k_{wl} = 1 / (1 + 2 \cdot A_{fn} / A_w)$$

As mentioned earlier, four different common stiffener cross-sections are being evaluated:

- Flat bar

- T-Section

- L-Section

- Bulb section

The stiffeners follow similar structural requirement calculations to the web frames. The shear area, plastic section modulus, and web stability criteria are the driving factors in determining the dimensions of stiffeners of specified cross-section types. It is difficult to design equivalent stiffeners of different geometries while still meeting structural rule requirements. For example, to achieve a similar plastic section modulus for both a T-section and a flat bar stiffener, one has to push the flat bar stiffener height to width ratio to close to the limit, and even then, the shear area (and therefore steel weight) of the flat bar stiffener is significantly greater than that of the T-section stiffener. For this reason, it

62

is hard to balance the driving factors of the stiffener design to achieve equivalent stiffeners.

It was decided that in order to design equivalent stiffeners using the different cross-sections; the plastic section modulus and shear area would meet the minimum requirements, while exceeding them as little as possible.

For the flat bar stiffener, the plastic section modulus was made to be close to that of the other stiffener types, while significantly exceeding its actual plastic section modulus and shear area requirements. The calculated dimensions of the longitudinal stiffeners and the required values are shown in Table 4-6.

Table 4-6: Longitudinal stiffener dimensions

| Factor | Value | | | |
|---|---|---|---|---|
| | T-Section | L-Section | Flat Bar | BP 200x9 Bulb Section |
| Web Height [mm] | 170 | 170 | 185 | 179.2 |
| Web Thickness [mm] | 9 | 9 | 15 | 9 |
| Flange Width [mm] | 75 | 75 | N/A | 34.2 |
| Flange Thickness [mm] | 11 | 11 | N/A | 20.8 |
| Required net effective plastic Section Modulus [cm$^3$] | 248.8 | 248.8 | 219.7 | 235.4 |
| Actual net effective plastic Section Modulus [cm$^3$] | 259.5 | 259.5 | 255.1 | 269.2 |
| Required Net effective Shear Area of Web Frame [cm$^2$] | 14.0 | 14.0 | 14.0 | 14.0 |
| Actual Net effective Shear Area of Web Frame [cm$^2$] | 14.4 | 14.4 | 25.8 | 15.9 |
| Actual Slenderness Ratio | 21.25 | 21.25 | 13.2 | 22.4 |
| Maximum Allowed Slenderness Ratio | 42.72 | 42.72 | 14.97 | 42.72 |

Bulb sections are manufactured in standard sizes, and therefore it was appropriate to

choose the size that best suits the structural requirements. That is, meeting the

requirements, but exceeding them as little as possible. The chosen bulb size is a BP200x9.

The dimensions of the bulb flat are shown in Table 4-7.

**Table 4-7: BP200x9 bulb flat dimensions**

| Factor | Value |
|---|---|
| h [mm] | 200 |
| $t_w$ [mm] | 9 |
| c [mm] | 28 |
| $A_{stiff}$ [cm2] | 23.6 |
| r [mm] | 8 |
| d [mm] | 28.8 |
| $A_b$ [cm2] | 5.6 |
| $h_w$ [mm] | 179.2 |
| $t_w$ [mm] | 9 |
| $w_f$ [mm] | 34.2 |
| $t_f$ [mm] | 20.8 |
| $b_w$ [mm] | 12.6 |

Due to the relatively complex shape of the blub flat, equivalent bulb section geometries are used for the structural calculations. The ABS standard method is used for this. This conversion of as-built bulb sections to the equivalent section geometry is shown in Figure 4-1. However, in the numerical analysis, the actual bulb shape is used.
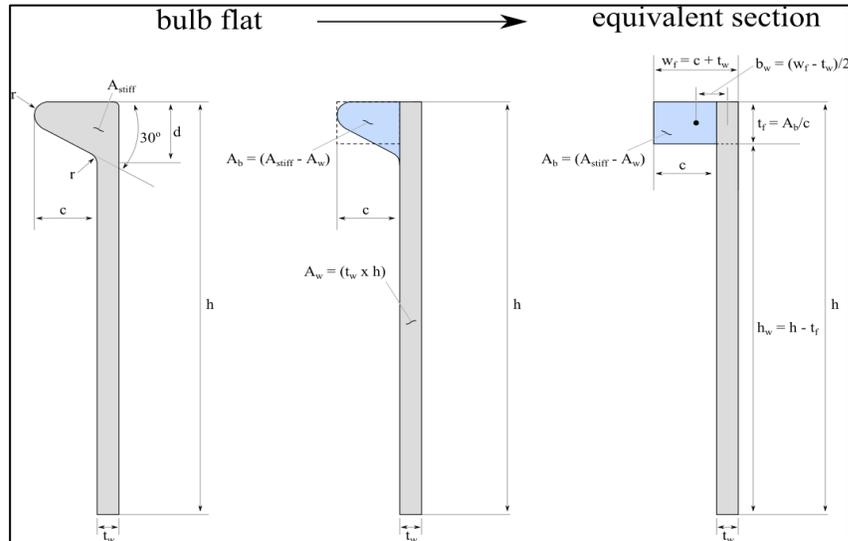


**Figure 4-1: ABS method of bulb flat geometry conversion**

### 4.2.5. Details of Longitudinal Stiffener Connection to Web Frames

The connection between web frames and longitudinal stiffeners is a fixed connection. There are no cut-outs for the longitudinal stiffeners to pass through the web frames, so the longitudinal stiffeners end at the web frames, and then begin again on the other side of the web frames. This was done in order to keep the different grillage designs as uniform as possible. As a result of there not being cut-outs in the web frames, all of the grillages are identical, except for the longitudinal stiffener cross-sections. If cut-outs were used on the

web frames, they would have to vary slightly in order to accommodate the different stiffener types.

## 4.3. Modeling

All solid modelling was done using SOLIDWORKS, and imported to ANSYS in IGES format. Each of the grillages has common major dimensions, web frame spacing, and stiffener spacing. The major dimensions are shown in Table 4-8.

**Table 4-8: Grillage model global dimensions**

| Dimension | Value |
|---|---|
| Total width [mm] | 3150 |
| Total length [mm] | 6000 |
| Web frame spacing [mm] | 2000 |
| Stiffener spacing [mm] | 350 |
| Number of web frames [mm] | 2 |
| Number of stiffeners [mm] | 9 |

An unmeshed 3D rendering of the T-stiffener grillage is shown in Figure 4-2.
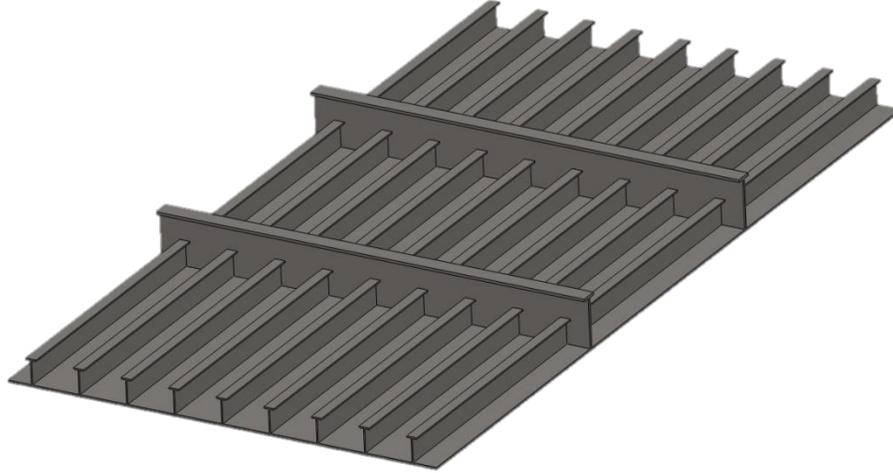
**Figure 4-2: 3D rendering of grillage structure with T-stiffeners**

## 4.4. Meshing

For all of the grillages, SOLID186 type elements were used. Mesh size was program-controlled, and user-input meshing refinements were utilized.

There are various methods of refining and controlling the mesh. Using simple refinements, one can further reduce the mesh size at a local level. Applying refinements to specific faces of critical interest can increase analysis fidelity.

For the analysis of the grillages in this section of this thesis, each grillage has a single level of refinement applied to all faces of the grillage. The mesh statistics for each of the four grillages are shown in Table 4-9.

**Table 4-9: Mesh statistics for PC7 grillages**

| Grillage Mesh Statistics | | | | |
|---|---|---|---|---|
| | Stiffener Type | | | |
| | Bulb | Flat bar | T-Section | L-Section |
| Total Nodes | 701359 | 481508 | 666131 | 615476 |
| Number of Elements | 350359 | 239957 | 334076 | 306099 |

Computation time for the bulb-stiffened grillage was the longest out of the different

stiffener types. The total number of nodes involved is greater than in the other grillages.

This is due to the complex shape of the bulb cross-sectioned stiffeners. In contrast, the

number of elements in the flat bar-stiffened grillage was significantly less than that of the

other grillages, and computation time was reduced as well.

## 4.5. Boundary Conditions

Fixity is assumed at the edges of the grillages. The outer edges of the grillages in the

longitudinal direction are at the locations of what would be the next web frames.

In ANSYS, the outer four edges of the grillage are fixed in X, Y, Z translation, as well as

fixed in X, Y, Z rotation.

## 4.6. Loading

The grillages are loaded in the IACS design load patch. The design load patch size is

2213 mm wide by 614.8 mm high. This patch is centered on the center longitudinal

stiffener. Transversely, it does not meet the neighboring longitudinal stiffeners.

69

Longitudinally, it spans the two web frames that are perpendicular to the center stiffener.

The location of the design load patch on the grillages is shown in Figure 4-3.
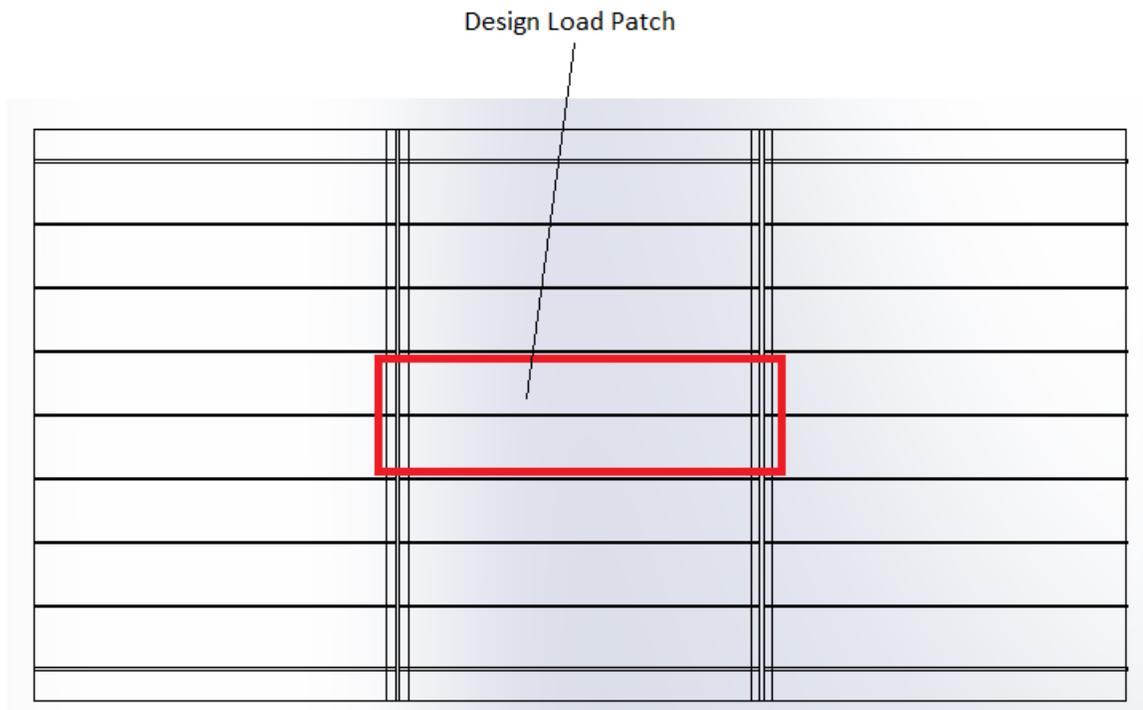


**Figure 4-3: Location of design load patch**

In ANSYS, the load is applied as a pressure across the area of loading on the outside of

the shell plating.

### 4.7. Material Properties

A bilinear isotropic hardening model was used for the material properties of the steel

structure. The material properties of the steel used in the analysis is shown in Table 4-10.

**Table 4-10: IACS grillage material properties**

| IACS Grillage Material Properties | |
|---|---|
| Yield Strength [Mpa] | 355 |
| Ultimate Strength [MPa] | 460 |
| Young's Modulus [GPa] | 200 |
| Poisson's Ratio | 0.3 |
| Tangent Modulus | 1500 |

## 4.8. FE Analysis Results

FE analysis of the four grillages was completed for two load cases. In the first case, the

grillages were loaded up to the design load, and subsequently unloaded. In the second

loading case, the grillages are loaded up to triple the design load.

### 4.8.1. Design Load FE Analysis

The results of the FE analysis for design load conditions are observed in the form of load

vs. deflection data, shown in Figure 4-4, to Figure 4-7.

It can be seen in Figure 4-4 that while being loaded to 100% of the design load, 1.4031

MN, the T-stiffened grillage experiences 11.5 mm of total deflection, and when unloaded,

the grillage retains 1.3 mm of permanent plastic deformation. It is useful to express the

plastic deformation as a percentage of frame span length. With a frame span of 2000 mm,

and a plastic deformation of 1.3 mm, the T-stiffened panel has a total plastic deformation

under 100% design load of 0.065%. Expressing the deformation as a percentage of the

71

frame span provides a method of demonstrating the relative extent of the permanent

deformation.
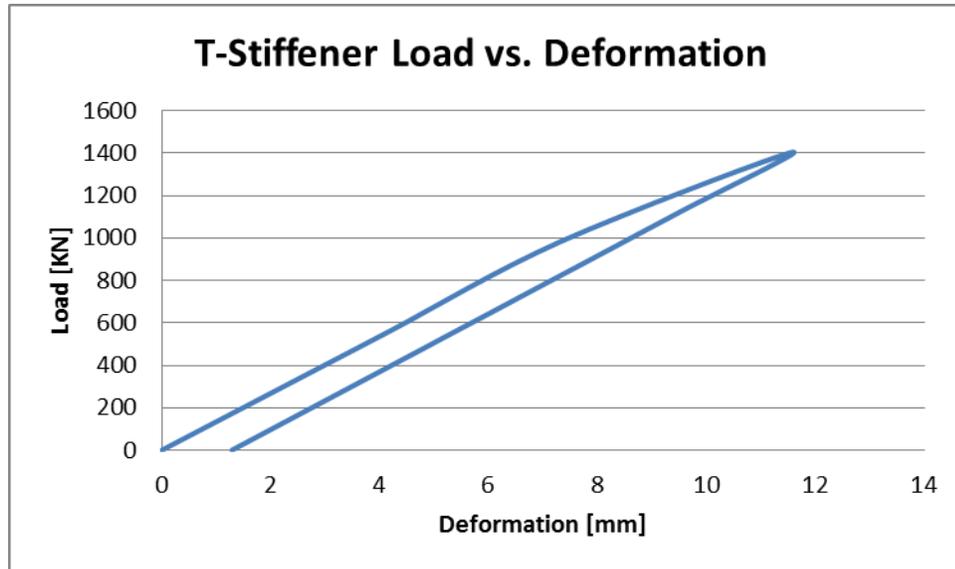


**Figure 4-4: T-Stiffener load vs. deformation for design load**

Figure 4-5 shows the load vs. deformation plot for the L-stiffener grillage while being

loaded to 100% of the design load, 1.4031 MN. Under this load, the L-stiffened grillage

experiences 15.0 mm of total deflection, and when unloaded, the grillage retains 1.3 mm

of permanent plastic deformation. With a frame span of 2000 mm, and a plastic

deformation of 1.3 mm, the L-stiffened panel has a total plastic deformation under 100%

design load of 0.065%.
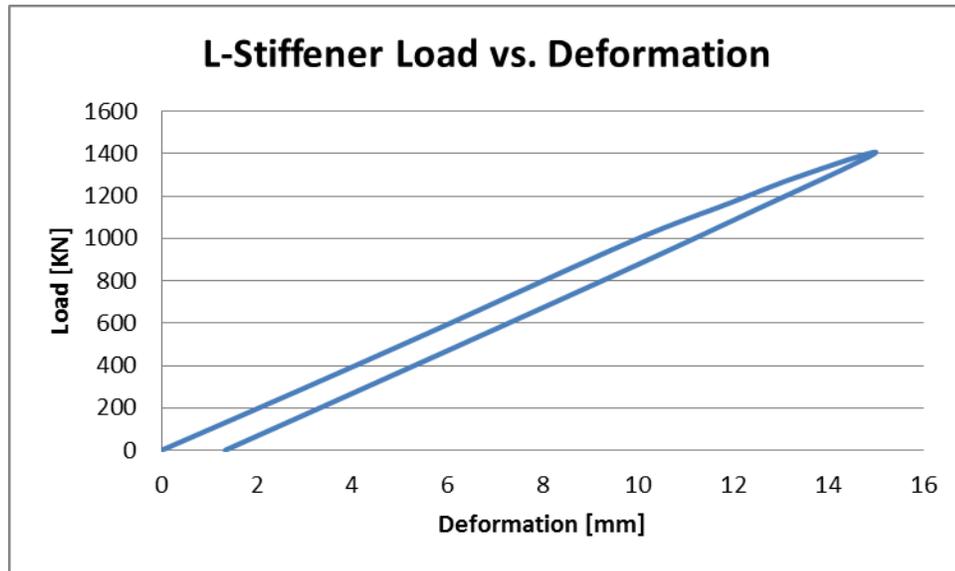
**Figure 4-5: L-Stiffener load vs. deformation for design load**

Figure 4-6 shows the load vs. deformation plot for the bulb-stiffener grillage while being loaded to 100% of the design load, 1.4031 MN. Under this load, the bulb-stiffened grillage experiences 11.2 mm of total deflection, and when unloaded, the grillage retains 1.27 mm of permanent plastic deformation. With a frame span of 2000 mm, and a plastic deformation of 1.27 mm, the bulb-stiffened panel has a total plastic deformation under 100% design load of 0.0635%.
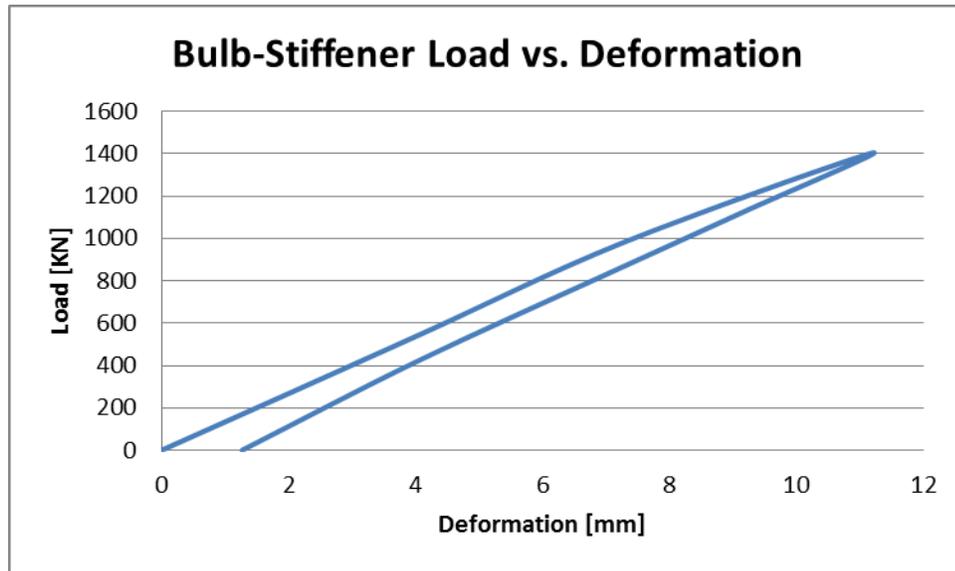
**Figure 4-6: Bulb-Stiffener load vs. deformation for design load**

Figure 4-7 shows the load vs. deformation plot for the flat bar-stiffener grillage while being loaded to 100% of the design load, 1.4031 MN. Under this load, the flat bar-stiffened grillage experiences 9.65 mm of total deflection, and when unloaded, the grillage retains 0.73 mm of permanent plastic deformation. With a frame span of 2000 mm, and a plastic deformation of 0.73 mm, the flat bar-stiffened panel has a total plastic deformation under 100% design load of 0.0365%.
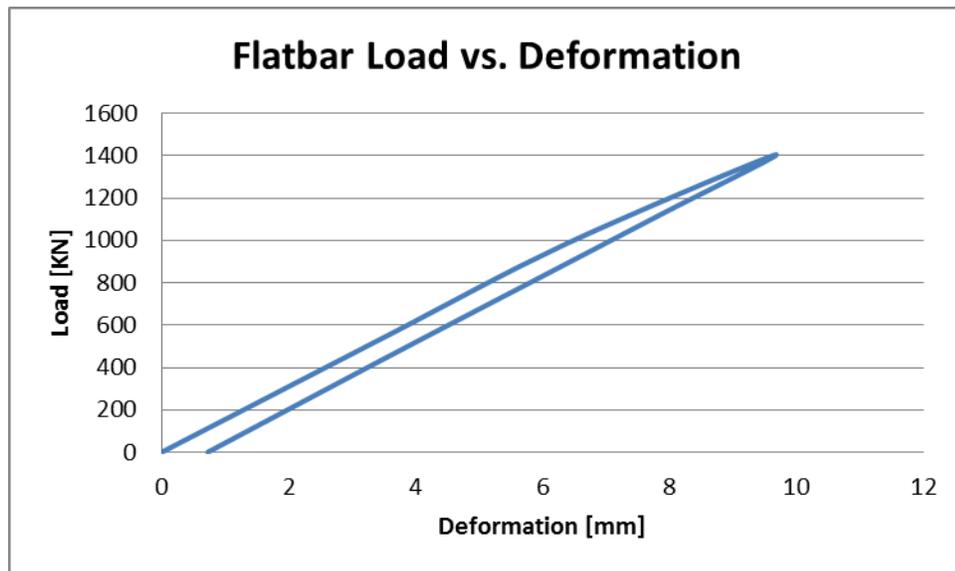
**Figure 4-7: Flat bar-stiffener load vs. deformation for design load**

Figure 4-8 shows the load-deformation curves for the four grillages on one plot. It can be seen that the flat bar stiffener performs the best, followed by the bulb-stiffener, then the T-stiffener, while the L-stiffened grillage performed the worst under design load conditions. This data makes it look like the flat bar stiffener is the best stiffener for this scenario. However, due to the excessive cross-sectional area of the flat bar stiffener, it may be too heavy and costly to use. A review of the UR I2 requirements for the flat bar stiffener could result in lighter structures being used, as the requirements are currently more conservative than required.

It should also be noted that none of the stiffeners tested had the webs buckle in this analysis. This may be due to the uniform loading and the lack of cut-outs through the web frames (which would increase non-symmetry in the grillages). It has been seen through experience that the webs of T-stiffeners can buckle during ice loading, resulting in a loss of capacity in the stiffeners, while bulbflat stiffeners have been shown to perform better

75

under similar conditions. A comparison of the buckling of the webs of the different

stiffener types would be a very useful study, however it is outside the scope of this work.
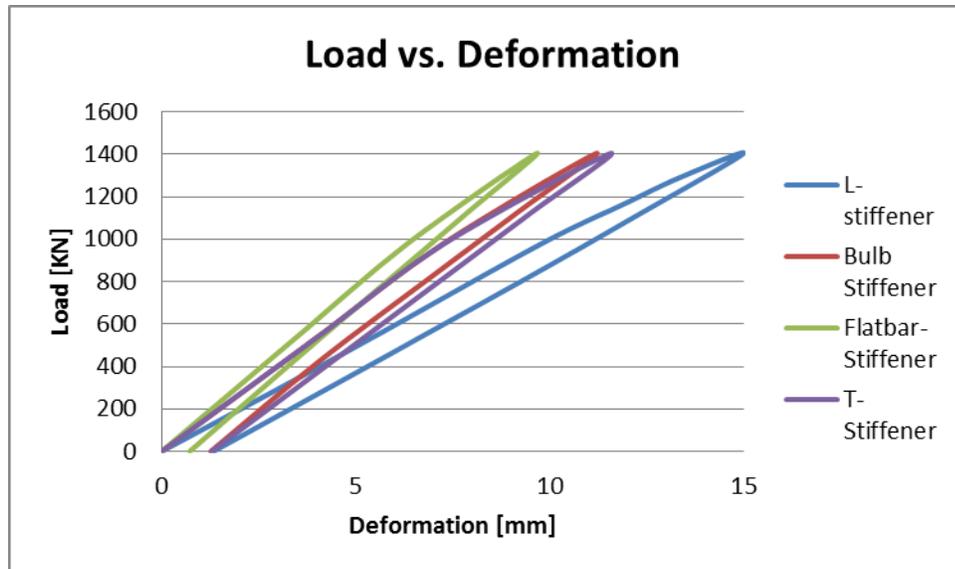


**Figure 4-8: Comparison of load vs. deflection for 100% design load**

Figure 4-9 shows the load vs. deflection curve for the web frames while experiencing

100% of design load. This plot for the web frames is common to the grillages of all

stiffener types. There was no appreciable difference in the response of the web frames on

the grillages with different stiffener types. It can be seen that the web frames experience a

total deflection of 2.83 mm under 100% design load, and a resulting plastic deformation

of 0.024 mm. This is a virtually undetectable amount of permanent deformation.
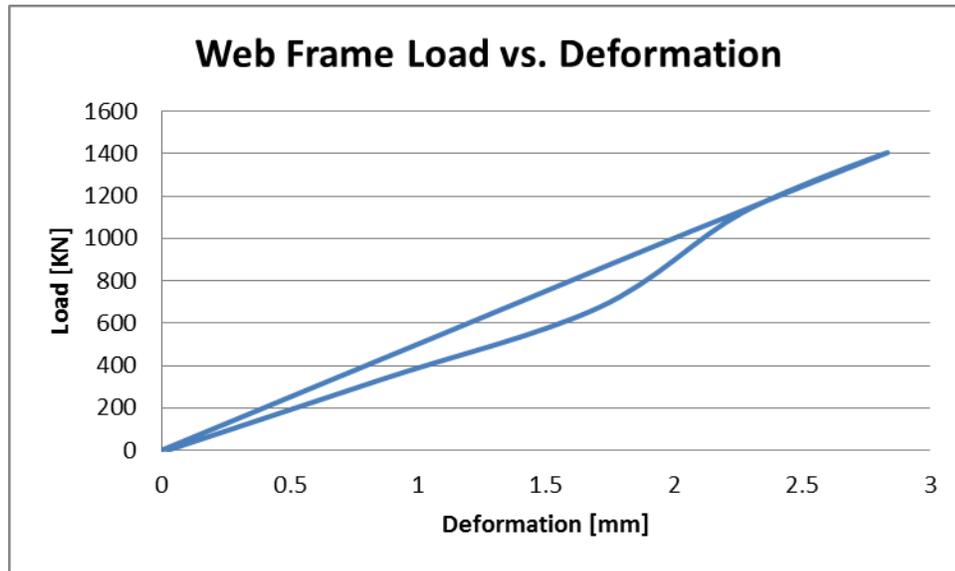
**Figure 4-9: Web frame load vs. deformation for 100%**

A common design point for plastic limit-state design is for the structure to undergo 0.1% plastic deformation under design conditions. All of the longitudinal stiffeners discussed above experience less than that amount of plastic deformation at the design load. Based on the results of the above FE analysis, it seems that the UR I2 structural requirements are conservative enough. The flat bar stiffeners may be over-penalized in the UR I2 requirements, and a review of the stiffener requirements could prove useful. A lighter structure would still perform well under overload conditions.

The amount of plastic deformation of the web frames under design loads is certainly an acceptable amount of plastic response.

### 4.8.2. Overload FE Analysis Results

The results of the FE analysis for overload conditions are observed in the form of load vs. deflection data, shown in Figure 4-10 to Figure 4-13.

It can be seen in Figure 4-10 that while being loaded to 220% of the design load, 3.178 MN, the T-stiffened grillage experiences 46.8 mm of total deflection, and when unloaded, the grillage retains 27.7 mm of permanent plastic deformation. It is useful to express the plastic deformation as a percentage of frame span length. With a frame span of 2000 mm, and a plastic deformation, the T-stiffened panel has a total plastic deformation under 220% design load of 1.4%.
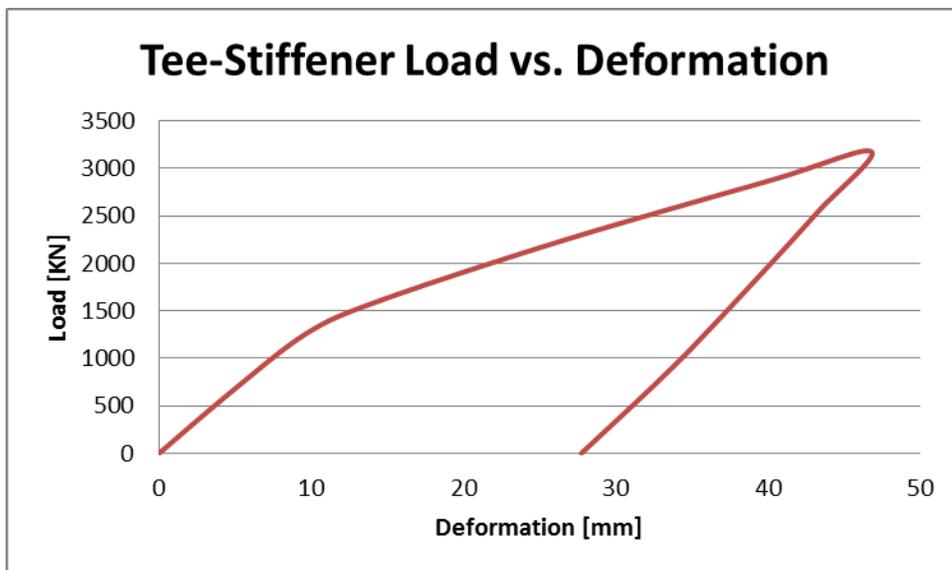


**Figure 4-10: T-stiffener load vs. deflection for 220% design load**

Figure 4-11 shows the load vs. deformation plot for the L-stiffener grillage while being loaded to 220% of the design load, 3.178 MN. Under this load, the L-stiffened grillage experiences 55.0 mm of total deflection, and when unloaded, the grillage retains 30.7 mm

of permanent plastic deformation. With a frame span of 2000 mm, and a plastic deformation of 30.7 mm, the L-stiffened panel has a total plastic deformation under 220% design load of 1.5%.
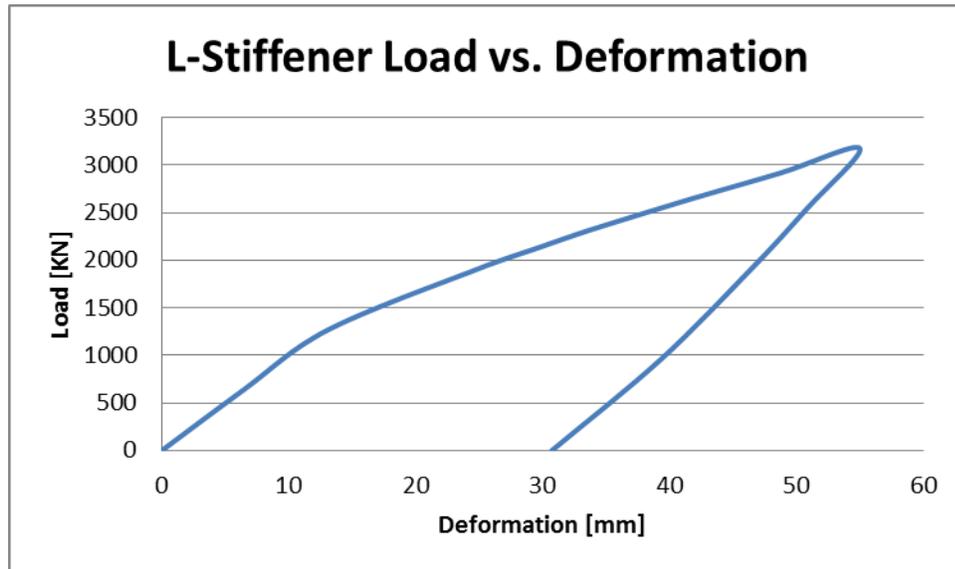


**Figure 4-11: L-stiffener load vs. deflection for 220% design load**

Figure 4-12 shows the load vs. deformation plot for the flat bar-stiffener grillage while being loaded to 220% of the design load, 3.178 MN. Under this load, the flat bar-stiffened grillage experiences 38.2 mm of total deflection, and when unloaded, the grillage retains 20.7 mm of permanent plastic deformation. With a frame span of 2000 mm, and a plastic deformation of 20.7 mm, the flat bar-stiffened panel has a total plastic deformation under 220% design load of 1.0%.

79
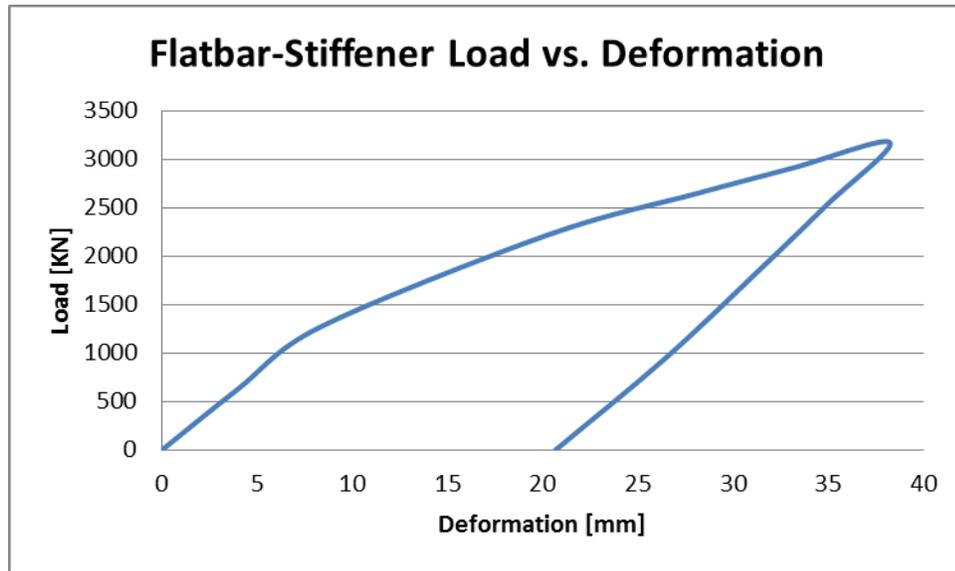
**Figure 4-12: Flat bar-stiffener load vs. deflection for 220% design load**

Figure 4-13 shows the load vs. deformation plot for the bulb-stiffener grillage while being loaded to 220% of the design load, 3.178 MN. Under this load, the bulbflat-stiffened grillage experiences 44.1 mm of total deflection, and when unloaded, the grillage retains 25.0 mm of permanent plastic deformation. With a frame span of 2000 mm, and a plastic deformation of 25.0 mm, the bulb-stiffened panel has a total plastic deformation under 220% design load of 1.25%.
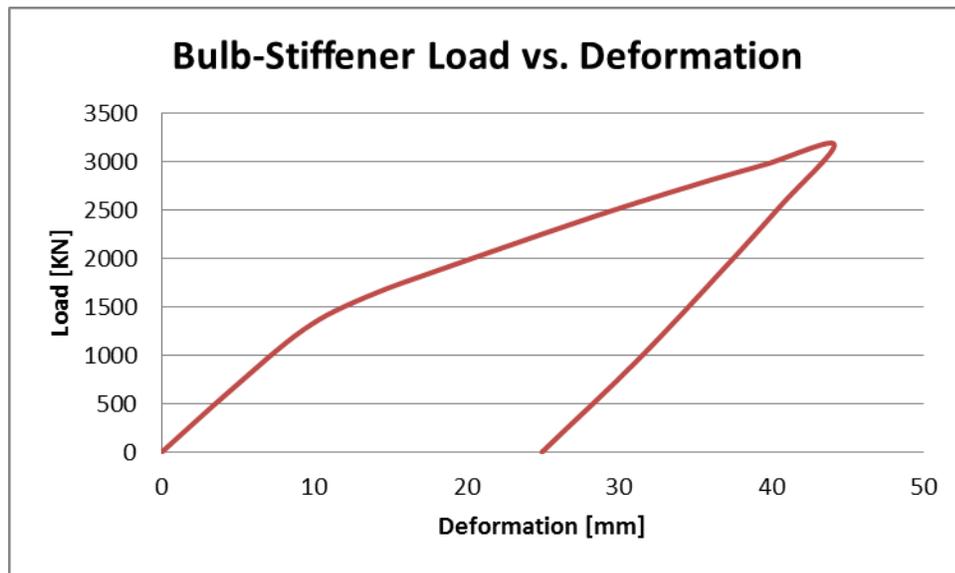
**Figure 4-13: Bulb-stiffener load vs. deflection for 220% design load**

Figure 4-14 shows the load-deformation curves for the four grillages on one plot. It can be seen that the flat bar stiffener performs the best, followed by the bulb-stiffener, then the T-stiffener, while the L-stiffened grillage performed the worst under overload conditions. This data makes it look like the flat bar stiffener is the best stiffener for this scenario. However, due to the excessive cross-sectional area of the flat bar stiffener, it may be too heavy and costly to use.

It should also be noted that none of the stiffeners tested had the webs buckle in this analysis. This may be due to the uniform loading and the lack of cut-outs through the web frames (which would increase non-symmetry in the grillages). It has been seen through experience that the webs of T-stiffeners can buckle during ice loading, resulting in a loss of capacity in the stiffeners, while bulbflat stiffeners have been shown to perform better under similar conditions. A comparison of the buckling of the webs of the different stiffener types would be a very useful study, however it is outside the scope of this work.

81
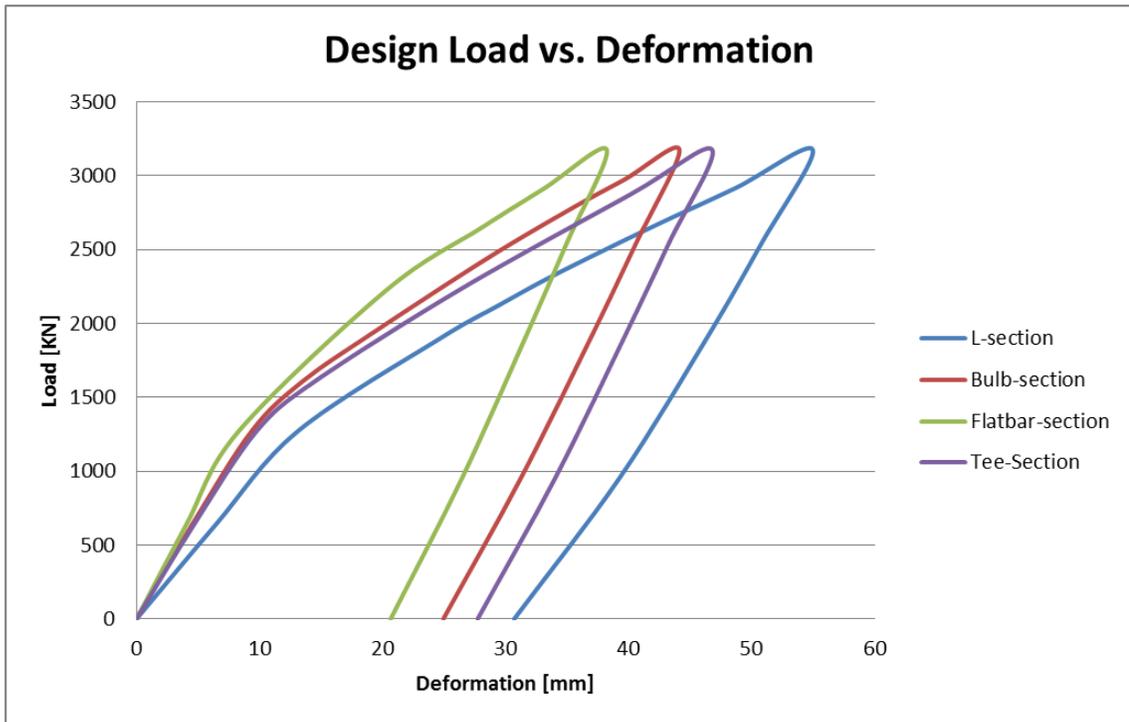
**Figure 4-14: Comparison of load vs. deflection at 220% design load**

Figure 4-15 shows the load vs. deflection curve for the web frames while experiencing a

220% overload. This plot for the web frames is common to the grillages of all stiffener

types. There was no appreciable difference in the response of the web frames on the

grillages with different stiffener types. It can be seen that the web frames experience a

total deflection of 7.0 mm under 220% design load, and a resulting plastic deformation of

0.9 mm. The unloading portion of this curve is not linear. This is due to the plastic

deformation of the other components of the grillage around the web frames. In all loading

cases, the load-deformation curve takes a similar shape during the unloading portion.

82
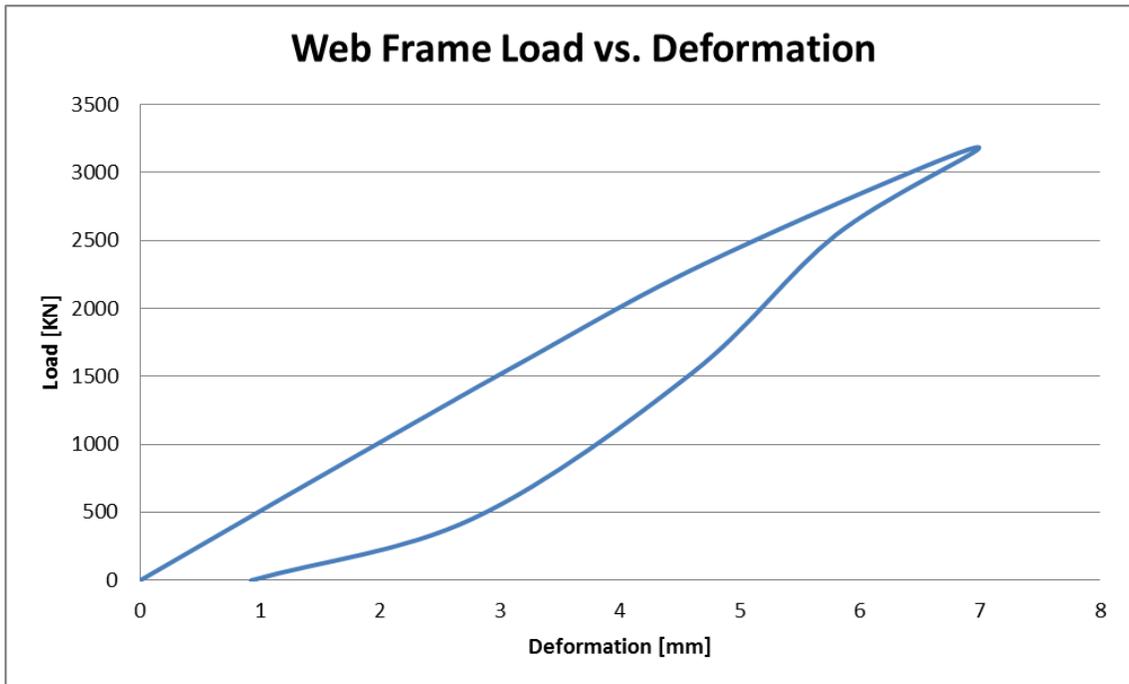
**Figure 4-15: Web frame load vs. deflection for 220% design load**

### 4.8.3. Extreme Overload FE Analysis Results

In this analysis, the grillages were loaded up to 700% of the design load, to 9.576 MN. The loads vs. deformation curves for each of the four grillages up to 700% design load are shown in Figure 4-16, Figure 4-17, Figure 4-18, and Figure 4-19.
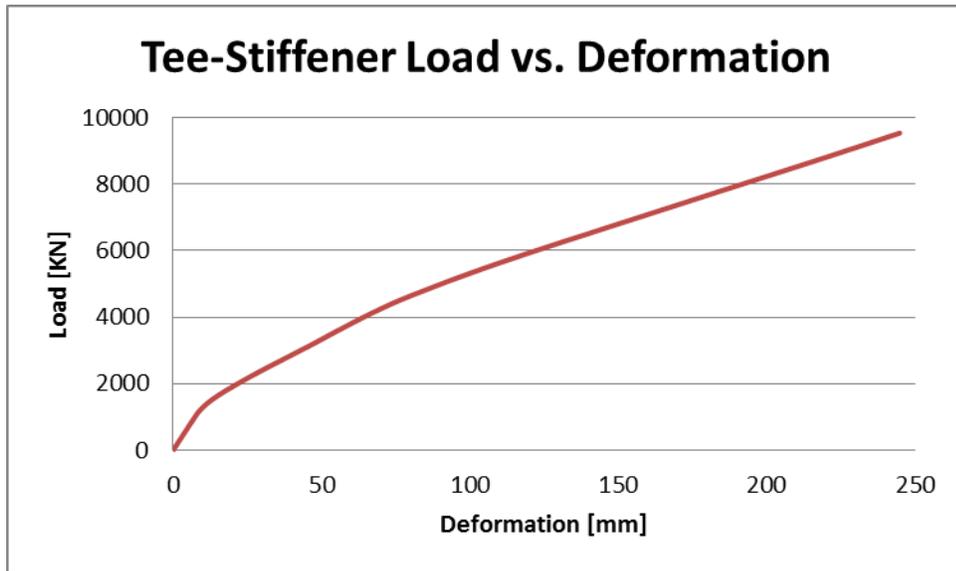
**Figure 4-16: T-stiffener load vs. deflection for 700% design load**
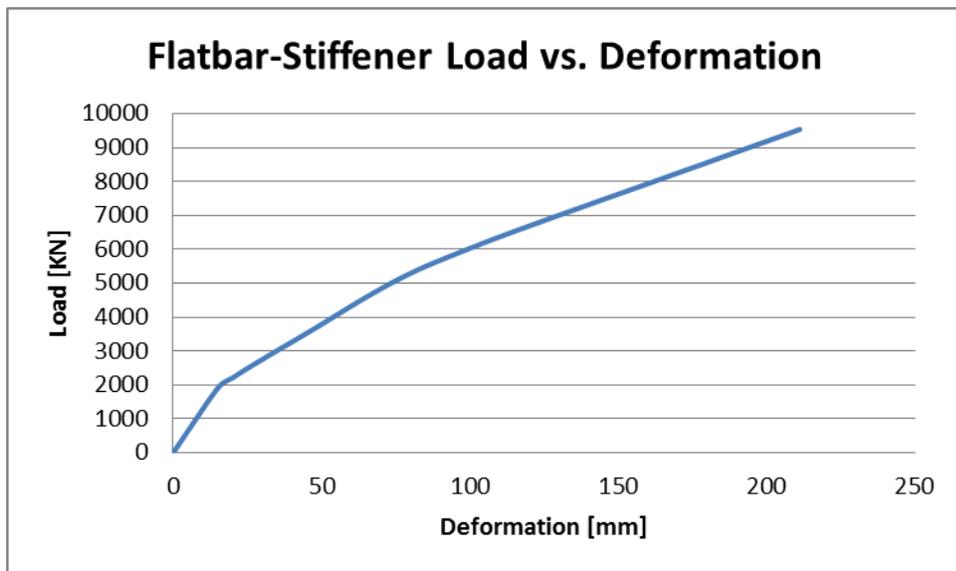


**Figure 4-17: Flat bar-stiffener load vs. deflection for 700% design load**

84
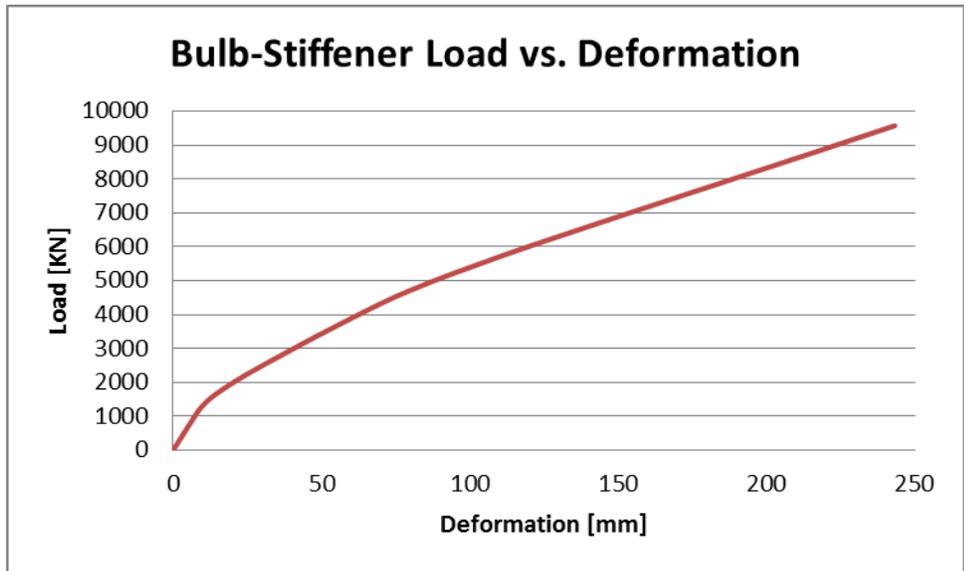
**Figure 4-18: Bulb-stiffener load vs. deflection for 700% design load**
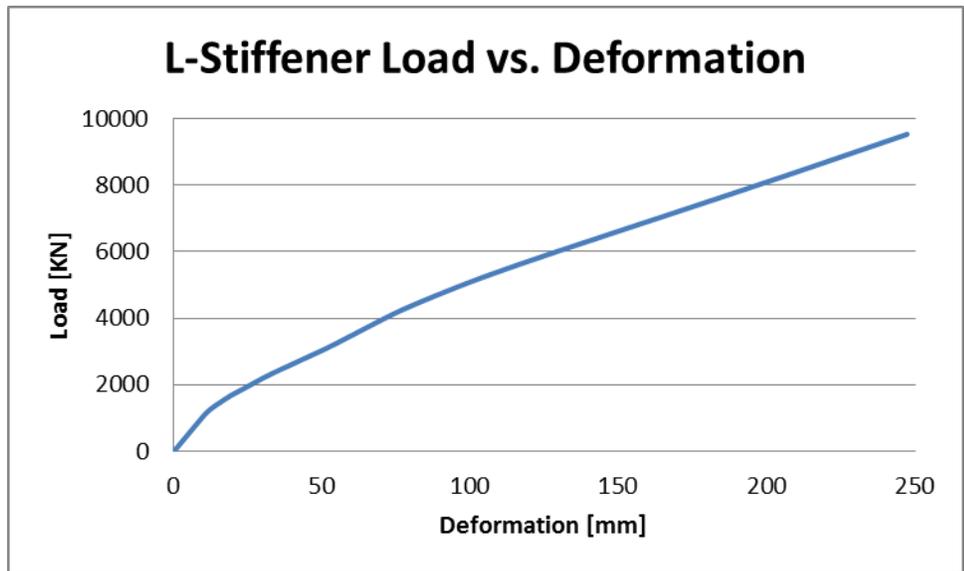


**Figure 4-19: L-stiffener load vs. deflection for 700% design load**

85

Comparing the FE analysis results for the grillages using the different stiffener types (see Figure 4-20), it is observed that all of the grillages have significant overload capacity. Defining deformation as a percentage of the frame span (web frame spacing), the greatest deformation under 700% design load that is encountered is slightly more than 12% of the frame span. This is a significant amount of deformation under load, and the resultant permanent plastic deformation would be in the range of 9% of the length of the frame span.

It can be seen that the frame with the least amount of deformation is the flat bar stiffener type. However, if one considers the cross-section of the stiffeners, it is seen that the steel weight of the rule-compliant flat bar stiffener is double that of the other stiffener types.
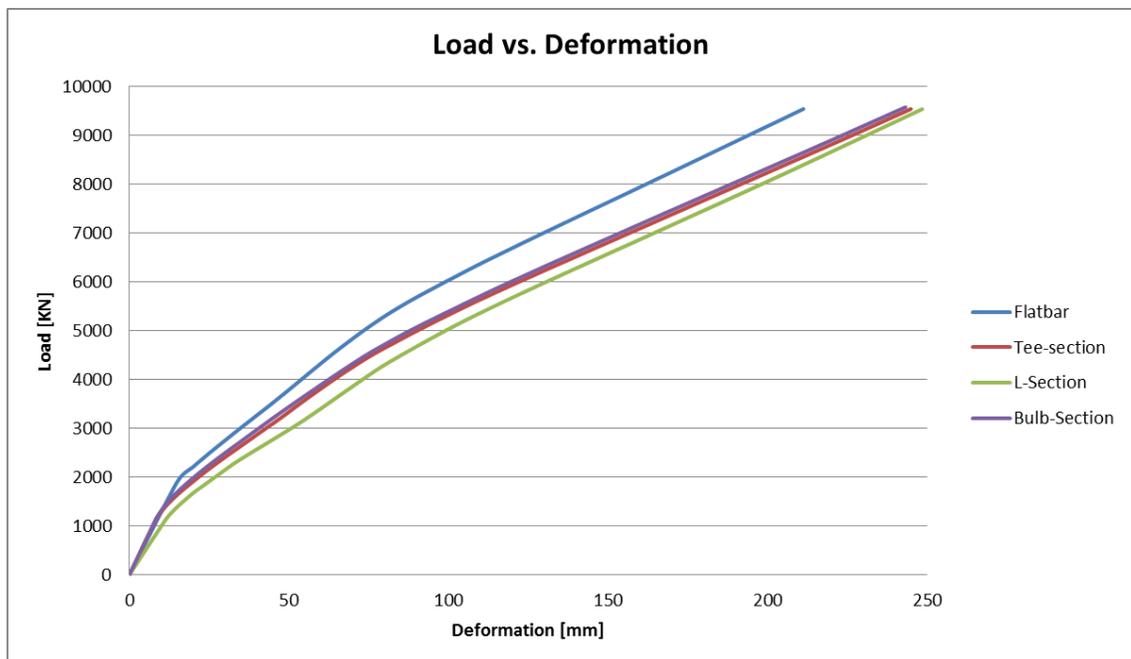


**Figure 4-20: Load vs. deformation ANSYS results for 700% design load**

Figure 4-21 shows the response of the four grillages, while experiencing loads of up to 2.5 MN. The slope of the elastic range of loading for the flat bar, tee, and bulb sections is very close, while the L-section is shown to be less stiff. The elastic range of the flat bar stiffener is seen to be longer, with a higher yield point.
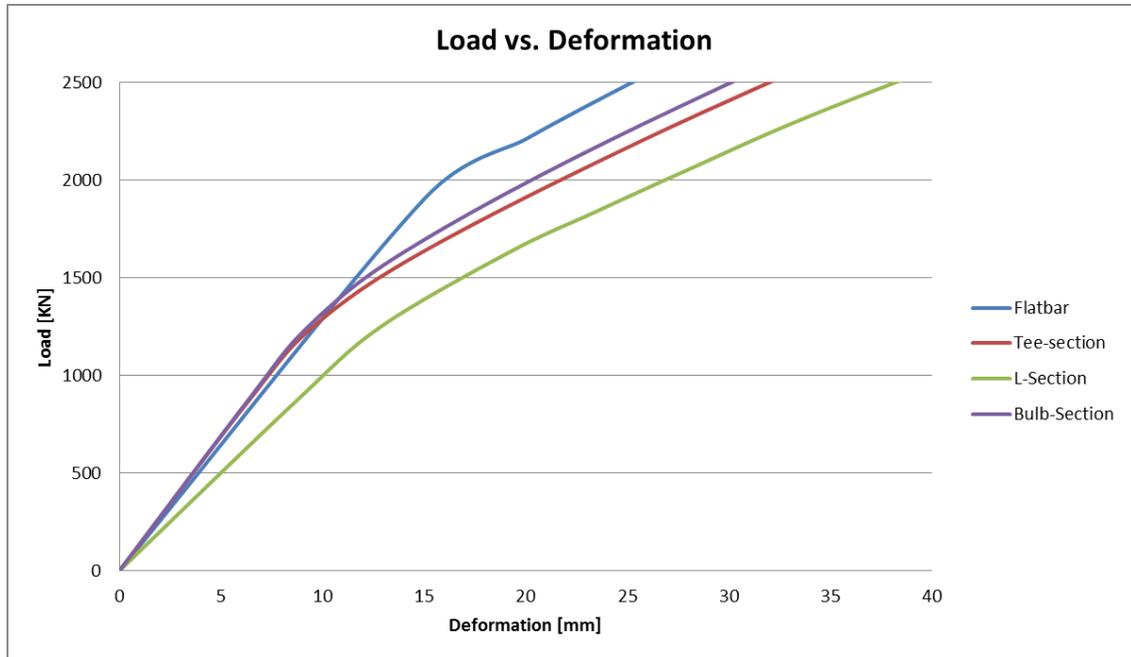


**Figure 4-21: Load vs. deformation results for 700% design load, elastic-plastic transition range**

### 4.9. Conclusion

The FE analysis results show that there is significant plastic deformation in both the web frames, as well as the longitudinal stiffeners under design load. It seems that the amount of plastic deformation over a frame span is well within the accepted range, and the UR I2 requirements are adequate.

The grillages of every stiffener type have been shown to result in extremely strong

87

designs with enormous reserve capacity. The fact that the structures can experience 7 times the design load and still be functional is a testament to this fact.

There is an enormous amount of further work that could be done in this area. Web height-width ratios for stiffeners and web frames, using web frame cut-outs, flange dimensions, stiffener spacing, and web frame spacing are all factors that would affect the performance of a stiffened panel, and there are nearly limitless combinations of different configurations that could be tested. A parametric study or Design of Experiments study of the effects of even some of these parameters would require a huge amount of computing power and time, but would provide valuable information.

## 5. Conclusion

Relative to the original stated research objectives, all objectives have been met, and are addressed in the following discussion.

The large grillage test results provide practical, real-world information about ship-ice interaction. These tests are useful as a validation of existing ship design rules. They provide insight to the actual ice load a ship can handle without sustaining catastrophic structure failure (ie tearing or puncture of the shell plating). Although the structure was not pushed to the point of failure, and it is not known at what load level that might happen, it is a testament to the load capacity of these structures that they withstood several times the design load without failure.

In the results, it can be seen that the slope of the unloading phase is steeper than the slope of the loading phase. This demonstrates that, in addition to strengthening through strain

hardening, the grillage becomes stiffer as a result of the plastic deformation.

A major limitation of these experiments is that due to the size, man hours, and cost involved, it was not possible to repeat the tests with more grillages to get more experimental runs. Ideally, the large grillage tests would be repeated several times to display some consistency of the structural response to the ice loading and explore the effects of strain rate.

In Chapter 3, it can be seen that there is a great deal of understanding and experience required to accurately predict structural response using finite element methods. It took a lot of iterations and practice before realistic results could be achieved using FE analysis. Using finite element methods is an excellent tool to perform structural analysis. However, it is easy to make mistakes, and without experience or physical validation, one can easily achieve incorrect results.

The fidelity of the validation FE analysis is quite good. Having less than a 10% discrepancy between laboratory results and FE analysis results is very hard to achieve when the pressure distribution of the ice-structure interface is not known. Using a uniform pressure distribution resulted in excellent fidelity, and therefore in this case, it was not necessary to use a non-uniform pressure distribution. If one wanted to achieve a higher fidelity FE simulation of structural response to ice loading, there would have to be a focus on achieving an accurate estimate of the ice load pressure distribution, which is a very hard task.

While it is known that the pressure is not uniform during an ice loading event, it us much easier to model the interaction as having a uniform pressure. It was demonstrated that a

89

good agreement can be achieved based on a uniform pressure patch. The accuracy of the numerical results to the experimental results proves this.

Chapter 4 of this thesis used FE analysis to calculate the structural response of a stiffened panel against ice loading, under UR I2 design conditions, and in overload, and extreme overload conditions. It is show in in that section that the UR I2 requirements are adequate for longitudinal stiffener design at the midbody ice belt of a PC7 vessel, at least in the configuration studied in this thesis. The stiffened panels, regardless of the stiffener cross-section type, deformed plastically less than 0.1% of the frame span length, which is an acceptable amount of permanent deformation for design load conditions. 1-2 mm of deflection over a 2 m span is not detectable by the eye, and is not a significant amount of damage for a design scenario.

The rule-compliant flat bar stiffener type was shown to be the stiffest and most robust stiffener out of the four types evaluated. It would be a good idea to revisit the formulation of the UR I2 rules, and consider whether the flat bar stiffener requirements are overly conservative.

Overall, the analysis of ship structures for ice loading is an area where there could be an enormous amount of work done. Full-scale laboratory experiments are a great way to test ice-structure interaction in a controlled environment. Both continued quasi-static and dynamic ice loading experiments on stiffened panel structures would contribute to furthering understanding in this area. However, the magnitude and cost (both monetary and required time commitment) makes it unlikely that a great number of full-scale laboratory ice-structure tests will be done in the near future. The set of experiments

described in Chapter 2 of this thesis was a huge undertaking, and there were only two panels tested. FE analysis is a much faster way of analyzing structural response to ice loading, although the model must be validated by real-world results. The combination of laboratory experiments, followed by extensive FE analysis could result in greatly increasing the knowledge and understanding of the design of ship structures for ice environments.

The results of this thesis have provided and demonstrated a practical approach to analysing icebreaking ship structure. Having a validated FE analysis methodology for the analysis of full-scale ship structure is a very useful tool for the analysis and development of an optimized ship structural arrangement for icebreaking ships.

The current work is limited in its scope to a single area of one polar class of ship, but the same methodology can be employed to predict the structural response of any ship structure to ice loading.

Further research in this area should include more large-scale physical experiments with different stiffener types. An evaluation of the effects of web frame cut-out shape would be a useful study to perform in order to gain insight in that area. Dynamic loading of ship structure (ie. as an impact) in a laboratory setting is another area to explore. Investigating the effects of strain rate on stricture-ice loading events would be an interesting exercise.

# References

Abraham J (2008). Plastic response of ship structure subjected to ice loading. Master of Engineering Thesis, Memorial University.

ABS (2012). Rules for Materials and Welding 2012, Part 2. American Bureau of Shipping.

ANSYS 14.0 software.

Butler TR (2002). An analysis of stiffened plating subject to extreme ice loads. Master of Engineering Thesis, Memorial University.

Daley CG (2002). Derivation of plastic framing requirements for polar ships. Marine Structures 15 (2002) 543-559

Daley CG (2002). Application of plastic framing requirements for polar ships. Marine Structures 15 (2002) 533-542

Daley et al (2003) Ship frame and grillage structural experiments. NRC-IOT Publication Archives.

Daley CG (2004). A study of the process spatial link in ice pressure area relationships. PERD/CHC Report 7-108.

Daley CG, Kendrick A, and Pavic M (2007). New direction in ship structural regulations. 10th International Symposium on Practical Design of Ships and Other Floating Structures.

IACS (2011). I2 Structural requirements for polar class ships. International Association of Classification Societies.

Paik JK (2006). Towards limit state design of ships and offshore structures under impact pressure actions: a state of the art review. Marine Technology, Vol. 43, No. 3, 135-145

Reddy Gudimetla PS, Colbourne B, Daley CG, Bruneau SE, Gagnon R (2012). Strength and pressure profiles from conical ice crushing experiments. Icetech 2012.

Riska K, Kamarainen J (2013).
A review of ice loading and the evolution of the Finnish-Swedish ice class rules. SNAME Annual Meeting, 2013. Society of Naval Architects and Marine Engineers.

SolidWorks 2013 documentation.

# Appendix

**Appendix A:**

**Validation using large grillage experiment**

**ANSYS-generated report**

Project

| | |
|---|---|
| First Saved | Tuesday, October 22, 2013 |
| Last Saved | Sunday, June 08, 2014 |
| Product Version | 14.0 Release |
| Save Project Before Solution | No |
| Save Project After Solution | No |

Contents

- **Units**

- **Model (A4)**

    o Geometry

        ▪ Parts

    o Coordinate Systems

    o Connections

        ▪ Contacts

            ▪ Contact Regions

    o Mesh

Units

TABLE 1

| Unit System | Metric (mm, t, N, s, mV, mA) Degrees rad/s Celsius |
|---|---|
| Angle | Degrees |
| Rotational Velocity | rad/s |
| Temperature | Celsius |

Model (A4)

Geometry

TABLE 2

Model (A4) > Geometry

| Object Name | Geometry |
|---|---|
| State | Fully Defined |
| Definition | |
| Source | C:\Users\Mike M\Desktop\Thesis\Grillage ANSYS |

| | Analysis\updated boundary conditions\Grillage Fixed.IGS |
|---|---|
| Type | Iges |
| Length Unit | Meters |
| Element Control | Program Controlled |
| Display Style | Body Color |
| **Bounding Box** | |
| Length X | 6756.4 mm |
| Length Y | 381. mm |
| Length Z | 2425.7 mm |
| **Properties** | |
| Volume | 2.727e+008 mm³ |
| Mass | 2.1407 t |
| Scale Factor Value | 1. |
| **Statistics** | |
| Bodies | 18 |
| Active Bodies | 18 |
| Nodes | 345043 |
| Elements | 164842 |
| Mesh Metric | None |
| **Basic Geometry Options** | |
| Solid Bodies | Yes |

| | |
|---|---|
| Surface Bodies | Yes |
| Line Bodies | No |
| Parameters | Yes |
| Parameter Key | DS |
| Attributes | No |
| Named Selections | No |
| Material Properties | No |
| Advanced Geometry Options | |
| Use Associativity | Yes |
| Coordinate Systems | No |
| Reader Mode Saves Updated File | No |
| Use Instances | Yes |
| Smart CAD Update | No |
| Attach File Via Temp File | Yes |
| Temporary Directory | C:\Users\Mike M\AppData\Local\Temp |
| Analysis Type | 3-D |
| Mixed Import Resolution | None |
| Decompose Disjoint | Yes |

| Faces | |
|---|---|
| Enclosure and Symmetry Processing | Yes |

TABLE 3

Model (A4) > Geometry > Parts

| Object Name | Part 1 | Part 2 | Part 3 | Part 4 | Part 5 |
|---|---|---|---|---|---|
| State | Meshed | | | | |
| Graphics Properties | | | | | |
| Visible | Yes | | | | |
| Transparency | 1 | | | | |
| Definition | | | | | |
| Suppressed | No | | | | |
| Stiffness Behavior | Flexible | | | | |
| Coordinate System | Default Coordinate System | | | | |
| Reference Temperature | By Environment | | | | |
| Material | | | | | |
| Assignment | Structural Steel | | | | |
| Nonlinear Effects | Yes | | | | |
| Thermal Strain Effects | Yes | | | | |
| Bounding Box | | | | | |
| Length X | 120.65 mm | | 6032.5 mm | | |

| Length Y | 349.25 mm | | 210.32 mm | | |
|---|---|---|---|---|---|
| Length Z | 2425.7 mm | | 101.6 mm | | |
| **Properties** | | | | | |
| Volume | 1.9284e+007 mm³ | | 1.651e+007 mm³ | | |
| Mass | 0.15138 t | | 0.1296 t | | |
| Centroid X | 4022.7 mm | 2009.8 mm | 3016.2 mm | | |
| Centroid Y | 228.93 mm | | 149.72 mm | | |
| Centroid Z | -698.71 mm | | -348.71 mm | -1047.2 mm | -697.96 mm |
| Moment of Inertia Ip1 | 1942.7 t·mm² | | 648.91 t·mm² | | |
| Moment of Inertia Ip2 | 78475 t·mm² | | 3.9308e+005 t·mm² | | |
| Moment of Inertia Ip3 | 80305 t·mm² | | 3.9364e+005 t·mm² | | |
| **Statistics** | | | | | |
| Nodes | 28090 | | 60297 | 60311 | 60300 |
| Elements | 13833 | | 28943 | 28955 | 28946 |
| Mesh Metric | None | | | | |

TABLE 4

Model (A4) > Geometry > Parts

| Object Name | Part 6 | Part 7 | Part 8 | Part 9 | Part 10 |
|---|---|---|---|---|---|
| State | Meshed | | | | |
| **Graphics Properties** | | | | | |
| Visible | Yes | | | | |

| Transparency | 1 | | | | |
|---|---|---|---|---|---|
| **Definition** | | | | | |
| Suppressed | No | | | | |
| Stiffness Behavior | Flexible | | | | |
| Coordinate System | Default Coordinate System | | | | |
| Reference Temperature | By Environment | | | | |
| **Material** | | | | | |
| Assignment | Structural Steel | | | | |
| Nonlinear Effects | Yes | | | | |
| Thermal Strain Effects | Yes | | | | |
| **Bounding Box** | | | | | |
| Length X | 304.8 mm | | | | |
| Length Y | 196.85 mm | | | | |
| Length Z | 31.75 mm | | | | |
| **Properties** | | | | | |
| Volume | 1.3928e+006 mm³ | | | | |
| Mass | 1.0934e-002 t | | | | |
| Centroid X | -150.34 mm | | 6182.8 mm | | |
| Centroid Y | 109.97 mm | | | | |
| Centroid Z | -349.25 mm | -698.5 mm | -1047.8 mm | -349.25 mm | -698.5 mm |
| Moment of Inertia Ip1 | 90.263 t·mm² | | | | |

| | | | | | |
|---|---|---|---|---|---|
| Moment of Inertia Ip2 | 64.899 t·mm² | | | | |
| Moment of Inertia Ip3 | 27.2 t·mm² | | | | |
| **Statistics** | | | | | |
| Nodes | 143 | | | | |
| Elements | 15 | | | | |
| Mesh Metric | None | | | | |

TABLE 5

Model (A4) > Geometry > Parts

| Object Name | Part 11 | Part 12 | Part 13 | Part 14 | Part 15 |
|---|---|---|---|---|---|
| State | Meshed | | | | |
| **Graphics Properties** | | | | | |
| Visible | Yes | | | | |
| Transparency | 1 | | | | |
| **Definition** | | | | | |
| Suppressed | No | | | | |
| Stiffness Behavior | Flexible | | | | |
| Coordinate System | Default Coordinate System | | | | |
| Reference Temperature | By Environment | | | | |
| **Material** | | | | | |
| Assignment | Structural Steel | | | | |

| | | | | | | | |
|---|---|---|---|---|---|---|---|
| Nonlinear Effects | Yes | | | | | | |
| Thermal Strain Effects | Yes | | | | | | |
| **Bounding Box** | | | | | | | |
| Length X | 304.8 mm | | 361.95 mm | | | 31.75 mm | |
| Length Y | 196.85 mm | | 31.75 mm | | | 228.6 mm | |
| Length Z | 31.75 mm | | 1397. mm | | | | |
| **Properties** | | | | | | | |
| Volume | 1.3928e+006 mm³ | | 1.6054e+007 mm³ | | | 1.0139e+007 mm³ | |
| Mass | 1.0934e-002 t | | 0.12603 t | | | 7.9595e-002 t | |
| Centroid X | 6182.8 mm | | -180.97 mm | 6213.5 mm | 6048.4 mm | -15.875 mm | |
| Centroid Y | 109.97 mm | | 6.35 mm | | | 136.53 mm | |
| Centroid Z | -1047.7 mm | | -698.5 mm | | | | |
| Moment of Inertia Ip1 | 90.263 t·mm² | | 1386.4 t·mm² | | | 12952 t·mm² | |
| Moment of Inertia Ip2 | 64.899 t·mm² | | 21872 t·mm² | | | 353.31 t·mm² | |
| Moment of Inertia Ip3 | 27.2 t·mm² | | 20507 t·mm² | | | 13291 t·mm² | |
| **Statistics** | | | | | | | |
| Nodes | 143 | | 668 | | | 434 | |
| Elements | 15 | | 80 | | | 48 | |

| Mesh Metric | None |
|---|---|

TABLE 6

Model (A4) > Geometry > Parts

| Object Name | Part 16 | Part 17 | Part 18 |
|---|---|---|---|
| State | Meshed | | |
| **Graphics Properties** | | | |
| Visible | Yes | | |
| Transparency | 1 | | |
| **Definition** | | | |
| Suppressed | No | | |
| Stiffness Behavior | Flexible | | |
| Coordinate System | Default Coordinate System | | |
| Reference Temperature | By Environment | | |
| **Material** | | | |
| Assignment | Structural Steel | | |
| Nonlinear Effects | Yes | | |
| Thermal Strain Effects | Yes | | |
| **Bounding Box** | | | |
| Length X | 6756.4 mm | | 6032.5 mm |
| Length Y | 101.6 mm | | 9.525 mm |
| Length Z | 31.75 mm | | 1397. mm |

| Properties | | | |
|---|---|---|---|
| Volume | 2.1795e+007 mm³ | | 8.0271e+007 mm³ |
| Mass | 0.17109 t | | 0.63013 t |
| Centroid X | 3016.3 mm | | 3016.2 mm |
| Centroid Y | 28.575 mm | | 4.7625 mm |
| Centroid Z | -1412.9 mm | 15.875 mm | -698.5 mm |
| Moment of Inertia Ip1 | 161.55 t·mm² | | 1.0248e+005 t·mm² |
| Moment of Inertia Ip2 | 6.5085e+005 t·mm² | | 2.0134e+006 t·mm² |
| Moment of Inertia Ip3 | 6.5098e+005 t·mm² | | 1.9109e+006 t·mm² |
| Statistics | | | |
| Nodes | 1476 | | 101941 |
| Elements | 154 | | 49678 |
| Mesh Metric | None | | |

Coordinate Systems

TABLE 7

Model (A4) > Coordinate Systems > Coordinate System

| Object Name | Global Coordinate System |
|---|---|
| State | Fully Defined |
| Definition | |
| Type | Cartesian |
| Coordinate System ID | 0. |

| Origin | |
|---|---|
| Origin X | 0. mm |
| Origin Y | 0. mm |
| Origin Z | 0. mm |
| Directional Vectors | |
| X Axis Data | [ 1. 0. 0. ] |
| Y Axis Data | [ 0. 1. 0. ] |
| Z Axis Data | [ 0. 0. 1. ] |

Connections

TABLE 8

Model (A4) > Connections

| Object Name | Connections |
|---|---|
| State | Fully Defined |
| Auto Detection | |
| Generate Automatic Connection On Refresh | Yes |
| Transparency | |
| Enabled | Yes |

TABLE 9

Model (A4) > Connections > Contacts

| Object Name | Contacts |
|---|---|
| State | Fully Defined |

| Definition | |
|---|---|
| Connection Type | Contact |
| **Scope** | |
| Scoping Method | Geometry Selection |
| Geometry | All Bodies |
| **Auto Detection** | |
| Tolerance Type | Slider |
| Tolerance Slider | 0. |
| Tolerance Value | 17.972 mm |
| Use Range | No |
| Face/Face | Yes |
| Face/Edge | No |
| Edge/Edge | No |
| Priority | Include All |
| Group By | Bodies |
| Search Across | Bodies |

TABLE 10

Model (A4) > Connections > Contacts > Contact Regions

| Object Name | Contact Region 6 | Contact Region 12 | Contact Region 15 | Contact Region 17 | Contact Region 20 |
|---|---|---|---|---|---|
| State | Fully Defined | | | | |

| Scope | | | | |
|---|---|---|---|---|
| Scoping Method | Geometry Selection | | | |
| Contact | 4 Faces | | 1 Face | |
| Target | 1 Face | | | |
| Contact Bodies | Part 1 | Part 2 | Part 3 | Part 4 |
| Target Bodies | Part 18 | | Part 14 | Part 18 | Part 14 |
| Definition | | | | |
| Type | Bonded | | | |
| Scope Mode | Automatic | | | |
| Behavior | Program Controlled | | | |
| Suppressed | No | | | |
| Advanced | | | | |
| Formulation | Program Controlled | | | |
| Detection Method | Program Controlled | | | |
| Normal Stiffness | Program Controlled | | | |
| Update Stiffness | Program Controlled | | | |
| Pinball Region | Program Controlled | | | |

TABLE 11

Model (A4) > Connections > Contacts > Contact Regions

| Object Name | Contact Region 22 | Contact Region 25 | Contact Region 27 | Contact Region 41 | Contact Region 23 |
|---|---|---|---|---|---|
| State | Fully Defined | | | | |
| Scope | | | | | |
| Scoping Method | Geometry Selection | | | | |
| Contact | 1 Face | | | | |
| Target | 1 Face | | | | |
| Contact Bodies | Part 4 | Part 5 | | Part 12 | Part 1 |
| Target Bodies | Part 18 | Part 14 | Part 18 | Part 16 | Part 3 |
| Definition | | | | | |
| Type | Bonded | | | | |
| Scope Mode | Automatic | | | | |
| Behavior | Program Controlled | | | | |
| Suppressed | No | | | | |
| Advanced | | | | | |
| Formulation | Program Controlled | | | | |
| Detection Method | Program Controlled | | | | |

| | | | | | |
|---|---|---|---|---|---|
| Normal Stiffness | Program Controlled | | | | |
| Update Stiffness | Program Controlled | | | | |
| Pinball Region | Program Controlled | | | | |

TABLE 12

Model (A4) > Connections > Contacts > Contact Regions

| Object Name | Contact Region 24 | Contact Region 26 | Contact Region 28 | Contact Region 30 | Contact Region 32 |
|---|---|---|---|---|---|
| State | Fully Defined | | | | |
| Scope | | | | | |
| Scoping Method | Geometry Selection | | | | |
| Contact | 1 Face | | | | |
| Target | 1 Face | | | | |
| Contact Bodies | Part 1 | | | | Part 2 |
| Target Bodies | Part 4 | Part 5 | Part 16 | Part 17 | Part 3 |
| Definition | | | | | |
| Type | Bonded | | | | |
| Scope Mode | Automatic | | | | |
| Behavior | Program Controlled | | | | |

| Suppressed | No |
| --- | --- |
| Advanced | |
| Formulation | Program Controlled |
| Detection Method | Program Controlled |
| Normal Stiffness | Program Controlled |
| Update Stiffness | Program Controlled |
| Pinball Region | Program Controlled |

TABLE 13

Model (A4) > Connections > Contacts > Contact Regions

| Object Name | Contact Region 34 | Contact Region 36 | Contact Region 38 | Contact Region 40 | Contact Region 42 |
| --- | --- | --- | --- | --- | --- |
| State | Fully Defined | | | | |
| Scope | | | | | |
| Scoping Method | Geometry Selection | | | | |
| Contact | 1 Face | | | | |
| Target | 1 Face | | | | |
| Contact Bodies | Part 2 | | | | Part 3 |

| Target Bodies | Part 4 | Part 5 | Part 16 | Part 17 | Part 12 |
|---|---|---|---|---|---|
| Definition | | | | | |
| Type | Bonded | | | | |
| Scope Mode | Automatic | | | | |
| Behavior | Program Controlled | | | | |
| Suppressed | No | | | | |
| Advanced | | | | | |
| Formulation | Program Controlled | | | | |
| Detection Method | Program Controlled | | | | |
| Normal Stiffness | Program Controlled | | | | |
| Update Stiffness | Program Controlled | | | | |
| Pinball Region | Program Controlled | | | | |

TABLE 14

Model (A4) > Connections > Contacts > Contact Regions

| Object Name | Contact Region 43 | Contact Region 44 | Contact Region 45 | Contact Region 46 | Contact Region 47 |
|---|---|---|---|---|---|
| State | Fully Defined | | | | |
| Scope | | | | | |

| Scoping Method | Geometry Selection | | | | |
|---|---|---|---|---|---|
| Contact | 1 Face | | | | |
| Target | 1 Face | | | | |
| Contact Bodies | Part 3 | | | Part 4 | |
| Target Bodies | Part 13 | Part 15 | Part 12 | Part 13 | Part 15 |
| **Definition** | | | | | |
| Type | Bonded | | | | |
| Scope Mode | Automatic | | | | |
| Behavior | Program Controlled | | | | |
| Suppressed | No | | | | |
| **Advanced** | | | | | |
| Formulation | Program Controlled | | | | |
| Detection Method | Program Controlled | | | | |
| Normal Stiffness | Program Controlled | | | | |
| Update Stiffness | Program Controlled | | | | |
| Pinball Region | Program Controlled | | | | |

TABLE 15

Model (A4) > Connections > Contacts > Contact Regions

| Object Name | Contact Region 49 | Contact Region 51 | Contact Region 52 | Contact Region 53 | Contact Region 54 |
|---|---|---|---|---|---|
| State | Fully Defined | | | | |
| Scope | | | | | |
| Scoping Method | Geometry Selection | | | | |
| Contact | 1 Face | | | | |
| Target | 1 Face | | | | |
| Contact Bodies | Part 5 | | | Part 6 | |
| Target Bodies | Part 12 | Part 13 | Part 15 | Part 12 | Part 15 |
| Definition | | | | | |
| Type | Bonded | | | | |
| Scope Mode | Automatic | | | | |
| Behavior | Program Controlled | | | | |
| Suppressed | No | | | | |
| Advanced | | | | | |
| Formulation | Program Controlled | | | | |
| Detection Method | Program Controlled | | | | |

| | | | | | |
|---|---|---|---|---|---|
| Normal Stiffness | Program Controlled | | | | |
| Update Stiffness | Program Controlled | | | | |
| Pinball Region | Program Controlled | | | | |

TABLE 16

Model (A4) > Connections > Contacts > Contact Regions

| Object Name | Contact Region 55 | Contact Region 56 | Contact Region 57 | Contact Region 58 | Contact Region 59 |
|---|---|---|---|---|---|
| State | Fully Defined | | | | |
| Scope | | | | | |
| Scoping Method | Geometry Selection | | | | |
| Contact | 1 Face | | | | |
| Target | 1 Face | | | | |
| Contact Bodies | Part 7 | | Part 8 | | Part 9 |
| Target Bodies | Part 12 | Part 15 | Part 12 | Part 15 | Part 13 |
| Definition | | | | | |
| Type | Bonded | | | | |
| Scope Mode | Automatic | | | | |
| Behavior | Program Controlled | | | | |

| | | |
|---|---|---|
| Suppressed | No | |
| **Advanced** | | |
| Formulation | Program Controlled | |
| Detection Method | Program Controlled | |
| Normal Stiffness | Program Controlled | |
| Update Stiffness | Program Controlled | |
| Pinball Region | Program Controlled | |

TABLE 17

Model (A4) > Connections > Contacts > Contact Regions

| Object Name | Contact Region 60 | Contact Region 61 | Contact Region 62 | Contact Region 63 | Contact Region 64 |
|---|---|---|---|---|---|
| State | Fully Defined | | | | |
| **Scope** | | | | | |
| Scoping Method | Geometry Selection | | | | |
| Contact | 1 Face | | | | |
| Target | 1 Face | | | | |
| Contact Bodies | Part 9 | Part 10 | | Part 11 | |

| Target Bodies | Part 14 | Part 13 | Part 14 | Part 13 | Part 14 |
|---|---|---|---|---|---|
| Definition | | | | | |
| Type | Bonded | | | | |
| Scope Mode | Automatic | | | | |
| Behavior | Program Controlled | | | | |
| Suppressed | No | | | | |
| Advanced | | | | | |
| Formulation | Program Controlled | | | | |
| Detection Method | Program Controlled | | | | |
| Normal Stiffness | Program Controlled | | | | |
| Update Stiffness | Program Controlled | | | | |
| Pinball Region | Program Controlled | | | | |

TABLE 18

Model (A4) > Connections > Contacts > Contact Regions

| Object Name | Contact Region 65 | Contact Region 66 | Contact Region 67 | Contact Region 68 | Contact Region 69 |
|---|---|---|---|---|---|
| State | Fully Defined | | | | |
| Scope | | | | | |

| Scoping Method | Geometry Selection | | | | |
|---|---|---|---|---|---|
| Contact | 1 Face | | | | |
| Target | 1 Face | | | | |
| Contact Bodies | Part 12 | | | Part 13 | |
| Target Bodies | Part 15 | Part 17 | Part 18 | Part 14 | Part 16 |
| **Definition** | | | | | |
| Type | Bonded | | | | |
| Scope Mode | Automatic | | | | |
| Behavior | Program Controlled | | | | |
| Suppressed | No | | | | |
| **Advanced** | | | | | |
| Formulation | Program Controlled | | | | |
| Detection Method | Program Controlled | | | | |
| Normal Stiffness | Program Controlled | | | | |
| Update Stiffness | Program Controlled | | | | |
| Pinball Region | Program Controlled | | | | |

TABLE 19

Model (A4) > Connections > Contacts > Contact Regions

| Object Name | Contact Region 70 | Contact Region 71 | Contact Region 72 | Contact Region 73 | Contact Region 74 |
|---|---|---|---|---|---|
| State | Fully Defined | | | | |
| Scope | | | | | |
| Scoping Method | Geometry Selection | | | | |
| Contact | 1 Face | | | | |
| Target | 1 Face | | | | |
| Contact Bodies | Part 13 | | Part 14 | | Part 15 |
| Target Bodies | Part 17 | Part 18 | Part 16 | Part 17 | Part 16 |
| Definition | | | | | |
| Type | Bonded | | | | |
| Scope Mode | Automatic | | | | |
| Behavior | Program Controlled | | | | |
| Suppressed | No | | | | |
| Advanced | | | | | |
| Formulation | Program Controlled | | | | |
| Detection Method | Program Controlled | | | | |

| | | | | |
|---|---|---|---|---|
| Normal Stiffness | Program Controlled | | | |
| Update Stiffness | Program Controlled | | | |
| Pinball Region | Program Controlled | | | |

TABLE 20

Model (A4) > Connections > Contacts > Contact Regions

| Object Name | Contact Region 75 | Contact Region 76 | Contact Region 77 | Contact Region 78 |
|---|---|---|---|---|
| State | Fully Defined | | | |
| **Scope** | | | | |
| Scoping Method | Geometry Selection | | | |
| Contact | 1 Face | | | |
| Target | 1 Face | | | |
| Contact Bodies | Part 15 | | Part 16 | Part 17 |
| Target Bodies | Part 17 | Part 18 | | |
| **Definition** | | | | |
| Type | Bonded | | | |
| Scope Mode | Automatic | | | |
| Behavior | Program Controlled | | | |
| Suppressed | No | | | |

| Advanced | |
|---|---|
| Formulation | Program Controlled |
| Detection Method | Program Controlled |
| Normal Stiffness | Program Controlled |
| Update Stiffness | Program Controlled |
| Pinball Region | Program Controlled |

Mesh

TABLE 21

Model (A4) > Mesh

| Object Name | Mesh |
|---|---|
| State | Solved |
| Defaults | |
| Physics Preference | Mechanical |
| Relevance | 40 |
| Sizing | |
| Use Advanced Size Function | Off |
| Relevance Center | Fine |
| Element Size | Default |
| Initial Size Seed | Active Assembly |
| Smoothing | Medium |

| | |
|---|---|
| Transition | Fast |
| Span Angle Center | Coarse |
| Minimum Edge Length | 8.45470 mm |
| **Inflation** | |
| Use Automatic Inflation | None |
| Inflation Option | Smooth Transition |
| Transition Ratio | 0.272 |
| Maximum Layers | 5 |
| Growth Rate | 1.2 |
| Inflation Algorithm | Pre |
| View Advanced Options | No |
| **Patch Conforming Options** | |
| Triangle Surface Mesher | Program Controlled |
| **Advanced** | |
| Shape Checking | Standard Mechanical |
| Element Midside Nodes | Program Controlled |
| Straight Sided Elements | No |
| Number of Retries | Default (4) |
| Extra Retries For Assembly | Yes |
| Rigid Body Behavior | Dimensionally Reduced |
| Mesh Morphing | Disabled |

| Defeaturing | |
|---|---|
| Pinch Tolerance | Please Define |
| Generate Pinch on Refresh | No |
| Automatic Mesh Based Defeaturing | On |
| Defeaturing Tolerance | Default |
| Statistics | |
| Nodes | 345043 |
| Elements | 164842 |
| Mesh Metric | None |

TABLE 22

Model (A4) > Mesh > Mesh Controls

| Object Name | Refinement | Refinement 2 | Refinement 3 |
|---|---|---|---|
| State | Fully Defined | | |
| Scope | | | |
| Scoping Method | Geometry Selection | | |
| Geometry | 24 Faces | 29 Faces | 5 Faces |
| Definition | | | |
| Suppressed | No | | |
| Refinement | 1 | | |

Static Structural (A5)

TABLE 23

Model (A4) > Analysis

| Object Name | Static Structural (A5) |
|---|---|
| State | Solved |
| Definition | |
| Physics Type | Structural |
| Analysis Type | Static Structural |
| Solver Target | Mechanical APDL |
| Options | |
| Environment Temperature | 22. °C |
| Generate Input Only | No |

TABLE 24

Model (A4) > Static Structural (A5) > Analysis Settings

| Object Name | Analysis Settings |
|---|---|
| State | Fully Defined |
| Step Controls | |
| Number Of Steps | 2. |
| Current Step Number | 1. |
| Step End Time | 1. s |
| Auto Time | Program Controlled |

| | |
|---|---|
| Stepping | |
| Solver Controls | |
| Solver Type | Program Controlled |
| Weak Springs | Program Controlled |
| Large Deflection | On |
| Inertia Relief | Off |
| Restart Controls | |
| Generate Restart Points | Program Controlled |
| Retain Files After Full Solve | No |
| Nonlinear Controls | |
| Force Convergence | Program Controlled |
| Moment Convergence | Program Controlled |
| Displacement Convergence | Program Controlled |
| Rotation Convergence | Program Controlled |
| Line Search | Program Controlled |

| | |
|---|---|
| Stabilization | Off |
| **Output Controls** | |
| Stress | Yes |
| Strain | Yes |
| Nodal Forces | No |
| Contact Miscellaneous | No |
| General Miscellaneous | No |
| Calculate Results At | All Time Points |
| Max Number of Result Sets | Program Controlled |
| **Analysis Data Management** | |
| Solver Files Directory | C:\Users\Mike M\Desktop\Thesis\Grillage ANSYS Analysis\40cm patch load off center 2cm\corrected clearances- 375mpa yield-1500TM-test1_files\dp0\SYS\MECH\ |
| Future Analysis | None |
| Scratch Solver Files Directory | |
| Save MAPDL db | No |

| | |
|---|---|
| Delete Unneeded Files | Yes |
| Nonlinear Solution | Yes |
| Solver Units | Active System |
| Solver Unit System | nmm |

TABLE 25

Model (A4) > Static Structural (A5) > Analysis Settings

Step-Specific "Step Controls"

| Step | Step End Time |
|---|---|
| 1 | 1. s |
| 2 | 2. s |

TABLE 26

Model (A4) > Static Structural (A5) > Analysis Settings

Step-Specific "Output Controls"

| Step | Max Number of Result Sets |
|---|---|
| 1 | Program Controlled |
| 2 | 1000. |

TABLE 27

Model (A4) > Static Structural (A5) > Loads

| Object Name | Force | Fixed Support |
|---|---|---|

| State | Fully Defined | |
|---|---|---|
| Scope | | |
| Scoping Method | Geometry Selection | |
| Geometry | 1 Face | 6 Faces |
| Definition | | |
| Type | Force | Fixed Support |
| Define By | Vector | |
| Magnitude | Tabular Data | |
| Direction | Defined | |
| Suppressed | No | |

FIGURE 1

Model (A4) > Static Structural (A5) > Force
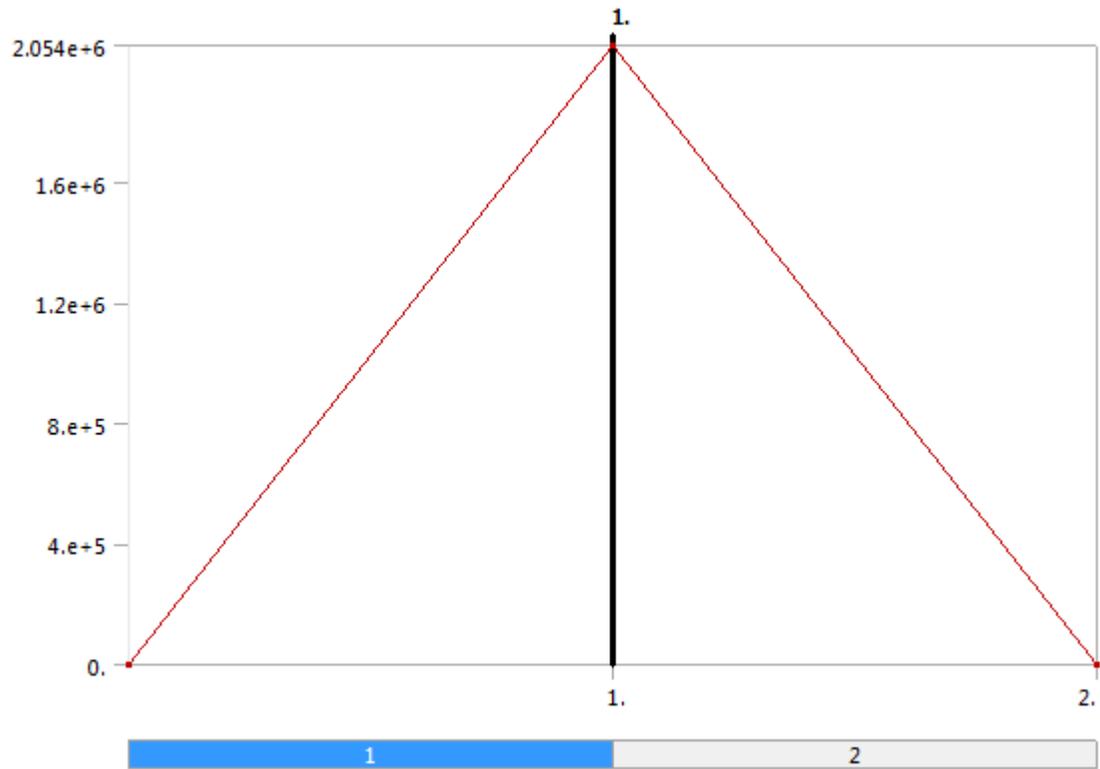
TABLE 28

Model (A4) > Static Structural (A5) > Force

| Steps | Time [s] | Force [N] |
|---|---|---|
| 1 | 0. | 0. |
| | 1. | 2.054e+006 |
| 2 | 2. | 0. |

Solution (A6)

TABLE 29

Model (A4) > Static Structural (A5) > Solution

| Object Name | Solution (A6) |
|---|---|

| State | Solved |
|---|---|
| Adaptive Mesh Refinement | |
| Max Refinement Loops | 1. |
| Refinement Depth | 2. |
| Information | |
| Status | Done |

TABLE 30

Model (A4) > Static Structural (A5) > Solution (A6) > Solution Information

| Object Name | Solution Information |
|---|---|
| State | Solved |
| Solution Information | |
| Solution Output | Force Convergence |
| Newton-Raphson Residuals | 0 |
| Update Interval | 2.5 s |
| Display Points | All |
| FE Connection Visibility | |
| Activate Visibility | Yes |
| Display | All FE Connectors |
| Draw Connections Attached To | All Nodes |
| Line Color | Connection Type |
| Visible on Results | No |

| Line Thickness | Single |
|---|---|
| Display Type | Lines |

FIGURE 2

Model (A4) > Static Structural (A5) > Solution (A6) > Solution Information
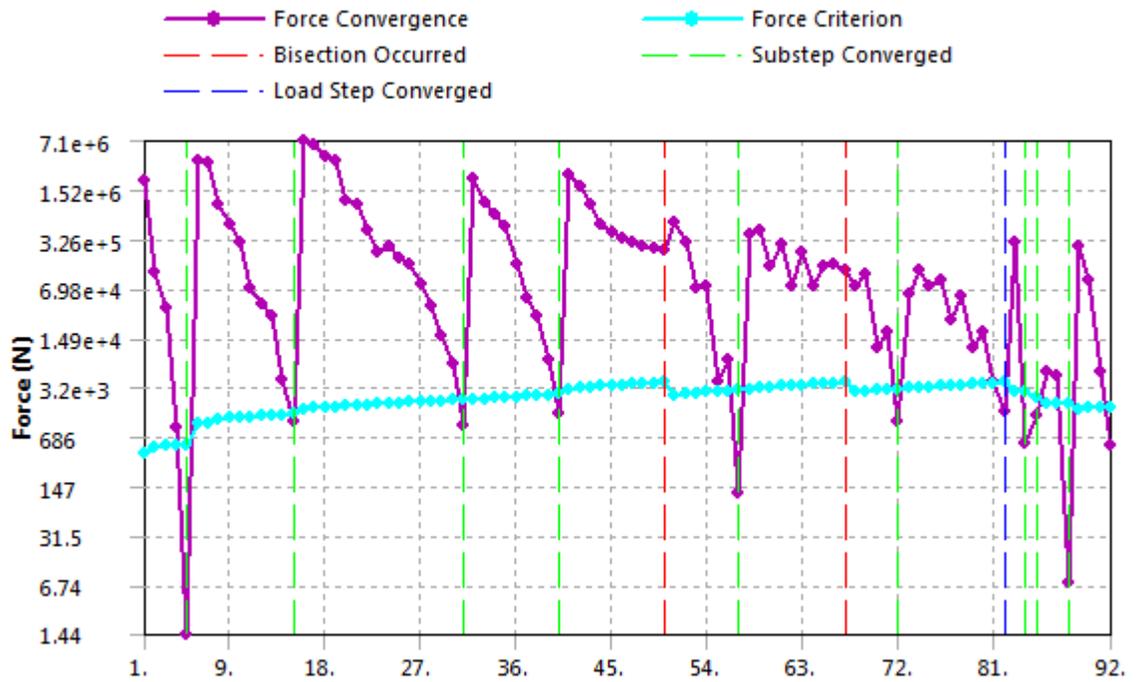


FIGURE 3

Model (A4) > Static Structural (A5) > Solution (A6) > Solution Information
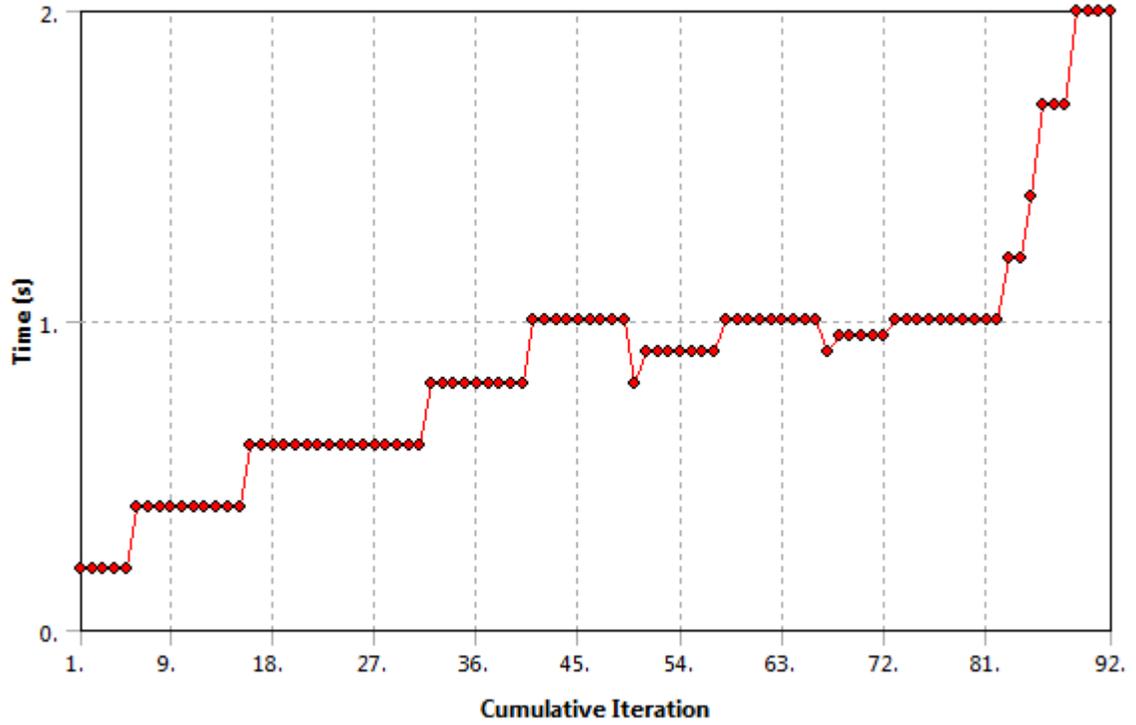
TABLE 31

Model (A4) > Static Structural (A5) > Solution (A6) > Results

| Object Name | Total Deformation |
|---|---|
| State | Solved |
| Scope | |
| Scoping Method | Geometry Selection |
| Geometry | All Bodies |
| Definition | |
| Type | Total Deformation |
| By | Time |

| | |
|---|---|
| Display Time | 1. s |
| Calculate Time History | Yes |
| Identifier | |
| Suppressed | No |
| **Results** | |
| Minimum | 0. mm |
| Maximum | 109.3 mm |
| Minimum Occurs On | Part 1 |
| Maximum Occurs On | Part 5 |
| **Minimum Value Over Time** | |
| Minimum | 0. mm |
| Maximum | 0. mm |
| **Maximum Value Over Time** | |
| Minimum | 8.397 mm |
| Maximum | 109.3 mm |
| **Information** | |
| Time | 1. s |
| Load Step | 1 |
| Substep | 7 |
| Iteration Number | 82 |

FIGURE 4

Model (A4) > Static Structural (A5) > Solution (A6) > Total Deformation
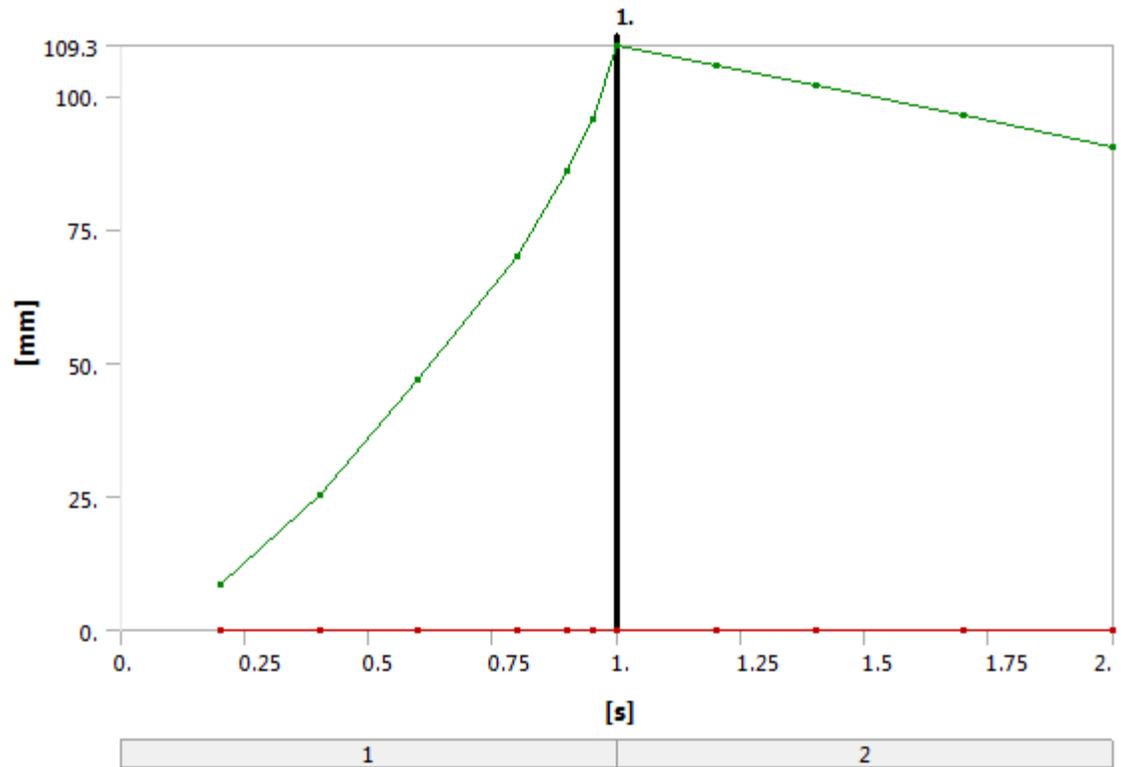


TABLE 32

Model (A4) > Static Structural (A5) > Solution (A6) > Total Deformation

| Time [s] | Minimum [mm] | Maximum [mm] |
|----------|--------------|--------------|
| 0.2      |              | 8.397        |
| 0.4      |              | 25.186       |
| 0.6      | 0.           | 46.786       |
| 0.8      |              | 69.886       |
| 0.9      |              | 85.931       |

| | | |
|---|---|---|
| 0.95 | | 95.723 |
| 1. | | 109.3 |
| 1.2 | | 105.53 |
| 1.4 | | 101.77 |
| 1.7 | | 96.286 |
| 2. | | 90.369 |

Material Data

Structural Steel

TABLE 33

Structural Steel > Constants

| Density | 7.85e-009 tonne mm^-3 |
|---|---|
| Coefficient of Thermal Expansion | 1.2e-005 C^-1 |
| Specific Heat | 4.34e+008 mJ tonne^-1 C^-1 |
| Thermal Conductivity | 6.05e-002 W mm^-1 C^-1 |
| Resistivity | 1.7e-004 ohm mm |

TABLE 34

Structural Steel > Compressive Ultimate Strength

| Compressive Ultimate Strength MPa |
|---|
| 460 |

TABLE 35

Structural Steel > Compressive Yield Strength

| Compressive Yield Strength MPa |
| --- |
| 409 |

TABLE 36

Structural Steel > Tensile Yield Strength

| Tensile Yield Strength MPa |
| --- |
| 409 |

TABLE 37

Structural Steel > Tensile Ultimate Strength

| Tensile Ultimate Strength MPa |
| --- |
| 460 |

TABLE 38

Structural Steel > Isotropic Secant Coefficient of Thermal Expansion

| Reference Temperature C |
| --- |
| 22 |

TABLE 39

Structural Steel > Alternating Stress Mean Stress

| Alternating Stress MPa | Cycles | Mean Stress MPa |
| --- | --- | --- |
| 3999 | 10 | 0 |
| 2827 | 20 | 0 |
| 1896 | 50 | 0 |
| 1413 | 100 | 0 |

| | | |
|---|---|---|
| 1069 | 200 | 0 |
| 441 | 2000 | 0 |
| 262 | 10000 | 0 |
| 214 | 20000 | 0 |
| 138 | 1.e+005 | 0 |
| 114 | 2.e+005 | 0 |
| 86.2 | 1.e+006 | 0 |

TABLE 40

Structural Steel > Strain-Life Parameters

| Strength Coefficient MPa | Strength Exponent | Ductility Coefficient | Ductility Exponent | Cyclic Strength Coefficient MPa | Cyclic Strain Hardening Exponent |
|---|---|---|---|---|---|
| 920 | -0.106 | 0.213 | -0.47 | 1000 | 0.2 |

TABLE 41

Structural Steel > Isotropic Elasticity

| Temperature C | Young's Modulus MPa | Poisson's Ratio | Bulk Modulus MPa | Shear Modulus MPa |
|---|---|---|---|---|
| | 2.e+005 | 0.3 | 1.6667e+005 | 76923 |

TABLE 42

Structural Steel > Isotropic Relative Permeability

| Relative Permeability |
|---|

| 10000 |
|---|

TABLE 43

Structural Steel > Bilinear Isotropic Hardening

| Yield Strength MPa | Tangent Modulus MPa | Temperature C |
|---|---|---|
| 409 | 1500 | |

**APENDIX B:**

**FE Analysis of PC7 Structure**

**ANSYS-generated reports**

**Appendix B:**

**FE Analysis of PC7 Structure**

**ANSYS-generated sample report**

Project

| | |
|---|---|
| First Saved | Monday, June 16, 2014 |
| Last Saved | Tuesday, June 17, 2014 |
| Product Version | 14.0 Release |
| Save Project Before Solution | No |
| Save Project After Solution | No |

Units

TABLE 1

| Unit System | Metric (mm, t, N, s, mV, mA) Degrees rad/s Celsius |
|---|---|
| Angle | Degrees |
| Rotational Velocity | rad/s |
| Temperature | Celsius |

Model (A4)

Geometry

TABLE 2

Model (A4) > Geometry

| Object Name | Geometry |
|---|---|
| State | Fully Defined |
| Definition | |
| Source | C:\Users\Mike M\Desktop\Thesis\FEA Section\Structure design documents\T-Bar stiffener Model\onepart-T-3.15mx6m.IGS |
| Type | Iges |
| Length Unit | Meters |
| Element Control | Program Controlled |
| Display Style | Body Color |
| Bounding Box | |
| Length X | 3150. mm |
| Length Y | 382. mm |
| Length Z | 6000. mm |
| Properties | |
| Volume | 4.3049e+008 mm³ |
| Mass | 3.3793 t |
| Scale Factor Value | 1. |
| Statistics | |
| Bodies | 1 |

| | |
|---|---|
| Active Bodies | 1 |
| Nodes | 666131 |
| Elements | 334076 |
| Mesh Metric | None |
| Basic Geometry Options | |
| Solid Bodies | Yes |
| Surface Bodies | Yes |
| Line Bodies | No |
| Parameters | Yes |
| Parameter Key | DS |
| Attributes | No |
| Named Selections | No |
| Material Properties | No |
| Advanced Geometry Options | |
| Use Associativity | Yes |
| Coordinate Systems | No |
| Reader Mode Saves Updated File | No |
| Use Instances | Yes |
| Smart CAD Update | No |
| Attach File Via Temp | Yes |

| File | |
|---|---|
| Temporary Directory | C:\Users\Mike M\AppData\Local\Temp |
| Analysis Type | 3-D |
| Mixed Import Resolution | None |
| Decompose Disjoint Faces | Yes |
| Enclosure and Symmetry Processing | Yes |

TABLE 3

Model (A4) > Geometry > Parts

| Object Name | Part 1 |
|---|---|
| State | Meshed |
| Graphics Properties | |
| Visible | Yes |
| Transparency | 1 |
| Definition | |
| Suppressed | No |
| Stiffness Behavior | Flexible |
| Coordinate System | Default Coordinate System |
| Reference Temperature | By Environment |

| Material | |
|---|---|
| Assignment | Structural Steel |
| Nonlinear Effects | Yes |
| Thermal Strain Effects | Yes |
| Bounding Box | |
| Length X | 3150. mm |
| Length Y | 382. mm |
| Length Z | 6000. mm |
| Properties | |
| Volume | 4.3049e+008 mm³ |
| Mass | 3.3793 t |
| Centroid X | 4.2983e-014 mm |
| Centroid Y | 73.459 mm |
| Centroid Z | 2.1492e-013 mm |
| Moment of Inertia Ip1 | 9.2669e+006 t·mm² |
| Moment of Inertia Ip2 | 1.2018e+007 t·mm² |
| Moment of Inertia Ip3 | 2.8177e+006 t·mm² |
| Statistics | |
| Nodes | 666131 |
| Elements | 334076 |
| Mesh Metric | None |

Coordinate Systems

TABLE 4

Model (A4) > Coordinate Systems > Coordinate System

| Object Name | Global Coordinate System |
|---|---|
| State | Fully Defined |
| Definition | |
| Type | Cartesian |
| Coordinate System ID | 0. |
| Origin | |
| Origin X | 0. mm |
| Origin Y | 0. mm |
| Origin Z | 0. mm |
| Directional Vectors | |
| X Axis Data | [ 1. 0. 0. ] |
| Y Axis Data | [ 0. 1. 0. ] |
| Z Axis Data | [ 0. 0. 1. ] |

Mesh

TABLE 5

Model (A4) > Mesh

| Object Name | Mesh |
|---|---|
| State | Solved |

| Defaults | |
|---|---|
| Physics Preference | Mechanical |
| Relevance | 40 |
| Sizing | |
| Use Advanced Size Function | Off |
| Relevance Center | Fine |
| Element Size | Default |
| Initial Size Seed | Active Assembly |
| Smoothing | Medium |
| Transition | Fast |
| Span Angle Center | Coarse |
| Minimum Edge Length | 11.0 mm |
| Inflation | |
| Use Automatic Inflation | None |
| Inflation Option | Smooth Transition |
| Transition Ratio | 0.272 |
| Maximum Layers | 5 |
| Growth Rate | 1.2 |
| Inflation Algorithm | Pre |
| View Advanced Options | No |
| Patch Conforming Options | |

| | |
|---|---|
| Triangle Surface Mesher | Program Controlled |
| **Advanced** | |
| Shape Checking | Standard Mechanical |
| Element Midside Nodes | Program Controlled |
| Straight Sided Elements | No |
| Number of Retries | Default (4) |
| Extra Retries For Assembly | Yes |
| Rigid Body Behavior | Dimensionally Reduced |
| Mesh Morphing | Disabled |
| **Defeaturing** | |
| Pinch Tolerance | Please Define |
| Generate Pinch on Refresh | No |
| Automatic Mesh Based Defeaturing | On |
| Defeaturing Tolerance | Default |
| **Statistics** | |
| Nodes | 666131 |
| Elements | 334076 |
| Mesh Metric | None |

TABLE 6

Model (A4) > Mesh > Mesh Controls

| Object Name | Refinement |
|---|---|

| | |
|---|---|
| State | Fully Defined |
| **Scope** | |
| Scoping Method | Geometry Selection |
| Geometry | 239 Faces |
| **Definition** | |
| Suppressed | No |
| Refinement | 1 |

Static Structural (A5)

TABLE 7

Model (A4) > Analysis

| Object Name | Static Structural (A5) |
|---|---|
| State | Solved |
| **Definition** | |
| Physics Type | Structural |
| Analysis Type | Static Structural |
| Solver Target | Mechanical APDL |
| **Options** | |
| Environment Temperature | 22. °C |
| Generate Input Only | No |

TABLE 8

Model (A4) > Static Structural (A5) > Analysis Settings

| | |
|---|---|
| Object Name | Analysis Settings |
| State | Fully Defined |
| **Step Controls** | |
| Number Of Steps | 2. |
| Current Step Number | 1. |
| Step End Time | 1. s |
| Auto Time Stepping | Program Controlled |
| **Solver Controls** | |
| Solver Type | Program Controlled |
| Weak Springs | Program Controlled |
| Large Deflection | On |
| Inertia Relief | Off |
| **Restart Controls** | |
| Generate Restart Points | Program Controlled |
| Retain Files After Full Solve | No |
| **Nonlinear Controls** | |
| Force | Program Controlled |

| | |
|---|---|
| Convergence | |
| Moment Convergence | Program Controlled |
| Displacement Convergence | Program Controlled |
| Rotation Convergence | Program Controlled |
| Line Search | Program Controlled |
| Stabilization | Off |
| Output Controls | |
| Stress | Yes |
| Strain | Yes |
| Nodal Forces | No |
| Contact Miscellaneous | No |
| General Miscellaneous | No |
| Calculate Results At | All Time Points |
| Max Number of Result Sets | Program Controlled |

| Analysis Data Management | |
|---|---|
| Solver Files Directory | C:\Users\Mike M\Desktop\Thesis\FEA Section\Structure design documents\T-Bar stiffener Model\T-stiffener model- 6x3.15 , loadunload_files\dp0\SYS\MECH\ |
| Future Analysis | None |
| Scratch Solver Files Directory | |
| Save MAPDL db | No |
| Delete Unneeded Files | Yes |
| Nonlinear Solution | Yes |
| Solver Units | Active System |
| Solver Unit System | nmm |

TABLE 9

Model (A4) > Static Structural (A5) > Analysis Settings

Step-Specific "Step Controls"

| Step | Step End Time |
|---|---|
| 1 | 1. s |
| 2 | 2. s |

TABLE 10

Model (A4) > Static Structural (A5) > Analysis Settings

Step-Specific "Output Controls"

| Step | Max Number of Result Sets |
|------|---------------------------|
| 1 | Program Controlled |
| 2 | 1000. |

TABLE 11

Model (A4) > Static Structural (A5) > Loads

| Object Name | Fixed Support | Force |
|-------------|---------------|-------|
| State | Fully Defined | |
| Scope | | |
| Scoping Method | Geometry Selection | |
| Geometry | 4 Faces | 1 Face |
| Definition | | |
| Type | Fixed Support | Force |
| Suppressed | No | |
| Define By | | Vector |
| Magnitude | | Tabular Data |
| Direction | | Defined |

FIGURE 1

Model (A4) > Static Structural (A5) > Force
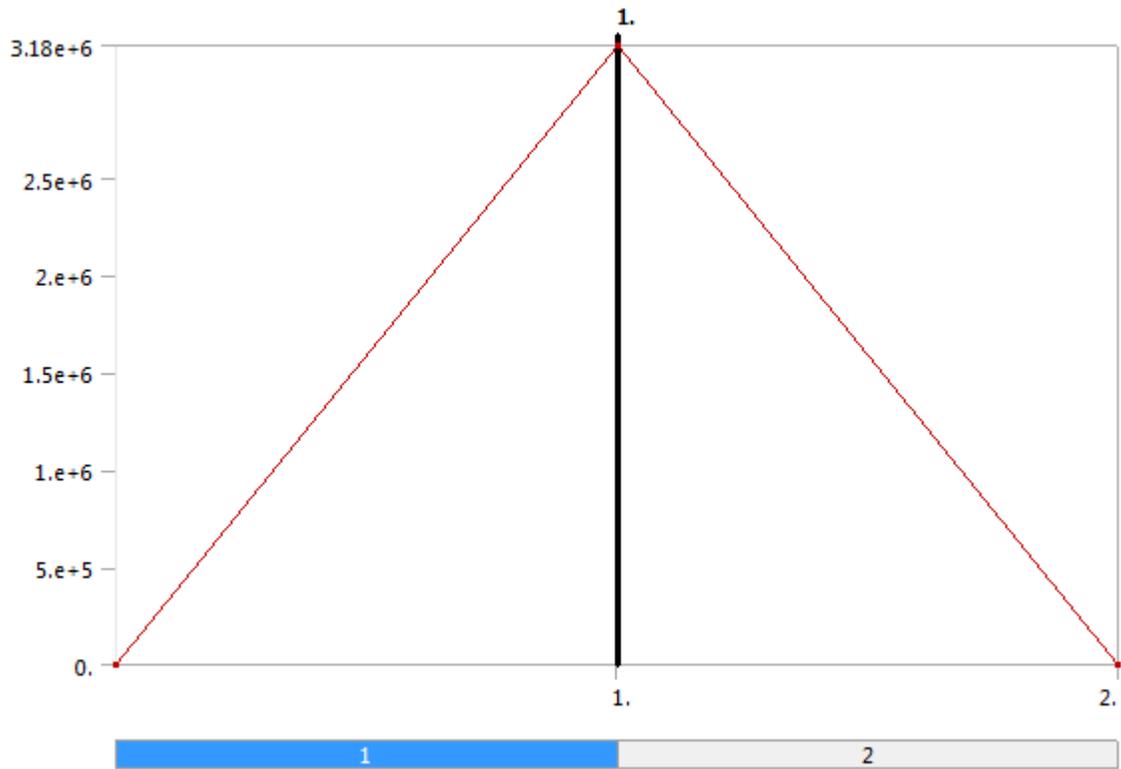
TABLE 12

Model (A4) > Static Structural (A5) > Force

| Steps | Time [s] | Force [N] |
|-------|----------|-----------|
| 1     | 0.       | 0.        |
|       | 1.       | 3.18e+006 |
| 2     | 2.       | 0.        |

Solution (A6)

TABLE 13

Model (A4) > Static Structural (A5) > Solution

| Object Name | Solution (A6) |
|-------------|---------------|

| State | Solved |
|-------|--------|
| **Adaptive Mesh Refinement** | |
| Max Refinement Loops | 1. |
| Refinement Depth | 2. |
| **Information** | |
| Status | Done |

TABLE 14

Model (A4) > Static Structural (A5) > Solution (A6) > Solution Information

| Object Name | Solution Information |
|-------------|---------------------|
| State | Solved |
| **Solution Information** | |
| Solution Output | Solver Output |
| Newton-Raphson Residuals | 0 |
| Update Interval | 2.5 s |
| Display Points | All |
| **FE Connection Visibility** | |
| Activate Visibility | Yes |
| Display | All FE Connectors |
| Draw Connections Attached To | All Nodes |
| Line Color | Connection Type |
| Visible on Results | No |

| Line Thickness | Single |
|---|---|
| Display Type | Lines |

TABLE 15

Model (A4) > Static Structural (A5) > Solution (A6) > Results

| Object Name | Total Deformation | Directional Deformation | Directional Deformation 2 |
|---|---|---|---|
| State | Solved | | |
| **Scope** | | | |
| Scoping Method | Geometry Selection | | |
| Geometry | All Bodies | 1 Edge | |
| **Definition** | | | |
| Type | Total Deformation | Directional Deformation | |
| By | Time | | |
| Display Time | Last | | |
| Calculate Time History | Yes | | |
| Identifier | | | |
| Suppressed | No | | |
| Orientation | | Y Axis | |
| Coordinate System | | Global Coordinate System | |

| Results | | | |
|---|---|---|---|
| Minimum | 0. mm | 0.89995 mm | 0.92501 mm |
| Maximum | 27.742 mm | 0.92473 mm | 27.734 mm |
| Minimum Value Over Time | | | |
| Minimum | 0. mm | 0.89995 mm | 0.92501 mm |
| Maximum | 0. mm | 6.9214 mm | 7.0673 mm |
| Maximum Value Over Time | | | |
| Minimum | 4.6493 mm | 0.92473 mm | 4.5715 mm |
| Maximum | 46.797 mm | 6.9877 mm | 46.789 mm |
| Information | | | |
| Time | 2. s | | |
| Load Step | 2 | | |
| Substep | 4 | | |
| Iteration Number | 42 | | |

FIGURE 2

Model (A4) > Static Structural (A5) > Solution (A6) > Total Deformation
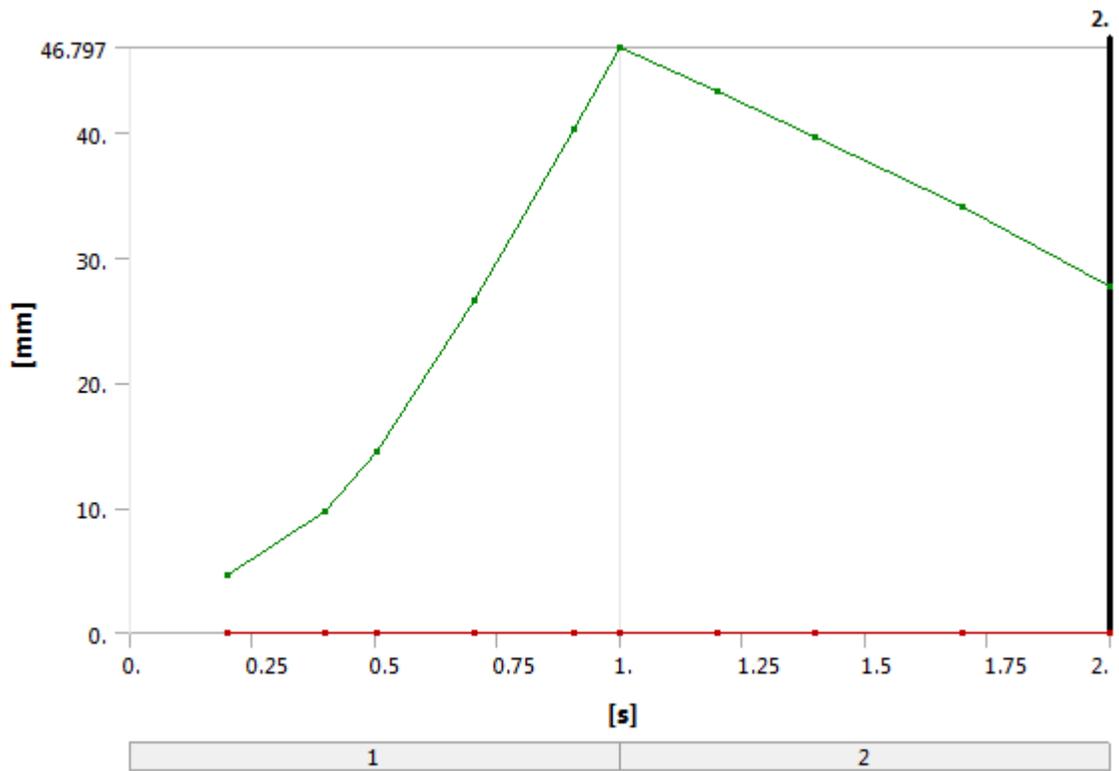
TABLE 16

Model (A4) > Static Structural (A5) > Solution (A6) > Total Deformation

| Time [s] | Minimum [mm] | Maximum [mm] |
|----------|--------------|--------------|
| 0.2      |              | 4.6493       |
| 0.4      |              | 9.7608       |
| 0.505    |              | 14.442       |
| 0.705    | 0.           | 26.509       |
| 0.905    |              | 40.199       |
| 1.       |              | 46.797       |
| 1.2      |              | 43.277       |

| | | |
|---|---|---|
| 1.4 | | 39.66 |
| 1.7 | | 34.04 |
| 2. | | 27.742 |

FIGURE 3

Model (A4) > Static Structural (A5) > Solution (A6) > Directional Deformation
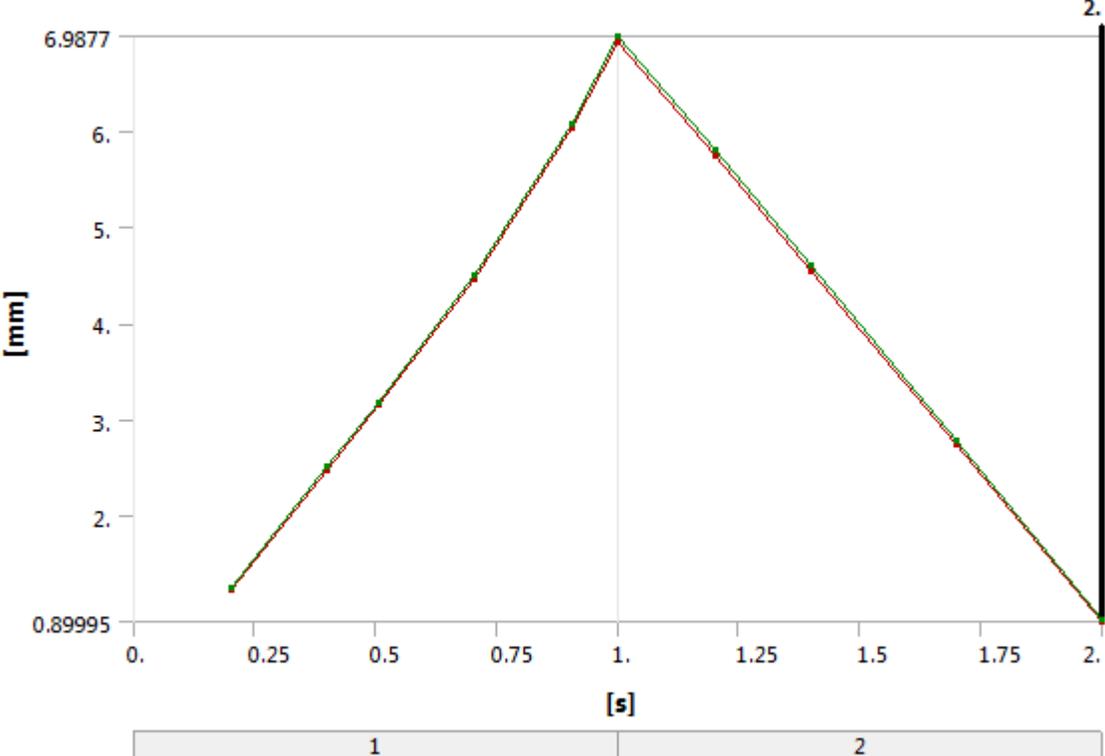


TABLE 17

Model (A4) > Static Structural (A5) > Solution (A6) > Directional Deformation

| Time [s] | Minimum [mm] | Maximum [mm] |
|---|---|---|
| 0.2 | 1.2341 | 1.2457 |
| 0.4 | 2.4835 | 2.5074 |

| | | |
|---|---|---|
| 0.505 | 3.1528 | 3.1807 |
| 0.705 | 4.4573 | 4.496 |
| 0.905 | 6.0276 | 6.0832 |
| 1. | 6.9214 | 6.9877 |
| 1.2 | 5.7407 | 5.7988 |
| 1.4 | 4.5497 | 4.5993 |
| 1.7 | 2.7441 | 2.7802 |
| 2. | 0.89995 | 0.92473 |

FIGURE 4

Model (A4) > Static Structural (A5) > Solution (A6) > Directional Deformation 2
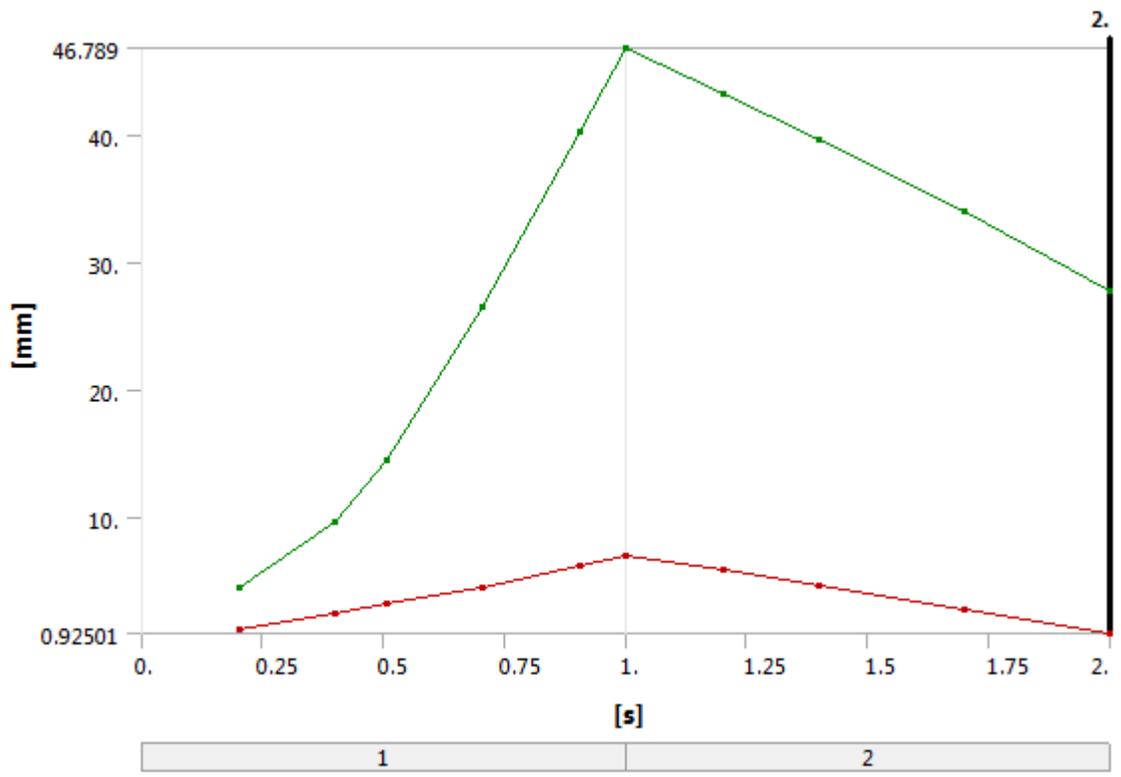
TABLE 18

Model (A4) > Static Structural (A5) > Solution (A6) > Directional Deformation 2

| Time [s] | Minimum [mm] | Maximum [mm] |
|----------|--------------|--------------|
| 0.2 | 1.2605 | 4.5715 |
| 0.4 | 2.5416 | 9.6701 |
| 0.505 | 3.2416 | 14.439 |
| 0.705 | 4.5819 | 26.504 |
| 0.905 | 6.1678 | 40.192 |
| 1. | 7.0673 | 46.789 |
| 1.2 | 5.861 | 43.269 |
| 1.4 | 4.6448 | 39.652 |
| 1.7 | 2.8024 | 34.032 |
| 2. | 0.92501 | 27.734 |

Material Data

Structural Steel

TABLE 19

Structural Steel > Constants

| | |
|---|---|
| Density | 7.85e-009 tonne mm^-3 |
| Coefficient of Thermal Expansion | 1.2e-005 C^-1 |
| Specific Heat | 4.34e+008 mJ tonne^-1 C^-1 |
| Thermal Conductivity | 6.05e-002 W mm^-1 C^-1 |

| Resistivity | 1.7e-004 ohm mm |
|---|---|

TABLE 20

Structural Steel > Compressive Ultimate Strength

| Compressive Ultimate Strength MPa |
|---|
| 460 |

TABLE 21

Structural Steel > Compressive Yield Strength

| Compressive Yield Strength MPa |
|---|
| 355 |

TABLE 22

Structural Steel > Tensile Yield Strength

| Tensile Yield Strength MPa |
|---|
| 355 |

TABLE 23

Structural Steel > Tensile Ultimate Strength

| Tensile Ultimate Strength MPa |
|---|
| 460 |

TABLE 24

Structural Steel > Isotropic Secant Coefficient of Thermal Expansion

| Reference Temperature C |
|---|
| 22 |

TABLE 25

Structural Steel > Alternating Stress Mean Stress

| Alternating Stress MPa | Cycles | Mean Stress MPa |
|---|---|---|
| 3999 | 10 | 0 |
| 2827 | 20 | 0 |
| 1896 | 50 | 0 |
| 1413 | 100 | 0 |
| 1069 | 200 | 0 |
| 441 | 2000 | 0 |
| 262 | 10000 | 0 |
| 214 | 20000 | 0 |
| 138 | 1.e+005 | 0 |
| 114 | 2.e+005 | 0 |
| 86.2 | 1.e+006 | 0 |

TABLE 26

Structural Steel > Strain-Life Parameters

| Strength Coefficient MPa | Strength Exponent | Ductility Coefficient | Ductility Exponent | Cyclic Strength Coefficient MPa | Cyclic Strain Hardening Exponent |
|---|---|---|---|---|---|
| 920 | -0.106 | 0.213 | -0.47 | 1000 | 0.2 |

TABLE 27

Structural Steel > Isotropic Elasticity

| Temperature C | Young's Modulus MPa | Poisson's Ratio | Bulk Modulus MPa | Shear Modulus MPa |
|---|---|---|---|---|
| | 2.e+005 | 0.3 | 1.6667e+005 | 76923 |

TABLE 28

Structural Steel > Isotropic Relative Permeability

| Relative Permeability |
|---|
| 10000 |

TABLE 29

Structural Steel > Bilinear Isotropic Hardening

| Yield Strength MPa | Tangent Modulus MPa | Temperature C |
|---|---|---|
| 355 | 1500 | 22 |